

ALPHA TRICALCIUM PHOSPHATE-BASED HYBRID BONE ANALOGS:
ASSESSMENT OF CEMENT BEHAVIOUR AND MECHANICAL PROPERTIES

A THESIS SUBMITTED TO
THE GRADUATE SCHOOL OF NATURAL AND APPLIED SCIENCES
OF
MIDDLE EAST TECHNICAL UNIVERSITY

BY

GÖZDE ALKAN

IN PARTIAL FULFILLMENT OF THE REQUIREMENTS
FOR
THE DEGREE OF MASTER OF SCIENCE
IN
METALLURGICAL AND MATERIALS ENGINEERING

SEPTEMBER 2014

Approval of the thesis:

**ALPHA TRICALCIUM PHOSPHATE-BASED HYBRID BONE ANALOGS:
ASSESSMENT OF CEMENT BEHAVIOUR AND MECHANICAL
PROPERTIES**

submitted by **GÖZDE ALKAN** in partial fulfillment of the requirements for the degree of **Master of Science in Metallurgical and Materials Engineering Department, Middle East Technical University** by,

Prof. Dr. Canan ÖZGEN _____
Dean, Graduate School of **Natural and Applied Sciences**

Prof. Dr. C. Hakan GÜR _____
Head of Department, **Metallurgical and Materials Engineering**

Assoc. Prof. Dr. Caner DURUCAN _____
Supervisor, **Metallurgical and Materials Engineering Dept. METU**

Examining Committee Members:

Prof. Dr. Abdullah ÖZTÜRK _____
Metallurgical and Materials Eng. Dept. METU

Assoc. Prof. Dr. Caner DURUCAN _____
Metallurgical and Materials Eng. Dept. METU

Prof. Dr. Cevdet KAYNAK _____
Metallurgical and Materials Eng. Dept. METU

Assist. Prof. Dr. Y. Eren KALAY _____
Metallurgical and Materials Eng. Dept. METU

Assoc. Prof. Dr. Ayşen TEZCANER _____
Engineering Sciences Dept. METU

Date: _____

I hereby declare that all information in this document has been obtained and presented in accordance with academic rules and ethical conduct. I also declare that, as required by these rules and conduct, I have fully cited and referenced all material and results that are not original to this work.

Name, Last name : Gözde ALKAN

Signature :

ABSTRACT

ALPHA TRICALCIUM PHOSPHATE-BASED HYBRID BONE ANALOGS: ASSESSMENT OF CEMENT BEHAVIOUR AND MECHANICAL PROPERTIES

Alkan, Gözde

M.Sc., Department of Metallurgical and Materials Engineering

Supervisor: Assoc. Prof. Dr. Caner DURUCAN

September 2014, 87 pages

The main theme of this thesis was to establish materials science and chemical issues for developing a self-hardening cement system, for potential use in bone defect filling operations. The cement comprises of a ceramic powder – alpha-tricalcium phosphate (α -TCP, α -Ca₃(PO₄)₂) – which hardens into inorganic ceramic part of the natural bone tissue, i.e. calcium deficient hydroxyapatite (CDHAp, Ca₉(HPO₄)(PO₄)₅(OH)) upon hydration. One of the primary objectives of this study therefore was, synthesis of phase pure α -TCP by solid state reactions, and investigation of its' hydraulic reactivity at around physiological temperature (37 °C) and evaluating the microstructural and mechanical changes upon cement conversion. These were accomplished by isothermal calorimetry studies and additional analytical characterization including x-ray diffraction, electron microscopy, chemical spectroscopy and mechanical testing. Additionally, in order to improve the strength of the hydration product, α -TCP based hybrid cement blends were obtained by the addition of an inorganic (calcium sulfate hemihydrate, CSH, CaSO₄·½H₂O) or an organic (polycaprolactone, PCL, (C₆H₁₀O₂)_n) component. α -TCP:CSH and α -TCP:PCL hybrid cements were again converted into

CDHAp:calcium sulfate dihydrate ($\text{CaSO}_4 \cdot 2\text{H}_2\text{O}$, CSD) or CDHAp:PCL cement-end products by hydration at 37 °C. For both systems, comparative and parametric studies were carried out to elucidate effect of these additives on hydraulic reactivity and mechanical properties of α -TCP cements. It was found that CSH dramatically suppresses α -TCP \rightarrow CDHAp conversion and retards setting reaction. However, CSH addition significantly improves strength of cement-end products. The fracture strength of cement end product of pure α -TCP was increased from 4.5 ± 0.1 MPa up to 9.28 ± 0.1 MPa upon addition of 25 wt. % CSH, as evaluated by diametral compressive tests. α -TCP:PCL hybrids were also investigated in terms of reaction kinetics, microstructural and mechanical properties. Isothermal calorimetry analysis revealed that PCL postpones α -TCP \rightarrow CDHAp conversion as also evidenced by detailed microstructural and phase analyses. Meanwhile, PCL addition improved mechanical integrity of the hardened mass leading to a maximum fracture strength value of 6.54 ± 0.1 MPa when added in optimum amount (3 wt. %).

Keywords: Bioceramics, Bone cements, alpha-tricalcium phosphate, calcium-deficient hydroxyapatite, calcium sulfates, polycaprolactone

ÖZ

ALFA-TRİKALSİYUM FOSFAT ESASLI HİBRİT KEMİK BENZEŞİKLERİ: ÇİMENTO DAVRANIMI VE MEKANİK ÖZELLİKLERİN BELİRLENMESİ

Alkan, Gözde

Yüksek Lisans, Metalurji ve Malzeme Mühendisliği Bölümü

Tez Yöneticisi: Doç. Dr. Caner DURUCAN

Eylül 2014, 87 sayfa

Bu tezde esas olarak, kemik dolgu operasyonlarında kullanılan ve kendiliğinden sertleşen çimento sistemlerinin geliştirilmesi yönünde, söz konusu biyomalzemelerin üretimi ve kullanımına yönelik için ilk kritik faz sayılabilecek malzeme özellikleri ve kimyasal faktörlerin aydınlatılması hedeflenmiştir. Alfa-trikalsiyum fosfat (α -TCP, α - $\text{Ca}_3(\text{PO}_4)_2$) esaslı bu toz çimento sistemi su ile hidrasyon sonucu sertleşerek doğal kemik dokusundaki anorganik bileşen olan kalsiyumca eksik hidroksiapatite (CDHAp, $\text{Ca}_9(\text{HPO}_4)(\text{PO}_4)_5(\text{OH})$) dönüşmektedir. Dolayısıyla, tezdaki genel amaçlardan biri; α -TCP'nin saf olarak katı hal reaksiyonuyla sentezi, fizyolojik sıcaklıkta (37°C) hidrasyon reaktivitesinin sınılanması, ve çimento dönüşümüne ilişkin mikroyapısal ve mekanik değişimlerin belirlenmesidir. Bu incelemeler, izotermal kalorimetre, x-ışını kırınımı, elektron mikroskopi, kimyasal spektroskopisi ve mekanik testlerle gerçekleştirilmiştir. Ayrıca, tez kapsamında hidrasyon ürünü sertleşmiş çimentonun mekanik dayanımını artırmaya yönelik olarak, yine α -TCP esaslı inorganik (CSH, kalsiyum sülfat hemihidrat, $\text{CaSO}_4 \cdot \frac{1}{2}\text{H}_2\text{O}$) veya organik (polikaprolakton, PCL, $(\text{C}_6\text{H}_{10}\text{O}_2)_n$) katkılı hibrit çimento karışımları oluşturulmuştur. α -TCP:CSH ve α -TCP:PCL hibrit çimentolarının 37°C de hidrasyonu sonucunda CDHAp: kalsiyum sülfat hemihidrat ($\text{CaSO}_4 \cdot 2\text{H}_2\text{O}$, CSD) veya CDHAp:PCL kompozitleri üretilmiştir.

Her iki sistem için de, bu eklentilerin hidrasyon reaktivitesine ve mekanik özelliklere olan etkisini görmek için karşılaştırmalı ve parametrik deneysel çalışmalar yapılmıştır. CSH eklentisinin α -TCP \rightarrow CDHAp reaksiyonunu bariz olarak ertelediği gözlemlenmiştir. Buna karşın, CSH eklentisiyle kırılma dayanımlarında artma olduğu belirlenmiştir. Saf α -TCP'nin hidrasyon ürünü çimenetonun dayanımı 4.5 ± 0.1 MPa iken, bu değer 25 % CSH eklentisiyle 9.28 ± 0.1 MPa'a yükselmiştir. α -TCP:PCL hibritlerinin de reaktivitesi ve mekanik özellikleri incelenmiştir. İzotermal kalorimetre bulguları, PCL'nin de α -TCP \rightarrow CDHAp reaksiyonunu geciktirdiğini ortaya koymuştur. Fakat, reaksiyon ürünlerinin mekanik özelliklerinde optimum miktarda (3 wt. %) PCL eklentisiyle 6.54 ± 0.1 MPa'a ulaşan artış gözlemlenmiştir.

Anahtar Kelimeler: Biyoseramikler, Kemik Çimentoları, Alfa Trikalsiyum Fosfat, Polikaprolakton, Kalsiyum Sülfat

To My Family

ACKNOWLEDGEMENTS

I would like to express my sincere appreciation to Assoc. Prof. Dr. Caner Durucan for his supervision, guidance, support and encouragement throughout the study.

I am grateful to and all my labmates; Tümerkan Kesim, Merve Güldiken, Özlem Yıldırım, Ekim Saraç and Barış Alkan and all the staff of the Department of Metallurgical and Materials Engineering especially; Bahadır Can Kocaoğlu and Halil İbrahim Yavuz for their moral support and friendship during my master's education.

I would like to express my special thanks to Hakan Yavaş for his professional support during my master's education and also for his support, guidance and trust outside school which helped me a lot through hard times.

I'm also grateful to my childhood friends Aybuke Doğan, Begüm Aydoğdu, Berna Turhan, Deniz Özüdoğru and Duygu Sarı for their unconditional friendship that always helps me to keep my motivation very high.

Finally, I owe a debt to my mom for her presence and support through the sleepless days and nights; to my dad for his unconditional love and smiling face; to my sister for showing me the light even in the darkest times and sharing everything in my life and to my little sunshine Duru for brightening up my life.

TABLE OF CONTENTS

ABSTRACT	V
ÖZ	VII
ACKNOWLEDGEMENTS	X
TABLE OF CONTENTS	XI
LIST OF TABLES	XIV
LIST OF FIGURES	XV
LIST OF ABBREVIATIONS	XIX
INTRODUCTION AND LITERATURE REVIEW	1
1.1 General introduction and rationale of the thesis	1
1.2 Related previous knowledge	3
1.2.1 Structure and properties of natural bone	3
1.2.2 Bone grafts	6
1.2.2.1 Bioinert ceramics	6
1.2.2.2 Calcium sulfates	7
1.2.2.3 Calcium phosphate ceramics	8
1.2.2.4 Hydroxyapatite	11
1.2.2.5 Calcium-deficient hydroxyapatite	12
1.2.2.6 Tricalcium phosphate	12
1.2.2.7 α -Tricalcium phosphate (α -TCP)	13
1.2.3 Bone cements	14
1.2.3.1 Calcium phosphate cements	15
1.2.3.2 Brushite cements	18
1.2.3.3 Apatite cements	19
1.2.4 Mechanical properties of calcium phosphate cements	22

1.2.4.1	Improving mechanical properties of calcium phosphate cements	22
1.2.5	Calcium phosphate cement based composites.....	23
1.2.5.1	Inorganic compound reinforced calcium phosphates.....	23
1.2.5.2	Calcium phosphate-polymer composites	24
1.2.5.3	Calcium phosphate based composites with natural polymers.....	26
1.2.5.4	Calcium phosphate based composites with synthetic polymers	27
1.3	Objective and structure of the thesis	29
MATERIAL CHARACTERIZATION AND EXPERIMENTAL PROCEDURE....		31
2.1	Materials.....	31
2.2	Experimental procedures.....	32
2.2.1	Synthesis of β -TCP.....	33
2.2.2	Preparation of HAp:calcium sulfate dihydrate composites	35
2.2.3	Preparation of HAp:polycaprolactone (PCL) composites	36
2.3	Characterization of solid state synthesis and cement end products	38
2.3.1	Particle size analysis.....	38
2.3.2	Phase identification: X-Ray Diffraction Analysis	38
2.3.3	Microstructural investigation: Scanning Electron Microscopy.....	38
2.3.4	Chemical analysis: Fourier Transformed Infrared Spectroscopy	38
2.3.5	Reaction kinetics studies: Isothermal Calorimetry.....	39
2.3.6	Mechanical testing: Diametrical Compression Test.....	39
2.3.7	Density measurement	40
CHARACTERIZATION OF β -TCP AND PRELIMINARY INVESTIGATION OF ITS' CEMENT TYPE REACTIVITY		41
3.1.	Characterization of β -TCP powders.....	41
3.2	Cement-type reactivity of TCP	45
3.3	Characterization of cement-end products.....	46
3.4	Mechanical properties of TCP and it's cement-end product.....	51

CHARACTERIZATION AND PROPERTIES OF	53
4.1 Effect of CSH incorporation on cement-type reaction kinetics of TCP	53
4.2 Characterization of cement-end products.....	54
4.3 Mechanical properties CSH incorporated hybrid cements.....	60
CHARACTERIZATION AND PROPERTIES OF	63
TCP:PCL HYBRID CEMENT BLENDS.....	63
5.1 Effect of PCL incorporation on cement-type reactivity of TCP	63
5.2 Microstructural and chemical properties of TCP:PCL hybrid cement blends	65
5.3 Compositional effects on cement behavior of TCP:PCL hybrid blends	72
5.4 Spectroscopic analysis of TCP:PCL hybrid blends	74
5.5 Mechanical properties of PCL incorporated hybrid cements.....	76
CONCLUSIONS.....	79
REFERENCES.....	83

LIST OF TABLES

TABLES

Table 1.1 List of existing calcium phosphate compounds with various Ca/P ratio.....	9
Table 1.2 The list of some commercial self-setting calcium orthophosphate formulations with the producer, product name, composition (when available) and main end-product. The end-product of the reactions can be either an apatite (CDHAp, carbonate apatite, <i>etc.</i>) or brushite (=DCPD) [Bohner, 2010].....	17
Table 2.1 The composition of TCP:CSH hybrid pre-cement blends and details for their cement conversion to HAp:CSD composites.....	36
Table 2.2 The composition of TCP:PCL hybrid pre-cement blends and details for their cement conversion to HAp:PCL composites.....	37
Table 3.1 Particle characteristics of TCP powders at different physical states.....	45
Table 4.1 Porosity values of mechanical test samples before and after hydration.....	64
Table 5.1 Porosity values of mechanical test samples before and after hydration.....	79

LIST OF FIGURES

FIGURES

Figure 1.1	A schematic shown of hierarchical structure of bone.....	4
Figure 1.2	Solubility isotherms of various calcium phosphates in water.....	10
Figure 1.3	CaO-P ₂ O ₅ binary phase diagram.....	13
Figure 1.4	An injectable bone cement system.....	15
Figure 1.5	Scanning electron micrographs of set apatite and brushite cements obtained by the hydrolysis of α -Tricalcium phosphate (α -TCP) and by reaction of β -Tricalcium phosphate (β -TCP) with monocalcium phosphate monohydrate (MCPM), respectively. [Ginebra et al., 2012].....	20
Figure 1.6	A schematic illustration of polymer incorporation into calcium phosphate cements a-b-c as dissolved in liquid phase d-e as solid additive to powder phase....	25
Figure 2.1	The diffractogram of the chemically synthesized monetite (CaHPO ₄).....	32
Figure 2.2	Experimental details and flowchart for solid state synthesis of α -TCP from CaCO ₃ and CaHPO ₄	34
Figure 2.3	The experimental details for TCP:CSH hybrid pre-cement blend preparation and processing of final HAp:CSD composite cement.....	36
Figure 2.4	The experimental details for TCP:PCL hybrid pre-cement blend preparation and processing of final HAp:PCL composite cements.....	38
Figure 2.5	Schematic representation of diametral compression test.....	40
Figure 3.1	The XRD diffractogram of the solid state synthesis product obtained according to the standard synthesis protocol.....	43
Figure 3.2	SEM micrograph of as-synthesized TCP.....	44
Figure 3.3	SEM micrograph of milled TCP.....	44

Figure 3.4 FTIR spectrum of TCP in 2000-450 cm^{-1} range.....	46
Figure 3.5 Typical isothermal calorimetry data (dQ/dt vs. time) for hydration of as-synthesized (α -TCP (A)) and milled TCP (α -TCP(M)). The reaction temperature was 37 °C	47
Figure 3.6 XRD diffractogram of hydration product of as-synthesized TCP powder.	48
Figure 3.7 XRD diffractogram of hydration product of milled TCP powder.....	49
Figure 3.8 SEM micrograph of hydration product of as-synthesized TCP powder...	51
Figure 3.9 SEM micrograph of hydration product of milled TCP powder.....	51
Figure 3.10 FTIR spectrum of hydrated TCP (i.e. after cement type conversion to HAp) in 2000-450 cm^{-1} range.....	52
Figure 3.11 Diametral compressive strength of TCP and its hydration product.....	54
Figure 4.1 The heat flow curves for hydration of plain TCP (α -TCP(M)), and 10 wt. (CS-10) or 25 wt.% (CS-25) calcium sulfate hemihydrate (CSH, $\text{CaSO}_4 \cdot \frac{1}{2}\text{H}_2\text{O}$) containing hybrid blends. The reaction temperature was 37 °C.....	56
Figure 4.2 XRD diffractogram of 10 wt. % CSH-containing hybrid TCP:CSH blend after hydration at 37 °C for 48 h.....	57
Figure 4.3 XRD diffractogram of 25 wt. % CSH-containing hybrid TCP:CSH blend after hydration at 37 °C for 48 h.....	58
Figure 4.4a SEM micrograph of 10 wt. CSH-containing hybrid TCP:CSH blend before hydration.....	60
Figure 4.4b SEM micrograph of 10 wt. CSH-containing hybrid TCP:CSH blend after hydration at 37 °C for 48 h.....	60

Figure 4.5a SEM micrograph of 25 wt. % CSH-containing hybrid TCP:CSH blend before hydration.....	61
Figure 4.5b SEM micrograph of 25 wt. CSH-containing hybrid TCP:CSH blend after hydration at 37 °C for 48 h.....	61
Figure 4.6 The images of CDHAp-based cement putty products after hydration of (a) plain TCP (b) 10 wt. (CS-10) or (c) 25 wt. % (CS-25) CSH containing hybrid TCP:CSH blends. (The scale is 1 cm)	62
Figure 4.7 Diametral compressive strength of TCP and hybrid TCP:CSH pellets; CS-10, CS-25 (10, and 25 wt. % CSH) (a) before and (b) after hydration.....	63
Figure 5.1 The heat flow curves for hydration (at 37 °C) of TCP and hybrid TCP:PCL pellets; T3CP, T6CP and T9CP (3, 6 or 9 wt.% PCL).....	66
Figure 5.2 The XRD diffractograms as a function of reaction time for (a) plain TCP pellet, (b) T3PC (3 wt. % PCL) hybrid pellets.....	68
Figure 5.3 Microstructural changes during hydration TCP pellet as a function of reaction (at 37 °C) time.....	69
Figure 5.4 SEM micrograph of 2 h hydrated TCP pellet.....	69
Figure 5.5 SEM micrograph of 42 h hydrated TCP pellet.....	70
Figure 5.6 Microstructural changes during hydrolysis of T3PC (3 wt. % PCL) as a function of reaction time.....	71
Figure 5.7 SEM micrograph of T3PC (3 wt. % PCL) after 2 h hydration.....	72
Figure 5.8 SEM micrograph of T3PC (3 wt. % PCL) after 8 h hydration.....	72
Figure 5.9 SEM micrograph of T3CP after 72 h hydration.....	73
Figure 5.10 XRD diffractograms of hydration products of T3CP, T6CP and T9CP (3, 6 or 9 wt. % PCL) pellets.....	75

Figure 5.11 SEM micrographs of hybrid pellets of T3CP, T6CP and T9CP (3, 6 or 9 wt. % PCL) (top line), and their hydration products (bottom line).....	75
Figure 5.12 FTIR spectra of PCL, TCP and hybrid TCP:PCL pellets; T3CP, T6CP and T9CP (3, 6 or 9 wt.% PCL) before hydration.....	77
Figure 5.13 FTIR spectra of TCP and hybrid TCP:PCL pellets; T3CP, T6CP and T9CP (3, 6 or 9 wt.% PCL) after hydration (at 37 °C).....	77
Figure 5.14 Diametral compressive strength of TCP and hybrid TCP:PCL pellets; T3CP, T6CP and T9CP (3, 6 or 9 wt.% PCL) (a) before and (b) after hydration.....	79

LIST OF ABBREVIATIONS

α -TCP	alpha tricalcium phosphate
HAp	hydroxyapatite
CDHAp	calcium deficient hydroxyapatite
PCL	polycaprolactone
CSH	calcium sulfate hemihydrate
CSD	calcium sulfate dehydrate
TTCP	tetracalcium phosphate
OCP	octa calcium phosphate
ACP	amorphous calcium phosphate
MCPM	monocalcium phosphate monohydrate

CHAPTER 1

INTRODUCTION AND LITERATURE REVIEW

1.1 General introduction and rationale of the thesis

Various metals, ceramics and polymers have been used in biomedical applications as bone implants, bone fracture fixation and bone defect filling devices. The main issue of designing these devices is achieving biocompatibility with comparable structural and mechanical properties with those of bone.

Small defects originated by factors such as traumas, natural aging and tumor removing operations have been augmented by natural and synthetic bone cements for many years. Bone cements that inserted into the defect by molding or injecting as in paste form exhibits self-setting nature and converts into a hardened mass after operation. The first generation bone cements were polymeric polymethylmethacrylate (PMMA) cements that is formed by polymerization reaction of MMA monomer. However, their highly exothermic polymerization reaction and release of unreacted MMA monomer pose a risk of bone necrosis. Despite these limitations, PMMA is currently the most widely used bone cement. On the other hand, bioactive and totally resorbable candidates are more promising for bone cement applications to be able to adhere natural bone and induce new bone formation. In this respect, calcium phosphate cements had been developed and have been used clinically as an alternative.

Calcium phosphate cements are classified according to their cement-end products; apatite and brushite cements. The inorganic mineral phase of natural bone is a carbonated, calcium deficient form of hydroxyapatite (HAp, $\text{Ca}_{10}(\text{PO}_4)_6(\text{OH})_2$). Apatite cement's chemical and structural resemblance to natural bone is the main motivation of their common use. Although there are various combinations of calcium phosphate compounds yield in apatite cement end product, α -tricalcium phosphate

(α -TCP, α -Ca₃(PO₄)₂ with its ability to harden into calcium deficient hydroxyapatite (Ca₉(HPO₄)(PO₄)₅(OH), CDHAp) from a single solid precursor is commonly preferred, especially in non-load bearing parts. Moreover, its cement end product, CDHAp resembles to natural bone more than the stoichiometric one in terms of chemistry and microstructure. This superior resemblance provides better integration with bone tissue. Furthermore, CDHAp with higher solubility than HAp degrades completely with clinically relevant time and provide new bone tissue generation.

Despite their good biological properties, cement end product of α -TCP as all calcium phosphate compounds exhibit poor mechanical properties especially fracture toughness with respect to natural bone, due to their ceramic origin. In order to attain mechanical properties similar to those for bone, a natural composite, processing of α -TCP based composite cements is a common strategy. Mainly by reinforcing α -TCP with inorganic compounds such as glass, alumina, calcium sulfates and biodegradable polymers such as polylactic acid ((C₃H₄O₂)_n, PLA), polyglycolide ((C₂H₂O₂)_n, PGA), polycaprolactone, ((C₆H₁₀O₂)_n, PCL), improving it's mechanical properties can be realized.

Another issue of α -TCP cements is slow cement reaction kinetics. It's complete conversion into CDHAp occurs slower than clinical requirements in as-synthesized conditions. Reaction time can be modified by controlling particle size of α -TCP, chemistry of reactant solution, reaction temperature, crystallinity and certain additives [Bohner, 2000]. Moreover, other phases incorporated to α -TCP for improving other cement properties should not deteriorate hydraulic reactivity.

In this thesis, phase pure and reactive α -TCP powders were synthesized. It was converted into CDHAp by cement-type reaction at near physiological temperature. Effect of particle size and specific surface area on reactivity of α -TCP was elucidated. In order to improve mechanical properties, an inorganic calcium sulfate hemihydrate (CaSO₄.1/2H₂O, CSH) and an organic (PCL) reinforcing agent were incorporated into α -TCP with varying amounts. α -TCP:CSH and α -TCP:PCL hybrid blends with various compositions were prepared. Comparative study was performed for both composite systems in terms of their mechanical properties and reaction kinetics.

Complete characterization (phase identification, morphological investigation, chemical and mechanical properties) were performed on all cement systems before and after hydration.

1.2 Related previous knowledge

1.2.1 Structure and properties of natural bone

Bone is a mineralized tissue with the primary function of load carrying and load transmission. It is a hierarchical composite material with three main constituents; calcium phosphate mineral (69 wt. %), collagen (20 wt. %), water (9 wt.%) [Park, 2008].

Main organic phase of bone is Type I collagen; however, there are more than two hundred other non-collagenous proteins and organics such as lipid and polysaccharides. Other organics only comprise of 10 % of total organic part of bone. Type I collagen typically 80-100 nm in diameter is present as fibrils in bone. Each fibril develops from 1000 amino acid long three polypeptide chains. Fibrils wound together in a triplehelix with cylindrical shape approximately 1.5 nm in diameter and 300 nm in length. Furthermore; fibrils packed in arrays create larger fiber structures as shown in Figure 1.1 [Weiner and Wagner, 1998]. Schematic representation of hierarchical structure of bone is also illustrated in Figure 1.1. In organic part of bone, blood vessels are also found. Three dimensional organic matrix of bone is reinforced by inorganic mineral part.

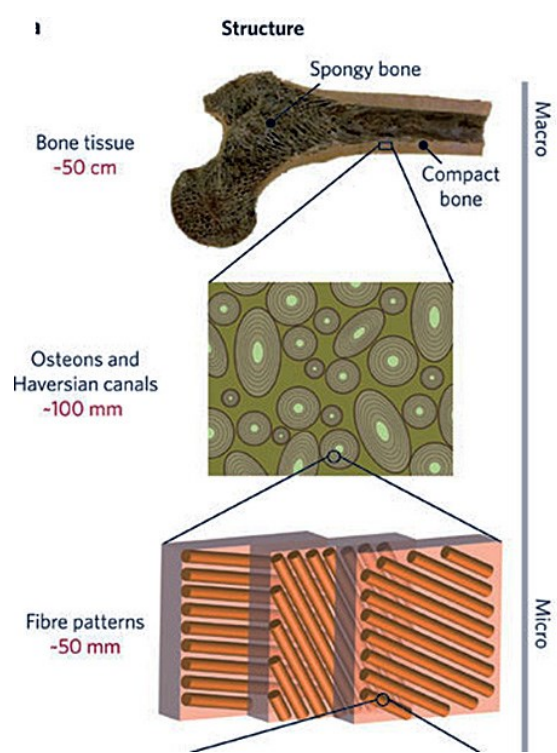
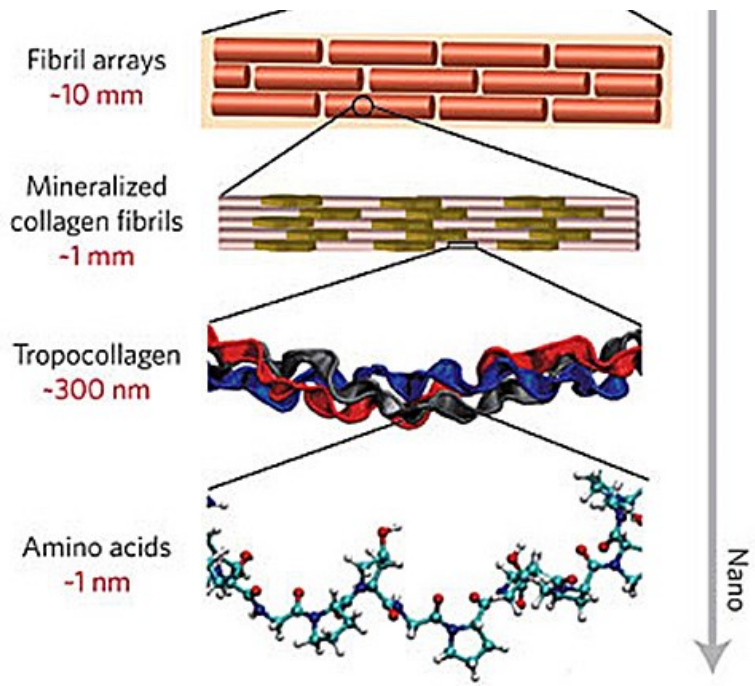


Figure 1.1 A schematic illustration of hierarchical structure of bone [Ritchie, 2011].

The mineral part of bone is submicroscopic crystals of biological apatite which are arranged parallel to collagen molecules. There are also other ions such as fluoride (F), citrate ($C_6H_5O_7^{4-}$), hydroxyl (OH^-) and carbonate (CO_3^{2-}) [Kokubo, 2008]. This apatitic calcium phosphate bone mineral differs from synthetic apatite in terms of stoichiometry (Ca/P ratio), crystal sizes and morphology [Dorozhkin, 2011]. Hap crystals found in the collagen fibers, named as dahhlite, are in calcium deficient ($Ca/P < 1.67$) and carbonated form $(Ca_{(10-x-y)}(HPO_4)_x(CO_3)_y(PO_4)_{(6-x-y)}(OH)_{(2-x-y)})$ as plate-shaped around the nanometric levels with values of 30–50 nm in length, 15–30 nm in width and 2–10 nm in thickness [Weiner and Wagner, 1998; Dorozhkin, 2011].

The third major component, water, is found within the fibrils, between the triple helix molecules and in the gaps. Structural properties of bone including porosity amount, mineral concentration, crystal size determines its load carrying ability. Bone with higher mineral content exhibits better supporting while the one with higher collagen content shows better flexibility [Dorozhkin, 2009]. Porosity is also important on mechanical load carrying abilities.

Depending on porosity level, bone can be categorized as cortical (dense) and cancellous (spongy). Generally, bone has a dense outer layer on internal porous structure. Compact bone consists 5-10 vol.% porosity with pore size varying between 1-100 μm . On the contrary, cancellous bone has 50-90 vol.% porosity even visible to naked eye and pore size of 200-400 μm [Dorozhkin, 2009; Weiner and Wagner, 1998]. Dense bone consists Haversian channel, canaliculi, Lacunae and Volkman's channels. As also represented in Figure 1.1, collagen fibers form lamellar sheets and lamellas form osteon around Haversian channel. Owing to its huge reservoir of calcium and orthophosphate ions, nanocrystalline apatite experience dynamic remodelling process which is continuous resorption and formation of nanodimensional apatite by osteoclasts (bone resorbing cells) and osteoblasts (bone forming cells), respectively [Kokubo, 2008; Lieberman and Frienlander, 2005]. In this way, bone regenerate and recover microdamages and microcracks by itself. Factors such as trauma, tumor removing operations or natural aging cause bone tissue failure that bone cannot recover itself. In such cases natural or synthetic bone graft materials are used to provide structural support by filling the bone defects and fixation of severe bone fractures.

1.2.2 Bone grafts

Natural bone grafts can be classified as; xenografts, allografts and autografts according to their origin. Grafts transplanted from one species to another species are named as xenografts. Due to viral infection risk after implantation, its low osteogenic (derived from bone forming tissue) nature and rapid resorption rate, xenografts usage is limited [Nandi et al., 2010].

Another graft type is allografts, tissue transplanted between individuals of the same species with different genetic composition. The risks of xenografts are also valid for this type of grafts. Tissues transferred from patient's body's different part are named as autograft. This type of grafts is considered as gold standard with minimum immune response risk, containing viable osteogenic cells and bone matrix proteins. In this way, autografts are osteoconductive (the ability of connecting to natural bone with chemical bonding), osteoinductive (the ability to induce new bone formation) and support bone growth. However, limited availability and harvest site morbidity limits its application.

Limitations of natural bone grafts have induced development of synthetic bone grafts which are promising owing to the fact that they can be malleable and fit to specific requirement of a certain application [Hench and William, 1984]. A variety of materials have been developed as synthetic bone analogs. Metals and alloys such as stainless steel, cobalt-chromium alloys and titanium alloys have been used in load bearing applications owing to their high toughness and strength. However, they are bioinert and do not exhibit osteoconductivity, osteoinductivity and osteointegration. They are limited for use in irregular defect filling operations.

1.2.2.1 Bioinert ceramics

Alumina (Al_2O_3) and yttria stabilized zirconia (Y-TZP) are in the class of tunable bioinert ceramic materials commonly used in biomedical applications. They do not

form chemical bond with natural bone and do not provide osteointegration. When they are implanted into the body, they form only mechanical interlocking with bone tissue.

Highly pure (99.9%) Al₂O₃ bioceramics are commonly preferred in articulating surfaces in orthopedic applications owing to their high hardness, low friction coefficient and high wear resistance [Hench, 2008]. They are also used as porous coatings on femoral stem and knee prosthesis. However, high brittleness of alumina induced development of Y-TZP ceramics which exhibit fracture strength of 1000 MPa and fracture toughness of 6-10 MPa.m^{1/2} [Park, 2008]. Y-TZP is mostly used in dental applications and also regarded as second generation of hip joint heads with relatively low wear rates. However, stress induced tetragonal to monoclinic transformation of zirconia may occur at the surface of implant in touch with body fluid which results in microcracking and progressive degradation. In order to overcome their drawbacks, Al₂O₃-ZrO₂ composites are favorable in biomedical applications [Kokubo, 2008].

1.2.2.2 Calcium sulfates

Calcium sulfates use as augmentation material by Dreesman goes back to 1892 to erase bone cavities sourced by tuberculosis and further developed by Peltier in following years [Peltier, 1961]. Depending on the water amount within a unit cell, calcium sulfate exists in anhydrate, dihydrate and hemihydrate forms [Kim, 2003]. Calcium sulfate is used in bone defect filling applications both as solid but more preferentially cement form. Calcium sulfate hemihydrate (CSH) converts into calcium sulfate dihydrate (CSD) when mixed with aqueous solutions via below highly exothermic cement-type reaction;



Reaction product, CSD, consists interlocking needle crystals which gives hardness to putty and has large surface area due to high porosity amount [Singh, 2007]. Porous macrostructure of calcium sulfate cements enables ingrowth of new bone tissue but the concern regarding this graft material is fast resorption rate before new tissue generation as reported by Thomas and Puleo [Thomas, 2008]. Moreover, CSD

dramatically loses mechanical properties upon degradation. Therefore, CSD generally is not used alone but with other bone graft materials [Singh, 2007].

1.2.2.3 Calcium phosphate ceramics

Calcium phosphate ceramics which are a class of chemically tunable bioactive compounds, have been studied and imparted as bone repair materials for almost 80 years. In 1920, Albee and Morrison examined the efficiency of calcium phosphates as bone substitutes by *in vivo* implantation of tricalcium phosphate into animals [Albee and Morrison, 1921]. In succeeding years, different calcium phosphate compounds' healing efficiency were examined. First implantation of hydroxyapatite was performed by Ray in rats and guinea pigs in 1951 [Ray et al., 1952]. After long term experiments, in 1970's, other calcium phosphates but mainly HAp were synthesized characterized and tried in medicine [Bohner, 2000]. In Table 1.1, the list of existing calcium phosphate compounds with Ca/P ratio varying between 0.5-2.0 are present.

Their chemical and structural resemblance to the natural bone and teeth is the main motivation of calcium phosphate usage as bone substitute materials. Due their bioactive nature, CaP's slowly degrade when inserted into human body. In this way, between the graft materials and bone tissue, a natural apatitic interface will be formed at atomic level. This physicochemical bond termed as osteointegration increases the stability of graft material under mechanical loading conditions.

Table 1.1 List of existing calcium phosphate compounds with various Ca/P ratio

Compound	Chemical Formula	Ca/P Ratio
Monocalcium phosphate monohydrate	$\text{Ca}(\text{H}_2\text{PO}_4)\cdot\text{H}_2\text{O}$	0.5
Monocalcium phosphate	$\text{Ca}(\text{H}_2\text{PO}_4)$	0.5
Dicalcium phosphate dehydrate	$\text{CaHPO}_4\cdot 2\text{H}_2\text{O}$	1.0
Dicalcium phosphate	CaHPO_4	1.0
Octacalcium phosphate	$\text{Ca}_8(\text{HPO}_4)_2(\text{PO}_4)_4\cdot 5\text{H}_2\text{O}$	1.33
α-tricalcium phosphate	$\alpha\text{-Ca}_3(\text{PO}_4)_2$	1.5
β-tricalcium phosphate	$\beta\text{-Ca}_3(\text{PO}_4)_2$	1.5
Amorphous calcium phosphate	$\text{Ca}_x\text{H}_y(\text{PO}_4)_z\cdot n\text{H}_2\text{O}$	1.33-1.5
Hydroxyapatite	$\text{Ca}_{10}(\text{PO}_4)_6(\text{OH})_2$	1.67
Calcium-deficient hydroxyapatite	$\text{Ca}_{10-x}(\text{HPO}_4)_x(\text{PO}_4)_{6-x}(\text{OH})_{2-x}$	1.5-1.67
Tetracalcium phosphate	$\text{Ca}_4(\text{PO}_4)_2\text{O}$	2

Some of the CaP compounds are biodegradable which means they will be completely dissolved in body and allow new natural tissue formation. Depending on the desired properties of application; a resorbable or bioactive CaP compound is used. Molar Ca/P ratio, solubility and acidity/basicity are the most important parameters of calcium phosphate compounds. By considering their solubility value, *in vivo* behaviour of calcium phosphates can be predicted. To illustrate, a CaP compound with relatively higher solubility than the mineral part of bone will be degraded [Bohner, 2000]. In Figure 1.2, solubility isotherms of CaP compounds in water are shown.

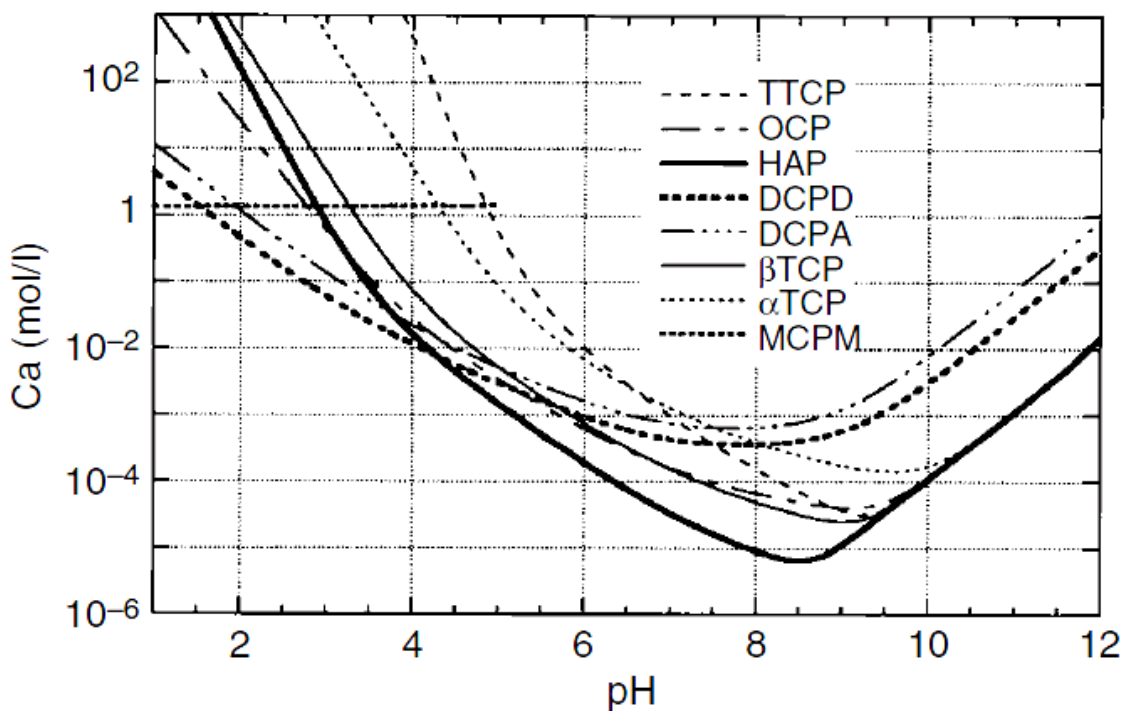


Figure 1.2 Solubility isotherms of various calcium phosphates in water [Dorozhkin, 2013]

As illustrated in Figure 1.2, stoichiometric HAp is the most stable compound in aqueous media in $\text{pH} > 4.2$ conditions. Its high stability yields in low degradation rates *in vivo* which makes it a long-term implant.

Generally, the lower Ca/P ratio yields in higher solubility and more acidity in water. Therefore; due to their high solubility and acidity, CaP compounds with Ca/P ratio lower than 1 are not suitable for medical applications. Monocalcium phosphate

monohydrate ($\text{Ca}(\text{H}_2\text{PO}_4)\cdot\text{H}_2\text{O}$) and monocalcium phosphate ($\text{Ca}(\text{H}_2\text{PO}_4)$) with a Ca/P ratio of 0.5 and tetracalcium phosphate (TTCP) with a Ca/P ratio of 2.00 are not used alone as bone graft substitutes due their high acidity and basicity; respectively [Dorozhkin, 2012]. However, they can be made suitable for implantation into body by combining with other calcium phosphates. Among various CaP compounds listed in Table 1.1, HAp and TCP based products are the most frequently used ones.

1.2.2.4 Hydroxyapatite

After years from the first tricalcium phosphate implantation, separate studies of de Groot [de Groot, 1980], Jarcho [Jarcho, 1981] and Aoki [Aoki et al., 1977] resulted in commercialization of synthetic and non-sintered HAp. Synthetic HAp is currently used as bone repair and regeneration material in granule, block and scaffold forms by itself and composite formulations mainly in non-load bearing parts [Kokubo, 2008].

Stoichiometric and pure HAp, $\text{Ca}_{10}(\text{PO}_4)_6(\text{OH})_2$, has a 1.67 Ca/P ratio and has a hexagonal crystal structure space group, $\text{P6}_3/\text{m}$. It is a highly crystalline and the most stable CaP compound in aqueous solutions [Bohner, 2000]. Synthetic HAp powders can be obtained via various methods including both high temperature and low temperature methods such as solid-state reaction, hydrothermal reactions, sol-gel method and hydrolysis reaction [Kokubo, 2008; Dorozhkin, 2011]. Dense HAp granules or blocks with porosity amount not exceeding 5 vol % is prepared by compacting HAp powders with 60-80 MPa pressure and sintering at a temperature between 950-1300 °C [Kokubo, 2008].

Despite their bioactive nature, dense and highly crystalline HAp behaves as a bioinert material. In order to improve bioactivity and also mimic the micro-and macroporous architecture of the mineral phase of the living bone; porous HAp scaffolds are prepared by incorporation of porogens such as naphthalene [Hubbard, 1974], foaming [Hattori and Iwadata, 1990], gel casting [Ramay and Zhang, 2003] and rapid prototyping techniques [Wilson et al., 2004]. Porous HAp structure with relatively higher surface area also promotes vascularization and tissue ingrowth by providing mechanical fixation and more sites for chemical bonding with bone [Tancred et al., 1998].

However, porosities deteriorate mechanical properties by lowering strength values and resulting in high brittleness. Bending, compressive and tensile strength values of dense HAp are 38-250 MPa, 120-900 MPa and 38-300 MPa. However, these decreased to 2-11 MPa, 2-100 MPa and ~3 MPa in the porous scaffold case [Suchanek and Yoshimura, 1998].

1.2.2.5 Calcium-deficient hydroxyapatite

Calcium deficient hydroxyapatite has a non-stoichiometric chemical formula $\text{Ca}_{(10-x)}(\text{HPO}_4)_x(\text{PO}_4)_{6-x}(\text{OH})_{2-x}$ where x changes between 0 and 1. CDHAp is commonly synthesized by wet precipitation techniques at $\text{pH} > 7$ and low temperature conditions from metastable CaP precursors such as amorphous calcium phosphate and α -tricalcium phosphate [Dorozhkin 2012; Bohner 2000]. Calcium deficiency which is an imperfection in the structure yields in less stability and higher solubility. CDHAp with relatively higher surface area of 25-100 m^2/g exhibits high dissolution rate which makes it propitious in temporary bone graft applications [Dorozhkin 2012]. An *in vivo* study performed by Bourgeo *et al.* revealed that CDHAp completely degrades within two weeks and induce rapid bone colonization [Bourgeois *et al.*, 2003].

1.2.2.6 Tricalcium phosphate

Tricalcium phosphate has three polymorphs; α' -TCP, β -TCP and α -TCP. Phase diagram illustrated in Figure 1.3 belongs to CaO- P_2O_5 system. α -TCP is the room temperature stable phase existing up to 1125 °C. Tricalcium phosphate exist in α -TCP form between 1125-1430 °C and α' -TCP above 1430 °C [Camire, 2011].

As illustrated in Figure 1.2, stoichiometric HAp is the most stable compound in aqueous media in $\text{pH} > 4.2$ conditions. Its high stability yields in low degradation rates *in vivo* which makes it a long-term implant.

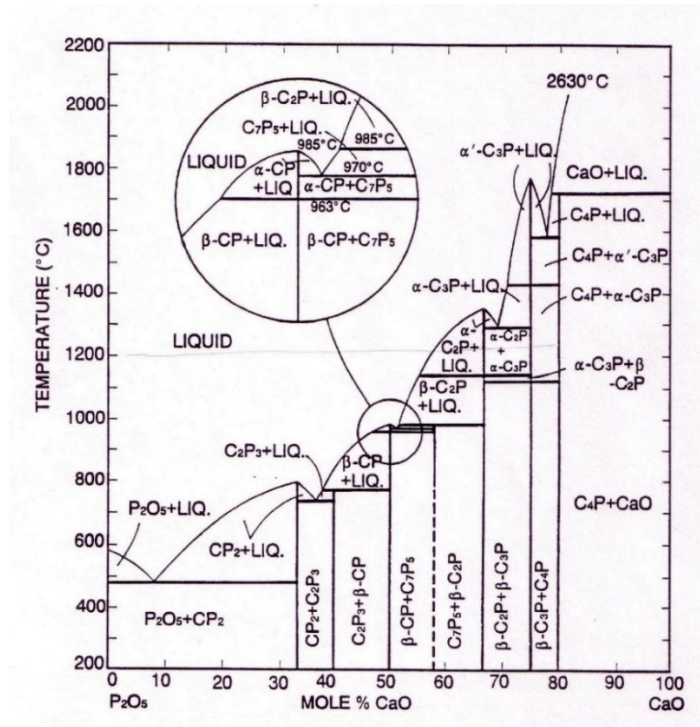


Figure 1.3 CaO-P₂O₅ binary phase diagram [Kokubo, 2008].

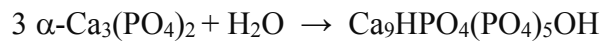
Despite their same chemical composition, their structure, density, solubility and therefore clinical applications are different. Among three polymorphs, α -TCP and β -TCP are frequently used in dental implants, orthopedics and maxillo facial applications. While α -TCP is commonly used as components of mono or biphasic bioceramics and composites, α -TCP is generally preferred as powder component of bone cements owing to its cement type reactivity.

1.2.2.7 α -Tricalcium phosphate (α -TCP)

α -TCP is a high temperature stable phase that is found at room temperature as metastable. Therefore; synthesis of phase pure α -TCP is a concern. α -TCP with a Ca/P ratio of 1.5 can be synthesized via high temperature techniques mainly by thermal transformation of an already obtained CaP with the same Ca/P ratio or solid state reaction of calcium and phosphate precursors [Camire, 2011]. Camire et al. synthesized α -TCP by firing CDHap formed by precipitation of a Ca(NO₃)₂ and (NH₄)₂HPO₄ solution, at 1250 °C for 2 h [Mathew et al., 1977]. α -TCP is also formed by heating α -TCP above 1125 °C followed by quenching [Monma et al., 1983].

Beside thermal transformation, solid-state synthesis of α -TCP is also a commonly used technique. $\text{CaCO}_3 : \text{CaHPO}_4$, $\text{CaCO}_3 : (\text{NH}_4)_2\text{HPO}_4$ and $\text{CaCO}_3 : \text{Ca}_2\text{P}_2\text{O}_7$ are mostly used precursor formulations yielding in α -TCP. Solid precursors milled together to obtain smaller particles and increase reaction surface area then fired at a temperature between 1200-1500 °C for 2-48 h and quenched to prevent reverse transformation [Camire, 2011].

When highly soluble α -TCP owing to its relatively loosely packed structure dissolves, it precipitates into the most stable CaP compound, HAp. This conversion is thermodynamic basis of α -TCP bone cements.



1.2.3 Bone cements

Bone cements are self setting, injectable or moldable systems allowing filling irregular shape bone defects without processing. They are formed by mixing one or more solid phase with a liquid reactant which sets into a viscous paste first and turns into a solid and hardened mass.

Setting time, injectability, degradability, microstructure and mechanical properties are the most important characteristics of a bone cement. Setting time is the time when cement paste loses its plasticity and harden. The optimum time for setting is between 5-15 min. Injectability, the ability of a cement paste to be extruded through a needle without solid liquid phase separation, is required for the ease of adequate filling operations of irregularly shaped defects. Degradation rate is another important issue for cements which should be low enough to allow natural bone tissue formation and high enough not to impair bone healing. Moreover, bone cements should consist a certain amount of macroporosity which facilitate bone colonization and tissue ingrowth. Firstly, poly (methyl methacrylate) (PMMA) was introduced and has been used as a bone cement. By polymerization of liquid monomer around pre-polymerized powders, hardened and self-setting PMMA cement was obtained [Albee and Marrison, 1920]. However, highly exothermic polymerization reaction of PMMA results in

temperature increase up to 67-124 °C and thermal necrosis of bone. Moreover, due to release of unreacted MMA monomer, there is also risk of chemical necrosis [Haldeman and Moore, 1934; Ray et al., 1952]. Furthermore, bioactive and totally resorbable candidates are more promising for bone cement applications to be able to adhere natural bone and induce new bone formation.



Figure 1.4 An injectable bone cement system [Retrieved from: <http://earlsview.com/2011/06/25/bone-cements-not-all-work-well/> Last accessed on 29.08.2014].

1.2.3.1 Calcium phosphate cements

Calcium phosphate cements (CPC) were first reported by Monma and Kazanowa in 1976 [Kokubo, 2008]. Initial report on CPC's was including setting reaction of α -TCP to CDHAp with Ca/P ratio of 1.5 when hydrated at 60-100 °C and pH between 8.1-11.4. Despite their first finding goes back to 1976, long setting time postponed their medical use. In 1982, CPC were reported as a dental restorative material candidate by Le Geros et al. In 1986, Brown and Chow formulated a bone cement that is the mixture of dicalcium phosphate and tetracalcium phosphate set in 30-60 min at physiological conditions to form an apatitic product. After invention of apatitic cements, brushite cements were reported by La Maitre consisting α -TCP and monocalcium phosphate monohydrate (MCPM) or phosphoric acid in 1987 [Dorohkin, 2012].

Calcium phosphate cements consist one or more calcium phosphate powder(s) and mixed with liquid phase. After the hardening reaction, cement mixture turns into a solid mass. Setting reaction of calcium phosphate cements initiates with dissolution of initial compounds and supplying calcium and phosphate ions into the solution. Then it is followed by precipitation of cement end product which determines the *in vivo* biodegradability of cement [Bohner, 2000; Durukan and Brown, 2000].

In the 1990's 15 different binary combinations of CaP compounds were established which set at body temperature into solid/hardened product upon mixing with aqueous solutions. Despite the diversity of combinations, according to solubility data provided in Figure 1.3, calcium phosphates yield only two end products; precipitated and poorly crystalline apatite when $\text{pH} > 4.2$, brushite when $\text{pH} < 4.2$. When pH value is lower than 1.5, thermodynamically stable phase is MCPM. However; due to its high acidity and solubility, fabrication of MCPM cements are not attempted [Kokubo, 2008; Dorozhkin, 2012]. In Table 1.2, a list of some commercial calcium phosphate cements are given:

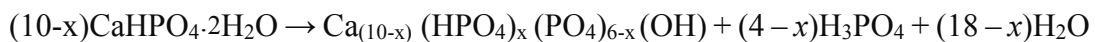
Table 1.2 The list of some commercial self-setting calcium orthophosphate formulations with the producer, product name, composition (when available) and main end-product. The end-product of the reactions can be either an apatite (CDHAp, carbonate apatite, *etc.*) or brushite (=DCPD) [Bohner, 2010].

Producer	Commercial Name	Composition	Product
Merck (GER) Biomet (U.S.A.)	Biocement D	Powder: 58% α -TCP, 24% DCPA, 8.5% CaCO_3 , 8.5% CDHA; Solution: 4 wt% Na_2HPO_4 in water	Apatite
Stryker(U.S.) Leibinger (Germany)	BoneSource™	Powder: TTCP (73%), DCPD (27%); Solution: H_2O , mixture of Na_2HPO_4 and NaH_2PO_4	Apatite
DePuy Synthes (U.S.A.)	Norian® SRS	Powder: α -TCP (85%), CaCO_3 (12%), MCPM (3%); Solution: H_2O , Na_2HPO_4	Apatite
DePuy Synthes (U.S.A)	ChronOS™ Inject	Powder: β -TCP (73%), MCPM (21%), $\text{MgHPO}_4 \cdot 3\text{H}_2\text{O}$ (5%), MgSO_4 (< 1%), $\text{Na}_2\text{H}_2\text{P}_2\text{O}_7$ (< 1%); Solution: H_2O , Na hyaluronate (0.5%)	Brushite
Teknimed (France)	Cementek®	Powder: α -TCP, TTCP, Na glycerophosphate; Solution: H_2O , $\text{Ca}(\text{OH})_2$, H_3PO_4	Apatite

1.2.3.2 Brushite cements

β -TCP + MCPM [Lemaître et al., 1987], β -TCP + H_3PO_4 [Bohner et al., 1996] and TTCP + MCPM + CaO [Constantz et al., 1998] are proposed brushite cement formulations [Dorozhkin, 2012]. Setting of brushite cements only take places by acid-base interaction. Due to the fact that precipitation of brushite can only occur when $pH < 6$; the paste of brushite cements is acidic while it is setting [Bohner et al., 1997; Elliott, 1999]. If basic compound of brushite cement is in excessive amount, intersection of the solubility isotherms of the basic phase with brushite determines the equilibrium pH value. The more basic CaP compounds have the less solubility in aqueous media. Since the setting reaction of cements starts with dissolution of initial compounds, the setting time depends on the solubility of the basic phase. If basic phase of the cement has higher solubility, setting time would be relatively short. To illustrate, HA+MCPM, α -TCP+MSPM, α -TCP+MCPM mixtures set in several minutes, 30-60 seconds and a few seconds; respectively. Improvement of workability of brushite cements by lowering their setting reaction kinetics are performed by chondroitin 4 sulfate [Marino et al., 2007], glycolic acid [Marino et al., 2007] and citric acid additions [Sarda et al., 2002].

Brushite has higher solubility with respect to apatite and it is stable under physiological conditions at $pH= 7.4$. Therefore; their high *in vivo* degradation rate cause rapid decrease in strength. Via following reaction a partial transformation to CDHAp was reported.

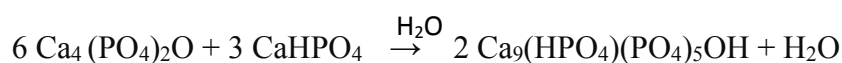


Brushite cements create an acidic environment during dissolution and conversion into CDHAp. *In vivo* and *in vitro* studies showed that acidic environment created by small quantities of brushite can be tolerated by bone tissue [Constant, 1998]. However, in the case of large quantities, tissue inflammation within the first weeks of implantation was reported due to release of phosphoric acid [Dorozhkin, 2011].

1.2.3.3 Apatite cements

Apatite cements consist a poorly crystalline HAp or calcium deficient HAp as hardening reaction product. There are two types of cement reactions yield in apatite cement products; cement mixtures of multiple solid precursors and hydrolysis of metastable CaP [Dorozhkin, 2011].

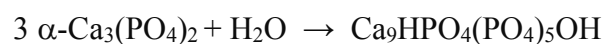
The setting reaction of this group occurs via acid-base reaction. An acidic CaP powder reacts with a relatively basic CaP in aqueous media and form a neutral CaP solid mass. Cement mixture formulations of TTCP and CaHPO₄ by Brown and Chow in 1986 is a typical example of this class of apatite cements [Brown and Chow, 1986].



By changing stoichiometric ratios of acidic and basic CaP compounds, both stoichiometric and calcium deficient forms of HAp can be obtained. TTCP and DCPA dissolve when mixed with liquid phase and supply Ca²⁺ and (PO₄)³⁻ ions to the solution. An issue of that Brown and Chow formulation is different solubility rates of two components. TTCP with Ca/P ratio of 2 dissolves rapidly and supplies more calcium ions to the solution than required for HAp precipitation. HAp formation takes place only if both Ca²⁺ and (PO₄)³⁻ ion concentrations are sufficient. Therefore; dissolution rate of DCPA and supplying required amount of (PO₄)³⁻ to the solution act as rate determining step for cement hardening. Setting time of apatite cement is also longer with respect to brushite cements. When DI water or saline solution are used as liquid phase, setting time of TTCP+DCPA cement mixtures was reported as 30-60 min which is not suitable for clinical use [Kokubo, 2008]. Ishikawa et al. reported a decrease in setting time of cement in the presence of hydrogen phosphate aqueous solution owing to their supply of phosphate ions [Ishikawa et al., 1995]. TEM analysis

of TTCP and DCPA powders mixed in a phosphate containing solution revealed that TTCP dissolves rapidly and dissolved Ca^{2+} and $(\text{PO}_4)^{3-}$ ions react with ions already existing in the solution and precipitate into HAp preferentially on the top of DCPA surfaces. As reaction progresses, linked DCPA particles via extensively grown apatite crystals and bridged TTCP particles were observed. Initially precipitated low crystalline HAp acts as seeding agent for precipitation of interlocked high crystalline HAp resulting in hardening [Chen et al., 2003].

This second type of calcium phosphate cement reaction is when the reactant and product have the same Ca/P ratio. The typical example of this class and also focus of this study is α -TCP cements that were invented by Monma and Kazanawa in 1976 [Monma and Kazanawa, 1976]. In aqueous media, α -TCP dissolves and precipitates into CDHAp via aforementioned reaction;



Cement reaction of α -TCP takes place in two main progressive stages; dissolution of α -TCP precursor and precipitation of HAp via nucleation and growth. The reaction product CDHAp forms in solid and hardened mass; resembles to natural bone more than the stoichiometric one in terms of microstructure and chemistry [Dorozhkin, 2011]. Figure 1.5 summarizes cement-type reaction and morphological properties for apatite and brushite cements.



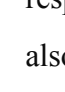
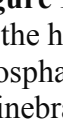
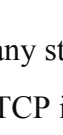
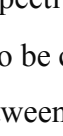
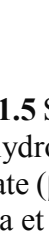
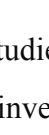
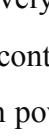
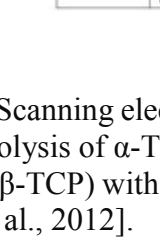
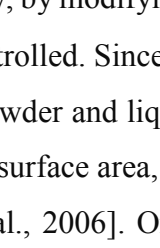
		Apatite cements		Brushite cements
		Single Component	Multiple Components	
Reactives		α -TCP	TTCP + DCPA/DCPD	β -TCP + MCPM/MCPA
Reaction		$3\alpha\text{-Ca}_3(\text{PO}_4)_2 + \text{H}_2\text{O} \rightarrow \text{Ca}_9(\text{HPO}_4)(\text{PO}_4)_7(\text{OH})$	$2\text{Ca}_3(\text{PO}_4)_2 + 2\text{CaHPO}_4 \rightarrow \text{Ca}_{10}(\text{PO}_4)_6(\text{OH})_2$	$\beta\text{-Ca}_3(\text{PO}_4)_2 + \text{Ca}(\text{H}_2\text{PO}_4)_2 \cdot \text{H}_2\text{O} + 7\text{H}_2\text{O} \rightarrow 4\text{CaHPO}_4 \cdot 2\text{H}_2\text{O}$
Type of Reaction		Hydrolysis	Acid-Base	Acid-Base
Setting mechanism and crystal morphology		 Initial α -TCP particles	 Initial TTCP/DCP particles	 Initial β -TCP/MCP particles
		 Dissolution - Precipitation	 Dissolution - Precipitation	 Dissolution - Precipitation
		 Final CDHA crystals	 Final HA crystals	 Final Brushite crystals
SEM			<div style="display: flex; align-items: center; justify-content: center;"> <div style="writing-mode: vertical-rl; transform: rotate(180deg);">APATITE</div> <div style="writing-mode: vertical-rl; transform: rotate(180deg);">BRUSHITE</div> </div>	

Figure 1.5 Scanning electron micrographs of set apatite and brushite cements obtained by the hydrolysis of α -Tricalcium phosphate (α -TCP) and by reaction of β -Tricalcium phosphate (β -TCP) with monocalcium phosphate monohydrate (MCPM), respectively [Ginebra et al., 2012].

Many studies have focused on setting and cement-type hardening reaction kinetics of α -TCP investigating effects of factors including temperature, chemistry, particle size, crystallinity and certain additives [Dorozkin, 2011; Bohner, 2007]. Since α -TCP to CDHAp cement-type reaction occurs with dissolution, nucleation and growth stages respectively, by modifying rates of these stages setting time and total reaction time can also be controlled. Since dissolution of α -TCP starts from surface, higher surface area between powder and liquid phase of cement yield in faster reaction kinetics. In order to increase surface area, long milling operations were performed [Bohner et al., 2006, Camire et al., 2006]. One limitation of this strategy is that powder size can not be decreased below a few micrometers [Camire et al., 2006]. Another approach to obtain nanosized calcium phosphate powders are flame synthesis [Lee et al., 1995] and precipitation techniques [Loher et al., 2005]. Dissolution reaction can be also accelerated by lowering pH value to 6-7 by Na_2HPO_4 , NaH_2PO_4 solutions as reactant solution [Bohner et al., 2007] and introducing surface defects and pits on material [Tang et al., 2001].

Second stage, nucleation of new CDHAp crystals, may be accelerated by introducing crystal nuclei such as stoichiometric or precipitated apatite which acts like nucleation site. In a study performed by Durucan and Brown, HAp nuclei was seeded to α -TCP and it was revealed that by seeding HAp between 1 wt.% and 5wt. % proportions shorten the hydration reaction [Durucan and Brown, 2002]. Another strategy which accelerates both nucleation and growth reactions is saturation of the mixing liquid with the presence of dissolved calcium and phosphate ions which phenomena named as common ion effect [Bohner, 2007].

1.2.4 Mechanical properties of calcium phosphate cements

Despite their good bioactivity and osteointegration, calcium phosphates suffer from lack of desired mechanical properties; low elasticity, low fracture toughness and unpredictable strength due to their ceramic origin. For bone graft materials in dental and orthopedic applications are subjected to a complex three dimensional load consisting bending, tension, compression and torsion. However, calcium phosphate cements only strong in compression. Another issue is initial mechanical properties of bone cements varies with implantation time. In vivo studies revealed that mechanical properties of apatite cements continuously increase as a function of implantation time while those brushite cements initially decrease and starts to increase after bone growth initiates [Ikenaga et al., 1998]. Apatite cement reach a tensile strength of 16 MPa [Camire et al., 2006] and compressive strength of 83 MPa [Lee et al., 1995]. Brushite cements exhibit relatively lower mechanical properties, a tensile strength of 10 MPa and a compressive strength of 60 MPa [Andrianjatovo et al., 1996]. Beside their low value, strength of calcium phosphate cements also shows large range of values which decreases their relatively and limits their applications [Dorozhkin, 2012].

1.2.4.1 Improving mechanical properties of calcium phosphate cements

Tensile strength and porosity level are related with a rule of thumb. Higher porosity levels in the material results in lower tensile strength [Bohner, 2000; Dorozhkin, 2011]. One approach to improve strength by lowering porosity amount is controlling liquid to solid ratio (L/S). High L/S ratio yields in higher porosity in the cement end

product and expedite crack initiation and propagation. By lowering excess amount of liquid, lowering the L/S ratio, higher strength values achieved. Hypothetically, a bone cement with zero porosity achieved a tensile strength of 103 MPa [Bohner et al., 2007]. However, bioresorbability and osteointegration concerns necessitate a certain amount of interconnected porosity.

1.2.5 Calcium phosphate cement based composites

In order to achieve mechanical properties of organic-inorganic composite structure of natural bone, single material alone is not satisfying. For this purpose, calcium phosphate cement based composites have been developed. Beside mechanical properties, reinforcing phases also effect cement properties such as setting times, injectability, cell adhesion and degradation rate etc. Two main approaches have been investigated and performed to improve mechanical and cement properties of calcium phosphates; reinforcing by inorganic additives and producing CaP-polymer composites; respectively. In previous studies; platelets, whisker and fiber reinforcements were examined.

1.2.5.1 Inorganic compound reinforced calcium phosphates

In order to improve mechanical properties of CaP's, calcium phosphate based biocomposites with inorganic reinforcements have been developed. Zirconia, alumina, titania, calcium sulfate, glass, various metals and alloys and silicon carbide are some of the inorganic additives have been investigated for this purpose. Most of these materials are bioinert; therefore, if they are used in significant amounts, biocomposites will be bioinert/bioactive. The ideal condition is imparting mechanical integrity to biocomposite without diminishing its bioactivity.

In a previous study, DCPA:TTCP cement with a flexural strength of 13 MPa was reinforced by carbon fibers with variable lengths [Xu et al., 2009]. Eventually, work of fracture increased and composites exhibited flexural strength between 32-59 MPa. Glass fibers were also used as reinforcing agent of CaP cements. An increase in elastic modulus, work of fracture and flexural strength was reported in consequence of short

and long E-glass fiber incorporation [Xu et al., 2000]. In another study performed by Gbureck et al., 80-100 MPa increase in compressive strength were achieved by incorporation of SiO₂ and TiO₂ particles [Gbureck et al., 2003].

Aforementioned compound, calcium sulfates (CS) have been used as component of CaP cement based composites. It's rapid degradation rates offers benefits in composite applications; since it creates pores in the structure and favors bone ingrowth and mechanical integrity. TTCP +DCPA cement mixtures with varying calcium sulfate addition were investigated in terms of setting time, mechanical properties and *in vitro* properties [Hu et al., 2000]. A slight decrease in setting times of CPC were observed in the presence of CS. Moreover, better cell proliferation, osteogenesis and faster degradation rates were achieved in composite cements with respect to pristine cement.

TCP/CS cement mixtures with both components exhibiting self setting nature, as also tried in this thesis, have been also studied. As reported by Nilsson et. al, fast absorption of CS in a TCP/CS mixture provide pores on the implant body that facilitate new tissue growth. Furthermore; it was stated that the mixture with excellent osteoconductivity exhibited improved properties without diminishing intrinsic properties of components [Nilsson et al, 2002]. In another study on α -TCP/CS cement mixture performed by Zhou et al., a significant decrease in the setting time of α -TCP was reported in the presence of low CS content. Moreover, with increasing CS concentration, improvement in the injectability of α -TCP cement was stated. In the same study, it was also shown that CS yielded in faster degradation rates by improving low degradation of α -TCP [Zhou et al., 2011].

1.2.5.2 Calcium phosphate-polymer composites

As mentioned earlier, bone is a natural organic/inorganic composite material. Therefore; polymer incorporation to calcium phosphate cements by polymers is promising for both improvement of mechanical properties and mimicking macrostructure of natural bone. Ceramics are too brittle and have high elastic modulus; while bone is a material exhibiting both high strength and toughness. Therefore; combination of bioactive ceramics with polymers suggests desirable

mechanical properties with high strength, toughness, deformability and relatively lower elastic modulus.

Since CaP cements consist a powder and a liquid phase, incorporation of polymer is performed by dissolving in liquid phase or as a solid additive to powder component of cement. Figure 1.6. illustrates preparation methods of calcium phosphate cement : polymer composites.

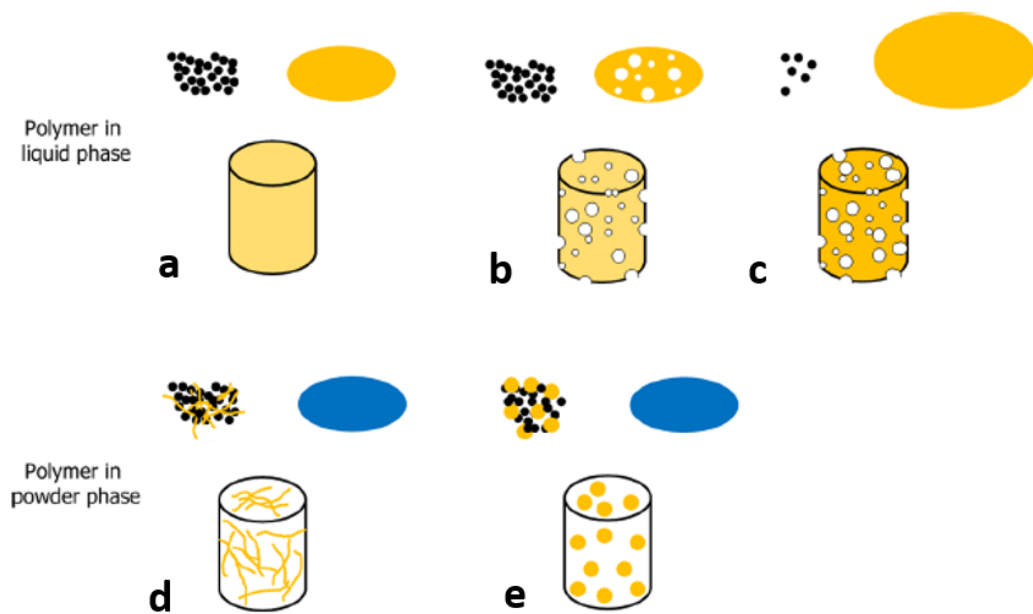


Figure 1.6 A schematic illustration of polymer incorporation into calcium phosphate cements a-b-c as dissolved in liquid phase d-e as solid additive to powder phase.

As illustrated in Figure 1.6a, dissolved polymer in solution can be mixed with powder and after cement setting, a continuous and homogeneous structure is obtained. CPC can also be obtained in macroporous form by foaming liquid phase and then mixing with powder as shown in Figure 1.6b. Incorporation of relatively small proportion of CPC powder in a relatively large polymer solution yields in slurry formation. After slurry is freeze-dried, again a macroporous CPC scaffold is obtained as illustrated in Figure 1.6c. Incorporation into powder phase may be performed with both fiber and powder polymers as shown in Figure 1.6 d and e.

Biomedically suitable polymers can be categorized as synthetic polymers and polymers with biological origin. While PLA, PGA, PCL are in the class of synthetic polymers, starch, alginate, chitosan, gelatin, cellulose, hyaluronic acid are those with biologic origin.

1.2.5.3 Calcium phosphate based composites with natural polymers

Gelatin which is a natural polymer with triple helix structure favoring cell adhesion has been studied in calcium phosphate cement based formulations. A fourfold increase in compressive strength of α -TCP cement was reported by Bigi et al. due to decreased amount of porosity. However, after a certain amount of gelatin incorporation, it was found that mechanical properties tend to decrease [Bigi et al., 2003]. An optimum amount of 2 wt. % for MCPM-CaCO₃, and 5 wt. % for α -TCP cements were determined in previous studies. Gelatin incorporation also increases paste viscosity and retards ion diffusion which results in increased setting times. For MCPM+ CaCO₃ and ACP+DCPD cements, increased setting times were reported.

Collagen is another natural polymer preferred as a CPC based composite constituent; since, it is also most abundant protein in organic part of natural bone. Incorporation of collagen improved cell adhesion of TTCP-DCPA, MCPM- β -TCP and α -TCP cements as evidenced by cell culture studies. Moreover, TTCP-DCPA cements with collagen incorporation exhibited relatively higher flexural strength and ten fold higher work of fracture with respect to pristine cement. Also, a slight increase in compressive strength of brushite cements was reported. Despite increased amount of collagen longers setting reaction, it does not exceed the range for medical applications [Moreau, 2009; Tamimi et al., 2008; Perez et al., 2012].

Chitosan, a polysaccharide with antibacterial properties, have been incorporating into different cement formulations including ACP-DCPD, α -TCP, TTCP, MCPM-CaCO₃, or DCPD-Ca(OH)₂ and increased their setting times [Yu et al., 2010; Xu et al., 2002; Carey et al., 2005; Wag et al., 2001; Rou et al., 2008]. In contrast DCPA-TTCP cement with chitosan addition exhibited shorter setting times and up to 15-20 wt. % chitosan improved its flexural and compressive strength [Sun et al., 2007]. Effect of chitosan

on setting times were investigated for ACP-DCPD, α -TCP, TTCP, MCPM-CaCO₃, DCPD-Ca(OH)₂ cements and increase in setting times were reported for all. Chitosan also affects degradation properties, lower degradation rates were stated for MCPM-CaO or DCPD-Ca(OH)₂ cements.

Cellulose is another natural polymer preferred as reinforcing phase of calcium phosphate cements. By variations in the monomer of cellulose, HPMC and CMC are obtained. Hydroxypropyl methyl cellulose (HPMC) incorporation has been studied for α -TCP-CaCO₃, DCPA-Ca(OH)₂, TTCP-DCPA, and TTCP-DCPD cement systems and enhancing dimetral tensile strength, work of fracture and compressive strength as increasing HPMC amount was reported. Moreover, increased setting times were observed for α -TCP-CaCO₃ and TTCP-DCPA cements [Takagi et al., 2003; Burguera et al., 2006; Cherng et al., 1998]. *In vitro* analyses revealed that CMC incorporation does not change biological properties of cements including cell proliferation.

1.2.5.4 Calcium phosphate based composites with synthetic polymers

Synthetic polymers incorporation into calcium phosphate cements suggest desirable properties, since their properties can be controlled and modified during their synthesis.

Polyamide 6.6, a non-resorbable polymer, exhibit high fracture strain (13%- 15%) and low elastic modulus (4 GPa) which yields in high fracture toughness [Beaudoin, 1990]. It's incorporation into α -TCP cement up to 8 wt. % in 3 mm length fibers increased compressive strength of pristine cement from 9.5 MPa to 12.5 MPa [Dos Santos et al., 2000]. Moreover, an increase in flexural strength of TTCP-DCPA cement reinforced with another class of polyamide, p-aramides from 13 MPa to 65 MPa was reported [Xu et al., 2000].

Polyesters are thermoplastic polymers containing ester functional group in their main chain. They are commonly preferred in calcium phosphate cement based composites owing to their biodegradable nature. Biodegradable polymer reinforcements provide extra porosity in addition to inherent porosities of calcium phosphate cements and enhance bone ingrowth and cell colonization.

PLLA fibers incorporated into α -TCP, CaHPO₄, CaCO₃, CDHAp cement mixture in 1-7 wt. %, progressively decreased setting time by absorbing liquid phase in cement and lowering L/S ratio. Moreover, an increase in total porosity amount was stated from pristine cement to cement with 7 wt. % PLLA fiber. PLLA also affects mechanical properties. Work of fracture of cement was increased from 10 J/m² to 258 J/m² by addition of 7 wt. % of PLLA fibers. Both flexibility of fibers and interaction between CPC matrix and polymer contributed to improvement in work of fracture [Zuo et al., 2010].

PLGA is another commonly used polyester that is a copolymer of glycolic and lactic acid. PLGA fibers in 8 mm length incorporated into TTCP-DCPA cements were investigated by in vitro studies and it was observed that fibers act as reinforcements within several weeks of implantation then degrade and form cylindrical macropores facilitates cell infiltration. In the same study, three times higher (25 MPa) flexural strength and two orders of magnitude work of fracture (34 kJ/m²) were reported [Xu and Quinn, 2002]. In another study, injectability of calcium phosphate cements reinforced with 5 m long PGA fibers with varying amount of 2.5- 7.5 vol. % were investigated. In the presence of PGA, higher injection forces were required independent from PGA composition. However; polymer amount more than 7.5 vol. % has not allowed injection [Xu et al., 2006].

Polycaprolactone, focus of this thesis, is another polyester considered as a long term implant owing to it's relatively longer degradation rate. PCL is a semicrystalline and hydrophobic biocompatible polymer synthesized by ring opening reaction of ϵ -caprolactone. It has a glass transition temperature (T_g) of -60 °C and melting point ranging between 59 and 64 °C. PCL releases non-toxic by products upon in vivo degradation and owing to it's slow degradation it does not create an acidic environment. Moreover, PCL exhibits higher fracture energy than most of the other biocompatible polymers. In a previous study α -TCP, CaHPO₄ and CaCO₃ cements reinforced by PCL exhibited shorter setting times with respect to pristine cement. Moreover, an increase in macroporosity amount was observed as a function of PCL content. Despite increase in work of fracture owing to fiber pullout and fiber matrix

interaction mechanisms, lower flexural strength and elastic modulus values in the presence of PCL was reported. Decrease in flexural strength was related to hydrophobic nature of PCL which prevent its well-integration into cement [Zuo et al., 2010].

1.3 Objective and structure of the thesis

One of the general objectives of this thesis is synthesis of phase-pure and reactive α -TCP, exhibiting high hydration efficiency in converting into hardened CDHAp by cement reaction. The secondary and somewhat more technical and specific objective was preparation of α -TCP based hybrid cement blends enabling acceptable cement type conversion for α -TCP and meanwhile improving mechanical properties of the final cement-type products. α -TCP was custom synthesized from calcium and phosphate precursors in solid state. α -TCP:calcium sulfate hemihydrate (CSH) and α -TCP:polycaprolactone (PCL) hybrid blends were prepared by solvent casting method and after hydration at 37 °C CDHAp:calcium sulfate dehydrate (CSD) and CDHAp:PCL composites were produced. The reaction kinetics and mechanical properties were examined in a parametric and comparative manner. Physical and chemical properties of products were also elucidated.

The experimental studies and results in the thesis are presented in four main chapters. *Chapter 2* gives the details in regard to experimental protocol and analytical work performed in the thesis. In the first results part (*Chapter 3*) α -TCP preparation methods and results for its cement behaviour has been introduced. α -TCP powders were synthesized by solid-state reaction between monetite and calcium carbonate. α -TCP powders with different particle size were hydrated with DI water at 37 °C and their conversion kinetics to CDHAp were evaluated. Complete characterization (phase identification, morphological investigations, chemical and mechanical properties) of α -TCP and it's hydration product have been performed.

The second part of the results focuses on preparation of α -TCP:CSH hybrid blends with varying CSH amount that hydrated into CDHAp:CSD composite cements. Cement-type reactivity of α -TCP in the presence of CSH elucidated in a comparative manner. Phase identification and morphological investigations were performed on α -TCP:CSH and CDHAp:CSD samples. Moreover, mechanical properties of hydrated and non-hydrated samples were evaluated to observe effect of CSH addition on mechanical integrity and fracture strengths of α -TCP and its cement end product. The related results are discussion have been given *Chapter 4*.

In the final part (*Chapter 5*), results related to properties of another composite blend has been introduced. α -TCP:PCL hybrid blends with varying PCL amount that hydrated into CDHAp:PCL composite cement were prepared. Effect of PCL on hydraulic reactivity of α -TCP were elucidated by direct comparison. Phase evaluations and morphological changes as a function of reaction time were analyzed for two selected cement systems for comparison purposes. Moreover, interaction between organic and inorganic constituent of cement system were examined by chemical analysis. Furthermore, the changes in mechanical properties of cement end products with various PCL content were investigated.

CHAPTER 2

MATERIAL CHARACTERIZATION AND EXPERIMENTAL PROCEDURE

The α -tricalcium phosphate (or α -Ca₃(PO₄)₂), α -TCP) used in this thesis was custom synthesized using proper starting materials of simple chemistry. This chapter presents the experimental details in regard to α -TCP synthesis and also processing of the two α -TCP based hybrid pre-cements; α -TCP:calcium sulfate hemihydrate (α -TCP:CSH) and α -TCP:polycaprolactone (α -TCP:PCL) blends. In both cases final hardened composite formation was achieved by cement type α -TCP→CDHAp conversion of powder or pre-shaped pellet forms of pre-cement blends. The analytical material characterization techniques used in the thesis and analyses details are also introduced in this chapter.

2.1 Materials

The calcium precursor was calcium carbonate (CaCO₃, reagent grade Merck, Germany) and phosphoric acid (H₃PO₄, reagent grade, 85% wt., Merck, Germany) was used as phosphorous source. The solid state synthesis of α -TCP was accomplished by firing stoichiometric amounts of CaCO₃ and chemically synthesized monetite (CaHPO₄) at 1200 °C for 2 h based on a previous study [Cicek et al., 2012].

In the first hybrid cement blend the additive was calcium sulfate hemihydrate or CSH, (CaSO₄·½H₂O) commercial grade product of Sigma-Aldrich, Germany). In the second hybrid blends an organic additive, a biodegradable polymer–polycaprolactone ((C₆H₁₀O₂)_n, PCL, Sigma-Aldrich, Germany) was used.

2.2 Experimental procedures

One of the precursors used in making α -TCP, CaHPO_4 , was chemically synthesized starting from CaCO_3 . First, calcium carbonate was calcined at $1010\text{ }^\circ\text{C}$ for 2 h to obtain CaO . 15.5 g CaO was hydrated with 100 mL excess de-ionized (DI) water at room temperature for 1 h and resultant $\text{Ca}(\text{OH})_2$ slurry was mixed with 31.75 g phosphoric acid at around $55\text{-}60\text{ }^\circ\text{C}$ for 1.5 h to precipitate CaHPO_4 . This was accomplished in open atmosphere by heating the aqueous mixture on a hot plate. The slurry was then vacuum filtered, the solid product was then dried and kept sealed at $70\text{ }^\circ\text{C}$ overnight. The XRD diffractogram of resultant solid product is given in Figure 2.1. The XRD pattern reveals that the reaction product was CaHPO_4 , and no additional phase for any other calcium phosphate compound was observed. Based on the JCPDS library the synthesis product is phase-pure monetite with the card no 9-008.

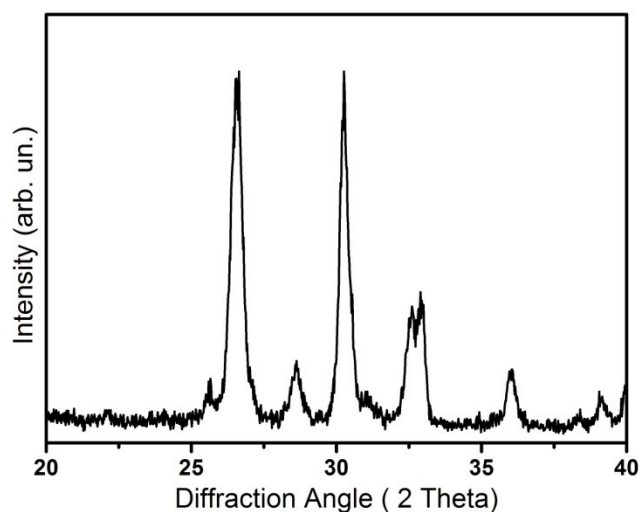


Figure 2.1 The diffractogram of the chemically synthesized monetite.

2.2.1 Synthesis of α -TCP

α -TCP was synthesized by solid-state reaction of calcium carbonate (CaCO_3) and CaHPO_4 . The proper amounts (1:2 mol proportion) of powder precursor was mixed in a Nalgene™ container in acetone and mixed using a Turbula mixer (Model T2F, System Schatz, Switzerland). After drying in air for overnight to completely evaporate acetone, the homogenized mixture was fired at 1200 °C for 2 h and to obtain α -TCP via following reaction;



Since α -TCP is metastable high temperature polymorph and may transform into β -TCP at 1150 °C under equilibrium cooling conditions, effective air quenching is required to avoid formation of β -TCP. So, after firing calcium carbonate: monetite mixture at 1200 °C (in alumina crucible) for 2 h, the red hot fired mass was immediately removed from the furnace and poured on a borosilicate glass plate. The quenched product was then ground into powder form using mortar and pestle. The flowchart summarizing the detailed synthesis protocol for TCP, including monetite precursor synthesis, is provided in Figure 2.2. The complete characterization of TCP will be given in the following Results chapter.

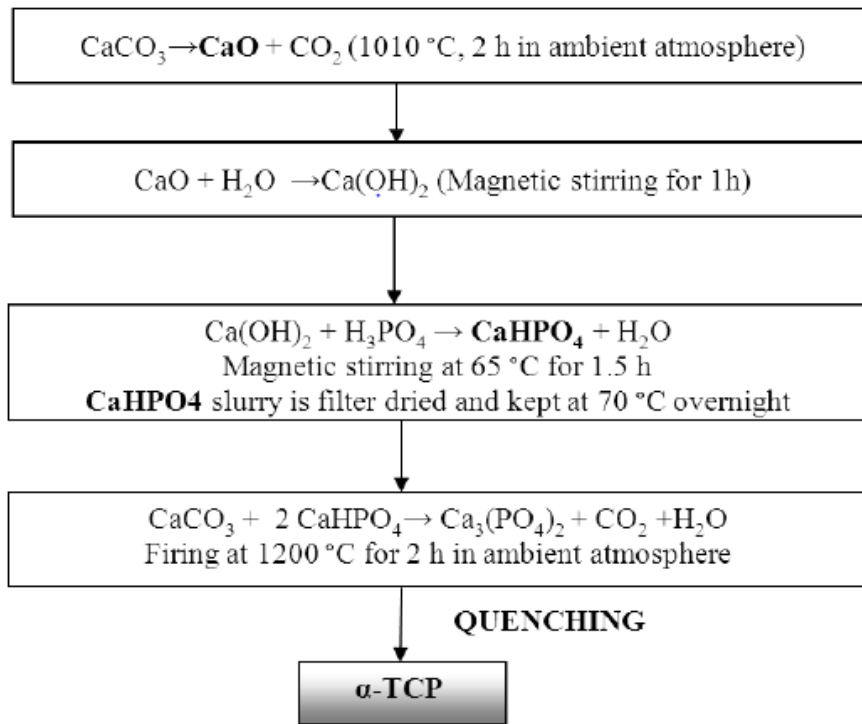


Figure 2.2 Experimental details and flowchart for solid state synthesis of α -TCP from CaCO_3 and CaHPO_4 .

The quenched product was ground into powder form using agate mortar and pestle, the average particle size of hand ground powder stock was measured as $17.8 \pm 1 \mu\text{m}$ using laser scattering (Malvern Mastersizer 2000) techniques. The reported particle size is volume equivalent diameter. As synthesized α -TCP powders were further elaborated for modification of particle characteristics. A Turbula T2F mixer (System Schatz, Switzerland) was used in milling operation where α -TCP was milled in a Nalgene™ cup for 60 min in acetone with 20 mm zirconia balls. The powder:acetone media weight proportion was 2 g:30 mL. After milling, acetone was removed by natural evaporation at room temperature for 5 h. The average particle size of the milled powder was measured as $8.4 \pm 1 \mu\text{m}$. (again measured by Malvern Mastersizer 2000), Most of the time milled powder was used in the thesis, i.e. subsequent composite cement preparation processes. As-synthesized α -TCP powder was only employed in preliminary comparative hydration kinetics studies as it will be discussed in the Results chapter.

2.2.2 Preparation of HAp:calcium sulfate dihydrate composites

For the first composite cements, the additive for hybrid pre-cement blends was $\text{CaSO}_4 \cdot \frac{1}{2}\text{H}_2\text{O}$ (CSH.), which also exhibits cement nature similar to α -TCP and converts to calcium sulfate dihydrate ($\text{CaSO}_4 \cdot 2\text{H}_2\text{O}$, or CSD or gypsum) by hydration. The α -TCP:CSH mixtures containing 10% and 25% (by weight) CSH were prepared by mechanical mixing. The mixing was accomplished in acetone in a Nalgene™ container using Turbula T2F mixer (System Schatz, Switzerland) and the wet mixture was dried in air after mixing operation. Hereafter, The α -TCP:CSH hybrid cement blends will be referred as CS-10 and CS-25, respectively.

Meanwhile, the hybrid pre-cement powder blends were consolidated into 3 mm thick pellets of 15 mm in diameter. For this purpose, 1.0 g of mixture powder were pressed (Model-C, Carver Inc., IN, USA) uniaxially in a cylindrical die at a pressure of 4 MPa at ambient temperature.

The powder mixtures were simply reacted with DI-water in order to start cement reaction and form final composite. In the case of pressed pellets, first they were inserted into plastic flasks with required amount of DI-water to initiate hydration leading to cement-type setting and kept in a closed water bath at 37°C. After allowing adequate time for cement-type reaction to be completed, these TCP-based pre-cement simply convert to HAp containing composite compacts. The liquid:solid ratio was 2:1 in all cases. The processing protocols for powder and pellet forms of pre-cement blends are given in Figure 2.3.

The cement characteristics of both of these forms, i.e. powder and pellets of pre-cement blends have been investigated for α -TCP:CSH system. It is worth to mention that, the powder forms of these pre-cement blends were mainly employed in reaction kinetics studies via by isothermal calorimetry, microstructural, phase and chemical analyses as it will be introduced in the following sections. The pellet forms solely produced for mechanical property evaluations/tests, usually requiring samples with simple geometry. (here pellets)

Table 2.1 The composition of α -TCP:CSH hybrid pre-cement blends and details for their cement conversion to HAp:CSD composites.

Cement	CSH (g)	α-TCP (g)	DI water (mL)	liquid:solid (by wt.)
CS-10	0.10	0.90	2.0	2
CS-25	0.25	0.75	2.0	2

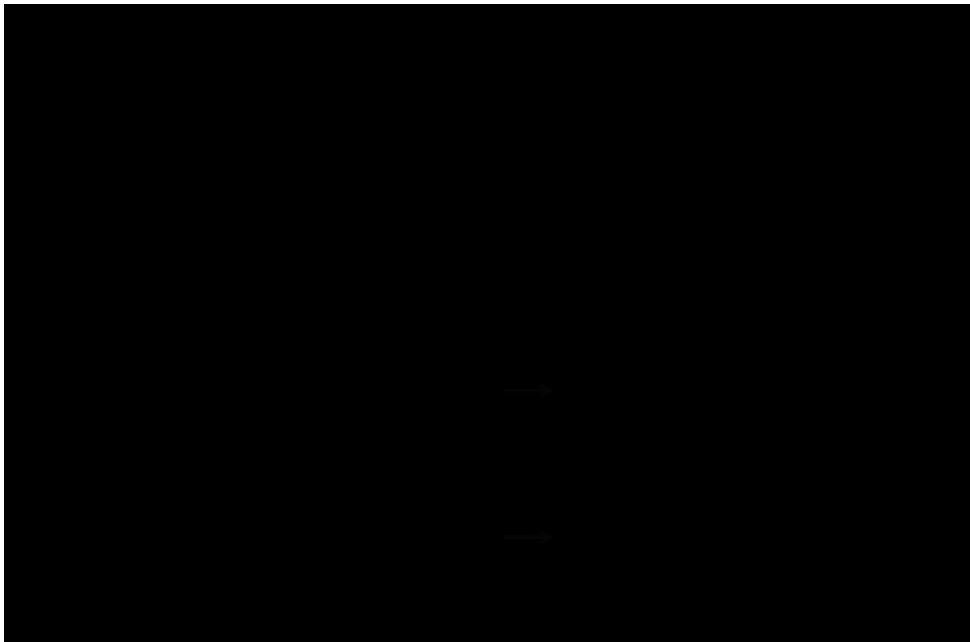


Figure 2.3 The experimental details for α -TCP:CSH hybrid pre-cement blend preparation and processing of final HAp:CSD composite cement.

2.2.3 Preparation of HAp:polycaprolactone (PCL) composites

In the second-type cement composites, three α -TCP-based hybrid pre-cements containing 3 wt. %, 6 wt. %, and 9 wt. % polycaprolactone (PCL) were prepared and then converted to HAp:PCL by hydration. The α -TCP:PCL hybrid pre-cements will be referred as T3CP, T6CP, T9CP; respectively. In preparing α -TCP:PCL hybrid pre-cements; initially, required amount of PCL was dissolved in chloroform and the solution was mechanically mixed by Turbula T2F mixer (System Schatz, Switzerland) after incorporating the α -TCP powders for 30 min at room temperature. The pre-

cement mixtures were kept in vacuum furnace (at room temperature) for 12 h to remove the solvent and achieve complete drying.

Later on, blends were ground to granule form using agate mortar and pestle. Granules were consolidated into pellets form (3 mm thick, 15 mm in diameter). Again, 1 g of hybrid pre-cement blend was pressed (Model-C, Carver Inc., IN, USA) uniaxially in a cylindrical die at a pressure of 4 MPa at ambient temperature. The pellets for each composition were hydrated at 37 °C again with a liquid: solid ratio of 2:1 allowing cement type conversion of α -TCP to HAp. The experimental details for HAp:PCL composite preparation are also provided in the flowchart shown in Figure 2.4. Different than the previous α -TCP:CSH composites, all analytical characterization, reaction kinetics and mechanical testing were performed on pellet forms.

Table 2.2 The composition of α -TCP:PCL hybrid pre-cement blends and details for theirs cement conversion to HAp:PCL composites.

Cement	PCL (g)	α-TCP (g)	DI water (mL)	liquid:solid (by wt.)
T3CP	0.03	0.97	2.0	2
T6CP	0.06	0.94	2.0	2
T9CP	0.09	0.91	2.0	2

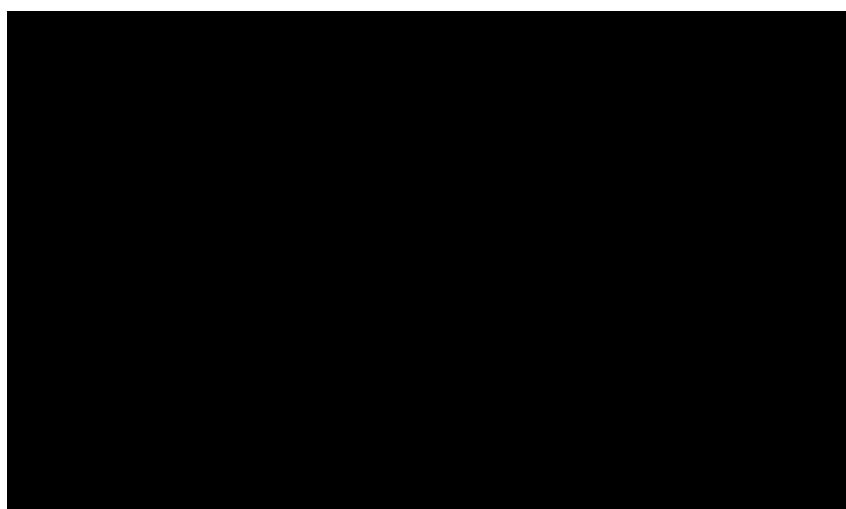


Figure 2.4 The experimental details for α -TCP:PCL hybrid pre-cement blend preparation and processing of final HAp:PCL composite cements.

2.3 Characterization of solid state synthesis and cement end products

2.3.1 Particle size analysis

Particle size analyses were performed for as-synthesized and milled α -TCP particles using Malvern Mastersizer 2000 particle size analyzer. In order to disperse agglomerated particles, powder was suspended in anhydrous ethanol and subjected to aggressive sonication using ultrasonic bath (Bandelin, Germany) prior to analysis.

2.3.2 Phase identification: X-Ray Diffraction Analysis

Phase identifications by X-Ray diffraction (XRD) measurements were performed for TCP, intermediate compounds formed during synthesis of α -TCP and hydration products of α -TCP, α -TCP:CSH and α -TCP:PCL cement systems. $\text{CuK}\alpha$ radiation was used at operation voltage of 40 kV and a current of 30 mA. Calcium phosphate powders and cement end products were scanned at 2θ of 20° - 40° and the systems including calcium sulfate from 10° - 40° at a scanning rate of $2^\circ/\text{min}$.

2.3.3 Microstructural investigation: Scanning Electron Microscopy

The microstructure of powders, pre-cement hybrids and composite samples were investigated by a FEI Quanta 400F model field emission scanning electron microscope (SEM). SEM examinations were performed after gold coating.

2.3.4 Chemical analysis: Fourier Transformed Infrared Spectroscopy

Fourier transform infrared (FTIR) spectroscopy analyses were performed using an FTIR Frontier spectrometer (Perkin Elmer, USA). The possible chemical interaction between organic and inorganic constituent of composites were explored. The spectra were collected between 450-2000 wavenumbers (cm^{-1}) with powder samples.

2.3.5 Reaction kinetics studies: Isothermal Calorimetry

The hydraulic reactivity (cement type conversion efficiencies) of α -TCP, α -TCP:CSH and α -TCP:PCL pre-cement hybrids were studied by isothermal microcalorimetry (TAM Air TA Instruments, Lindon USA). In a typical experiment, a glass ampoule containing pre-cement powder and a syringe with liquid reactant (DI water) were inserted into closed calorimetry chamber. Meanwhile, equivalent amount of inert $(\text{CaSO}_4) \cdot \frac{1}{2}\text{H}_2\text{O}$ powder including ampoule was inserted into the reference chamber. After establishing the thermal equilibrium, DI water was injected into the sample and the cement reaction was started. The heat flow rate due to hydration (dQ/dt) was continuously recorded as a function of time and interpreted to reveal reaction kinetics. The reaction temperature was at near physiological conditions (37 °C) in all experiments and solid: liquid ratio was 1:2.

2.3.6 Mechanical testing: Diametrical Compression Test

The fracture strengths of α -TCP, α -TCP:CSH and α -TCP:PCL hybrids pellets before and after hydration reaction were determined using diametrical compression test. In Figure 2.5, schematic for diametral compression test is given. Tests were performed using Shimadzu AGS-J 10 kN universal testing machine with 0.5 mm/min cross head speed at room temperature. The fracture strength (in MPa) of samples are computed by formula given in following equation;

$$\sigma = 2P/\pi Dt$$

where P is maximum compressive load (in N) that can be sustained by pellets until fracture, D is the diameter (in cm) of the pellet and t is thickness of sample (in cm). Typically at least five pellets were tested to be able to obtain representative data for each set of samples.

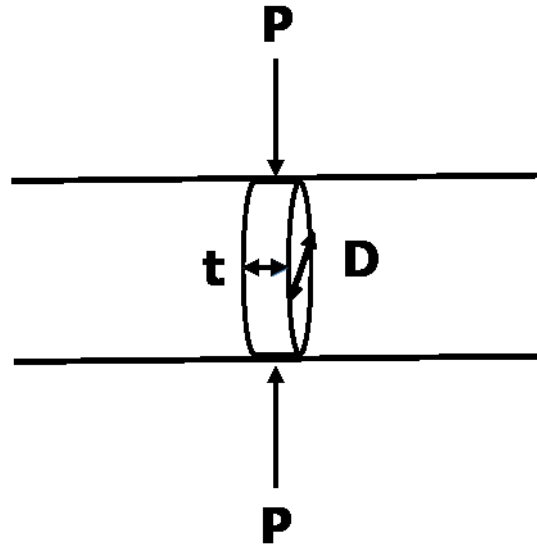


Figure 2.5 Schematic representation of diametral compression test.

2.3.7. Density measurement

The bulk densities of α -TCP, α -TCP:CSH and α -TCP:PCL hybrid pellets before and after hydration were determined by Archimedes method and compared with theoretical values. Total porosity was calculated by following formula;

$$\% \text{ Porosity} = (1 - \text{bulk density/theoretical density}) \times 100$$

The theoretical densities were calculated by rule of mixtures using respective values of the constituents. The theoretical density values for the α -TCP, CSH, CSD, HAp are 2.863, 2.73, 2.32 and 2.79 g/cm³, respectively. The theoretical density of organic constituent PCL is 1.145 g/cm³. [CRC Handbook of Chemistry and Physics].

CHAPTER 3

CHARACTERIZATION OF α -TCP AND PRELIMINARY INVESTIGATION OF ITS' CEMENT TYPE REACTIVITY

In this chapter, characterization of solid state reaction product synthesized by the preparation protocol explained in experimental methods (section 2.2.1) is presented. To begin with, a phase analysis was performed by XRD in order to ensure the phase characteristics of synthesized α -TCP. Microstructural properties were examined with SEM. Particle size and physical properties were investigated using laser diffraction techniques and also SEM. Chemical structure of synthesis product was also revealed by FTIR. Beside basic characterization, cement-type reactivity of both “as-synthesized” and “milled” α -TCP particles were investigated in a comparative manner by isothermal calorimetry. The microstructural features and chemistry of cement-end products were elucidated by SEM, XRD and FTIR.

3.1. Characterization of α -TCP powders

The diffractogram in Figure 3.1 shows the XRD pattern of the powder product obtained by solid state reaction between CaCO_3 and CaHPO_4 mixture at 1200 °C (in air) followed by air quenching. The XRD pattern completely matches with JCPDS card no 9-348 for α -TCP. Since there is no other diffraction peak corresponding to any other crystalline phase or calcium phosphate compound, it can be said that reaction product is phase pure α -TCP in as-synthesized condition. This data also reveals that the formation of β -TCP was completely suppressed, suggesting an effective and feasible quenching was performed. (α -TCP will be referred as only TCP hereafter.)

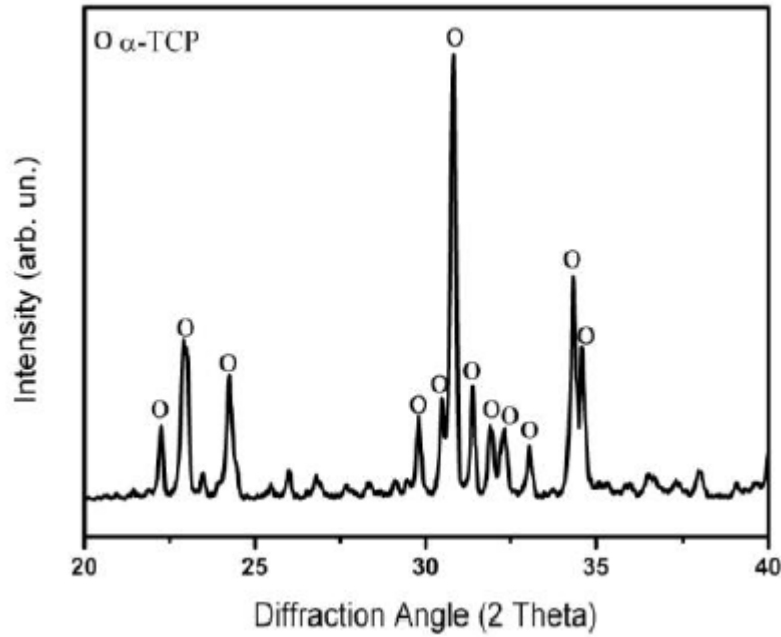


Figure 3.1 The XRD diffractogram of the solid state synthesis product obtained according to the standard synthesis protocol (peaks with low intensity are not marked; all correspond to α -TCP with JCPDS 9-348).

The SEM micrograph in Figure 3.2 shows the characteristics microstructural features of as-synthesized TCP. Irregular granulated, smooth and partially fused morphology of TCP particles consistent with solid-state synthesized ceramics powders as previously reported [Durucan and Brown, 2000; Cicek et al., 2012]. It is hard to talk about a representative average particle size at this state, as the particles are somewhat fused and agglomerated due to high temperature reaction.

Figure 3.3 shows SEM micrograph of 1 h milled TCP powders. The milled product exhibits relatively finer particles when compared with as-synthesized powders. This is consistent with particle size analyses results (obtained by light scattering) as shown in Table 3.1.

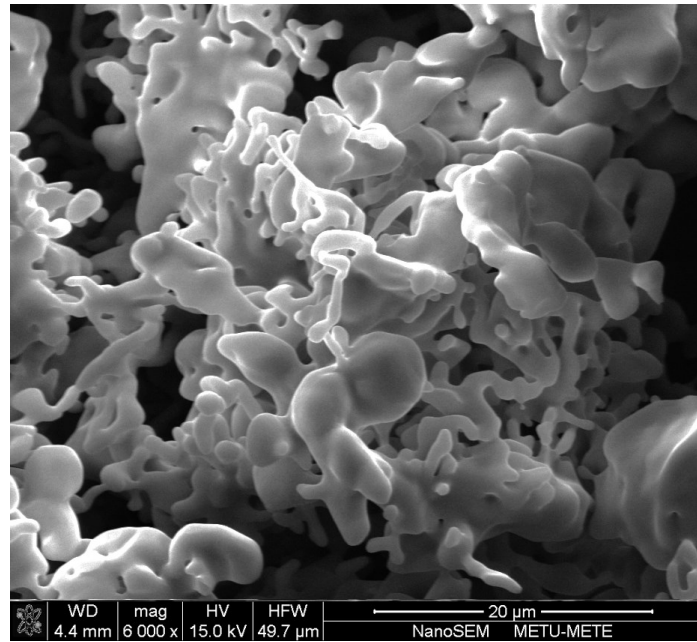


Figure 3.2 SEM micrograph of as-synthesized TCP.

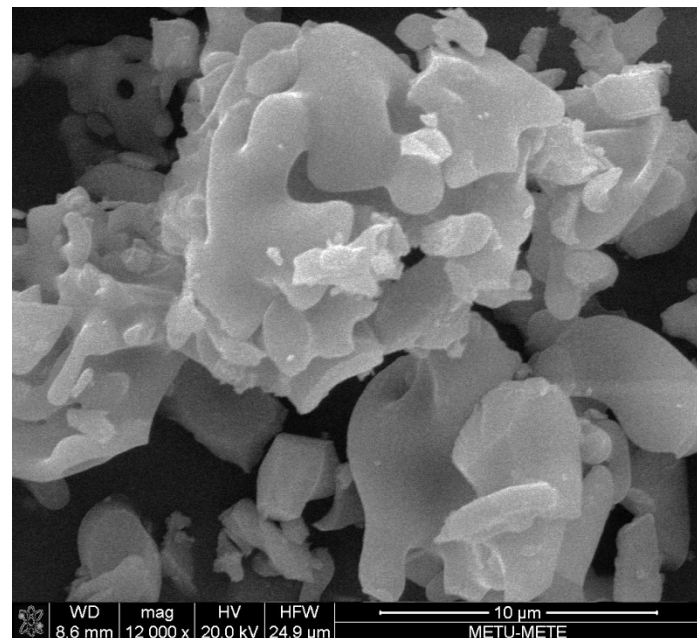


Figure 3.3 SEM micrograph of milled TCP.

Table 3.1 Particle characteristics of TCP powders at different physical states

	TCP (as-synthesized)	TCP (milled)
Specific surface area (m ² /g)	0.50	1.04
Average particle size (μm)	17.8 ± 1	8.4 ± 1

The chemical analysis of TCP (Ca₃(PO₄)₂) was performed by optical spectroscopy using FTIR. Figure 3.4 shows the transmittance spectrum of milled TCP powders in the range of 2000-400 cm⁻¹. The data shows the PO₄ structural group related chemical information based on two major phosphate absorption bands, and the details within these major bands. The IR absorption bands centering at around 565 cm⁻¹ and 600 cm⁻¹ for antisymmetric bending mode of P–O bonds. Meanwhile, the bands at 960 cm⁻¹, 1040 and 1090 cm⁻¹ are again assigned for different vibrational modes of P–O; for symmetric stretching and for antisymmetric stretching modes. The FTIR data does not provide any specific information especially for phase pure TCP. However, this analytical tool will be useful in understanding the chemical changes upon hydration, and exact chemical nature of cement product which will be a new calcium phosphate, most likely some type of HAp, consisting different chemical groups than TCP with a very general formula of Ca_{10-x-y}(HPO₄)_y(PO₄)_{6-x}(OH)_{2-x}.

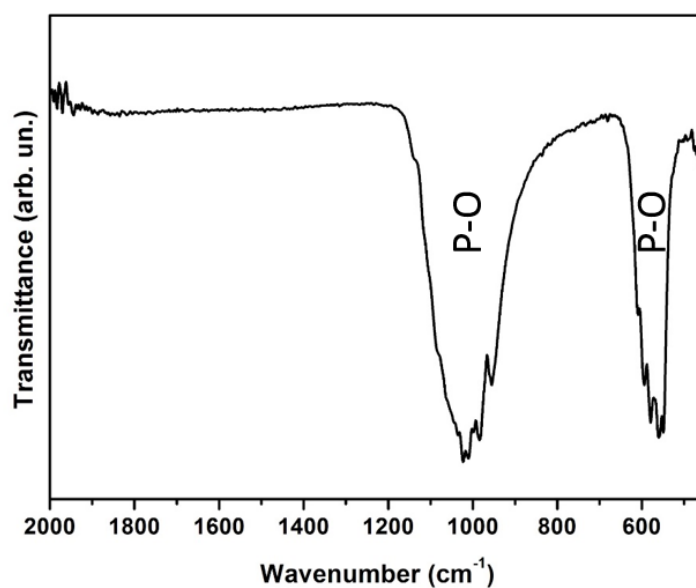


Figure 3.4 FTIR spectrum of TCP in 2000-450 cm⁻¹ range.

3.2 Cement-type reactivity of TCP

After determining chemical nature of TCP, further analysis was performed to elucidate its' cement type reactivity. Both as-synthesized and 1 h milled TCP powders were reacted with DI water to initiate the cement-type reaction and to achieve conversion to HAp. This was performed using isothermal calorimetry for precise and direct comparison purposes. Figure 3.5 shows typical isothermal calorimetry data (dQ/dt vs. time) for hydration of as-synthesized and milled TCP. The reaction temperature was 37 °C. These curves simply imply the heat evolution extent at different time periods during chemical reaction between TCP and DI-water.

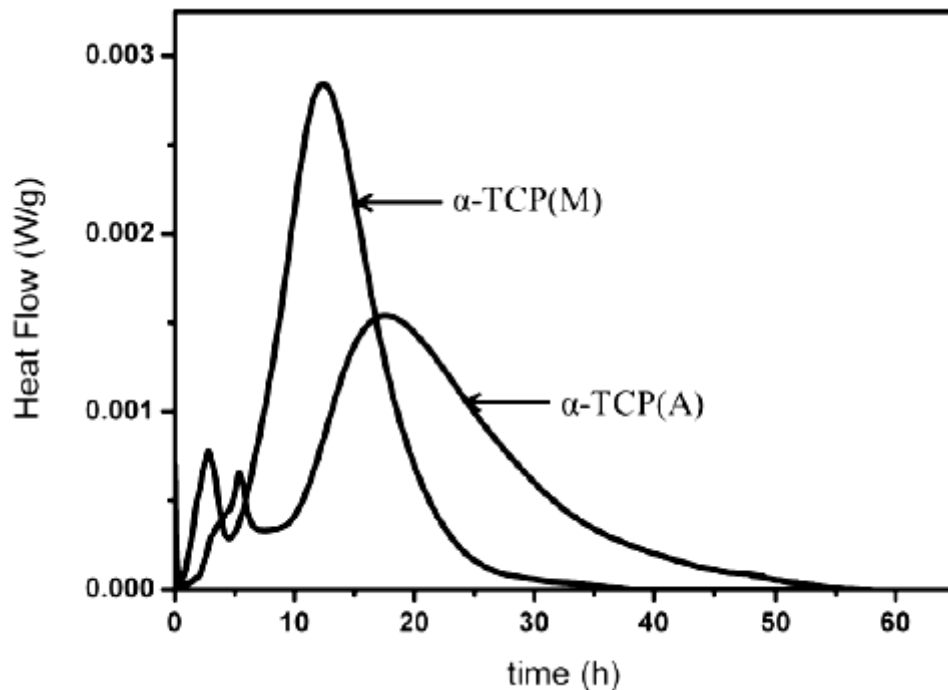


Figure 3.5 Typical isothermal calorimetry data (dQ/dt vs. time) for hydration of as-synthesized (α -TCP (A)) and milled TCP (α -TCP(M)). The reaction temperature was 37 °C.

These heat flow curves suggest that the hydration reaction was exothermic. The complete conversion was evidenced and determined by the time span after no further heat was evolved, i.e. heat flow becomes steady at around zero. The complete

conversion to cement-end product has occurred after 55 h and 36 h, for as-synthesized and for milled TCP, respectively. Even though the times for complete conversion times are different, the heat flow curves are similar and both consist a short low intensity heat peaks at around 3 h and 7 h, followed by a more broad and highly intense peak expanding to longer times, eventually saturating to zero at the end of conversion/reaction.

The heat events can be related to nucleation and growth of new phases during hydration. Isothermal calorimetry data reveal that the custom synthesized TCP exhibits a particle size-dependent cement-type reactivity. As clearly indicated by the calorimetry data, a decrease in particle size from $17.8 \pm 1 \mu\text{m}$ to $8.4 \pm 1 \mu\text{m}$ yields in faster reaction kinetics, leading much shorter completion times. The calorimetric analyses together with particle size measurement emphasize the importance of surface area for obtaining high reaction rates as reported by others [Bohner, 2007].

3.3 Characterization of cement-end products

The XRD diffractograms of end products of cement conversion for as-synthesized and milled TCP are shown in Figure 3.6 and 3.7. The data are for the samples that were obtained after 48 h-long hydration of powder forms. For both cases, after hydration at 37 °C for 48 h, the cement reaction was terminated by washing the wet cement putty with acetone and then air blowing to eliminate water from the system and to stop hydration. The morphological investigations and phase evaluations were performed on these 48h-hydrated samples in a comparative manner.

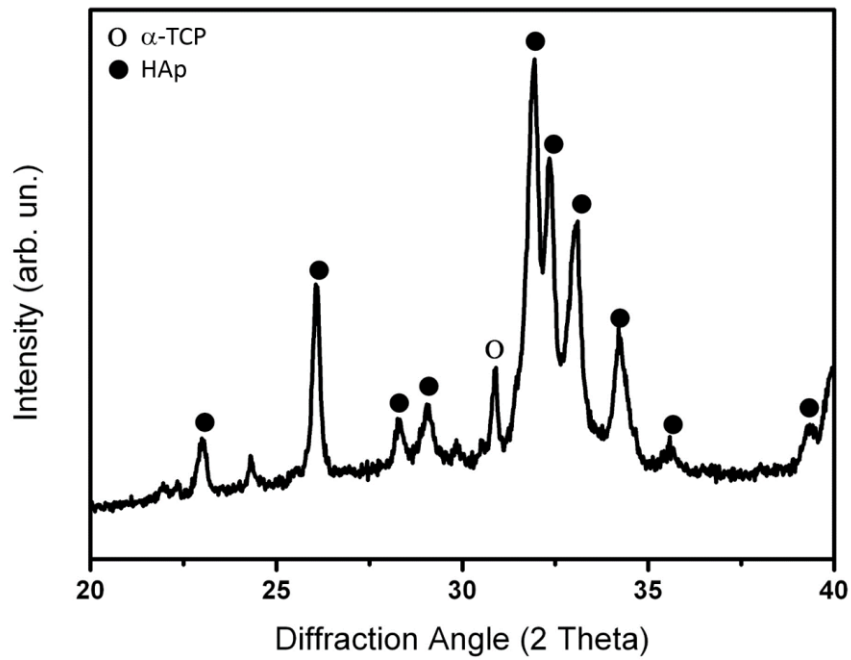


Figure 3.6 XRD diffractogram of hydration product of as-synthesized TCP powder (peaks with low intensity are not marked; all correspond to HAp with JCPDS 9-432).

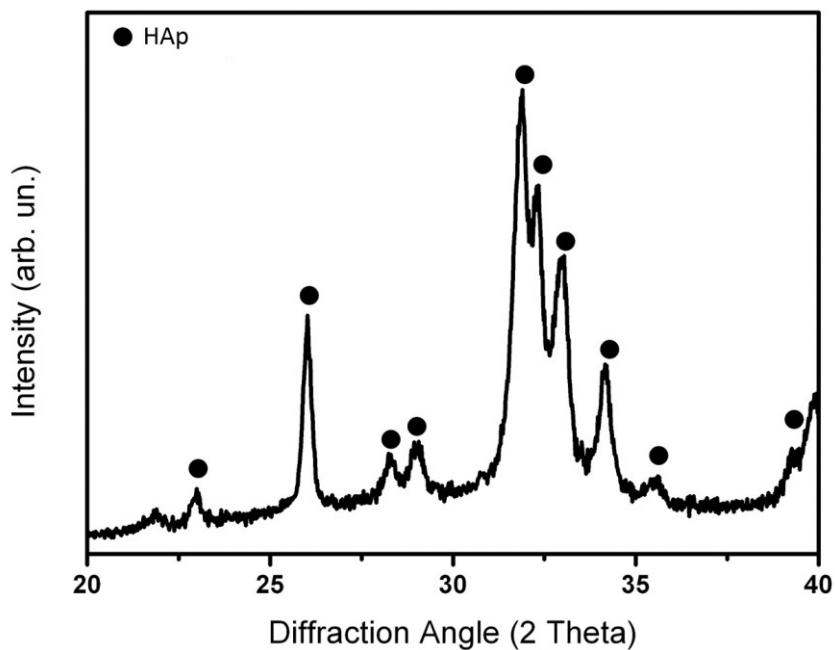


Figure 3.7 XRD diffractogram of hydration product of milled TCP powder. (peaks with low intensity are not marked; all correspond to α -TCP with JCPDS 9-432).

The XRD findings point out somewhat limited transformation to HAp (Figure 3.6) during hydration of as-synthesized TCP. The hydration product is a phase mixture of un-reacted TCP and HAp (JCPDS card no 9-342). The presence of left-over reactant is evidenced by low intensity diffraction peak at around $2\theta = 31-32^\circ$ matching with the position of the highest intense diffraction peak of TCP. For the milled TCP, on the other hand, complete conversion to HAp was achieved and no other crystalline was identified after hydration (Figure 3.7).

Accompanying SEM micrographs shown in Figures 3.8 and 3.9 give some insights about the morphology of the HAp products as well as nature of hardening/setting realized by hydration. The HAp crystals develop in flake-like morphology which are entangled in a reticulated form for both cases as consistent with the results reported by other [Leamy et. al., 1998; Durucan and Brown, 2000]. These morphological changes are typical for almost any dissolution and precipitation based setting reaction leading to self-hardening for granular shaped initial cement powders. SEM micrographs also show the difference in extent of HAp conversion for the two α -TCP powders. The circular marked region in Figure 3.8 shows some unreacted α -TCP particles in granular form embedded in HAp flakes formed by hydration, again suggesting a poor cement-type hydraulic reactivity and incomplete transformation to HAp for as-synthesized TCP powder). However, milled TCP exhibits complete conversion into HAp implied by entangled flake like morphology without any TCP granules.

The hydration product of milled TCP exhibiting complete and efficient conversion to HAp according to XRD and SEM results, was further investigated by FTIR spectroscopy to reveal its chemical structure. XRD and SEM analyses alone do not directly give information about exact chemical nature of HAp, as it can easily accommodate a variety of ions and chemical groups due to its intrinsic crystal arrangement involving different functional groups. The XRD of course show that the cement product is phase pure HAp, however nothing can be said about its stoichiometry, such (Ca/P ratio) number and presence of other chemical groups hydrogen phosphates (HPO_4), hydroxyl (OH), carbonates (CO_3) from XRD findings. For example, when stoichiometric HAp, with a Ca/P=1.67 and fully calcium-deficient HAp with Ca/P=1.5 are considered they would not exhibit any difference in their XRD

diffractograms and will have almost identical diffraction patterns. However, presence of additional groups $(\text{HPO}_4)^{-2}$ and/or OH^- , or stoichiometrical variations can be easily identified by FTIR.

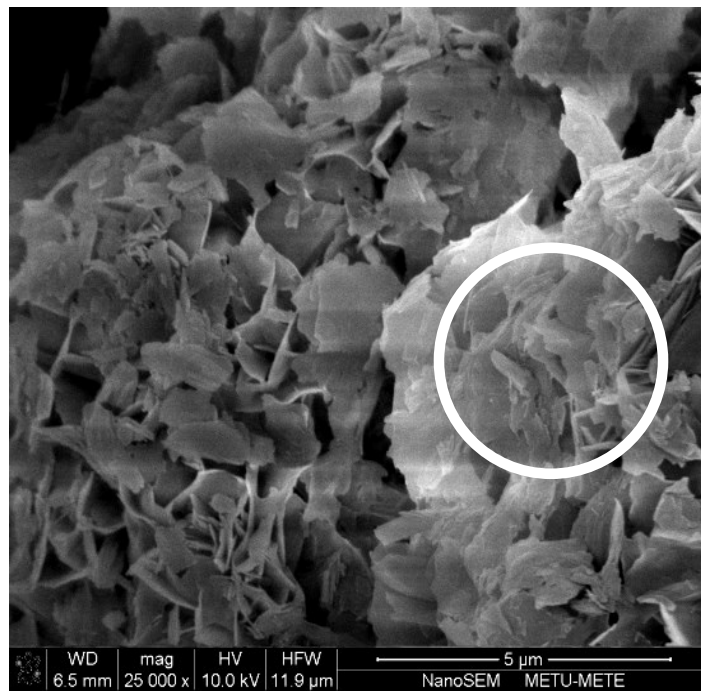


Figure 3.8 SEM micrograph of hydration product of as-synthesized TCP powder.

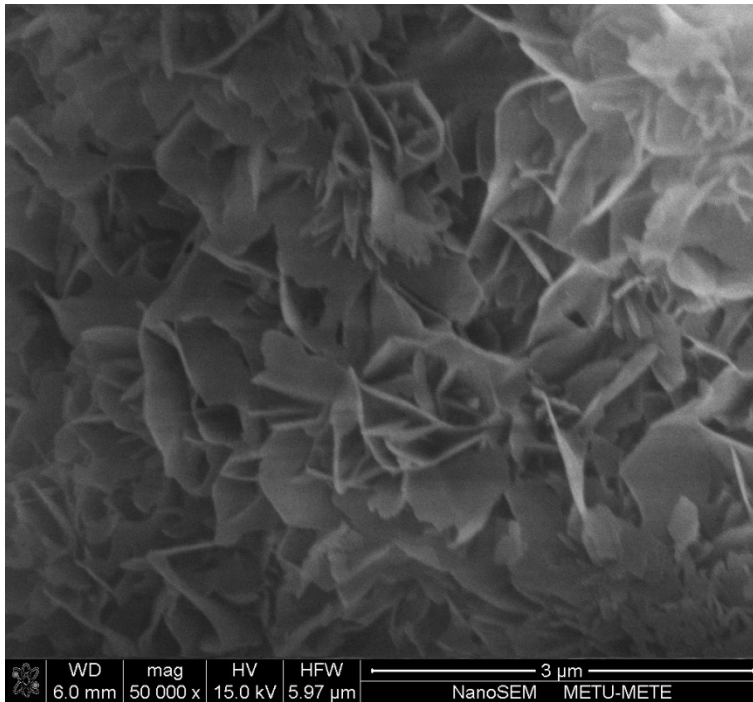


Figure 3.9 SEM micrograph of hydration product of milled TCP powder

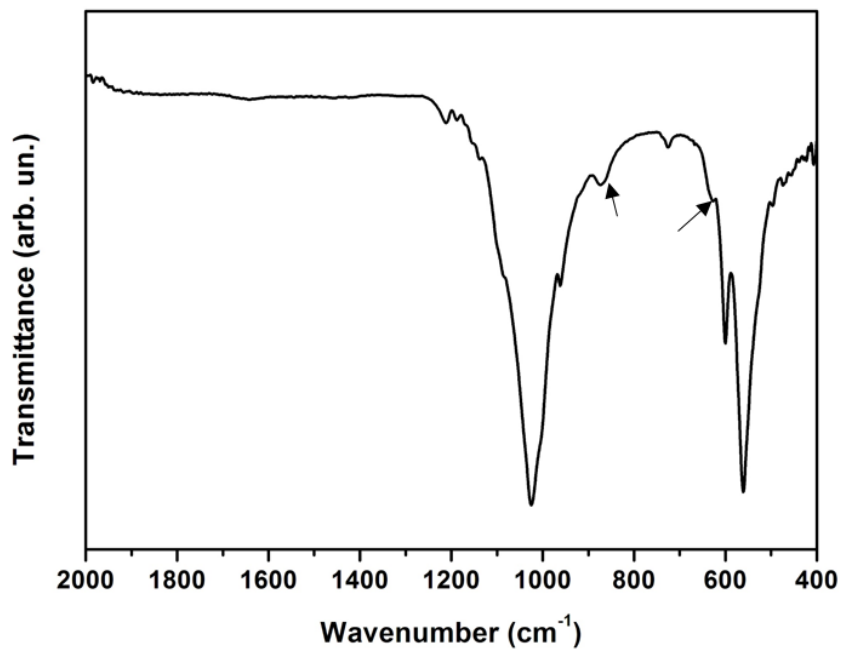


Figure 3.10 FTIR spectrum of hydrated TCP (i.e. after cement type conversion to HAp) in 2000-450 cm⁻¹ range.

Figure 3.10 shows the FTIR spectrum of hydration product of TCP, which is HAp according to XRD analyses. When this spectrum for hydrated sample (HAp) is compared with that of non-hydrated one (i.e. for TCP) provided in Figure 3.4, there are a couple of differences. The PO_4 asymmetric absorption bands at 565 and 600 cm^{-1} poorly recorded for TCP converted into distinctly separated forms as previously reported [Durucan and Brown, 2000]. Similarly, the other main phosphate group absorption band, including individual bands at 960 cm^{-1} , 1040 and 1090 cm^{-1} (assigned vibrational modes of P–O) characteristics change slightly. These differences are due to change in crystal structure and resultant chemical neighborhood and bonding variations. However, phosphate groups are common both for TCP and cement end product.

Additionally, FTIR spectrum proves that apatitic structure at the end of hydration is HAp in calcium-deficient form. The cement-end products of TCP contain two additional peaks indicated by arrows in Figure 3.10 at 630 cm^{-1} and 872 cm^{-1} assigned to the $(\text{OH})^-$ librational mode, and P–OH stretching of $(\text{HPO}_4)^{2-}$, respectively [LeGeros et al., 1989]. The $(\text{HPO}_4)^{2-}$ group bands which is characteristic to calcium-deficient HAp (CDHAp),

$\text{Ca}_9(\text{HPO}_4)(\text{PO}_4)_5(\text{OH})$ suggest that HAp is not stoichiometric [LeGeros et al., 1991]. In conclusion, based on XRD, SEM findings and FTIR analyses TCP completely converts to HAp as CDHAp. The cement type product will be referred as CDHAp for the rest of the thesis.

3.4 Mechanical properties of TCP and it's cement-end product

The mechanical property change and possible strength enhancement upon hydration of TCP have been evaluated by diametral compression tests. First, proper samples were obtained for mechanical testing. For this purpose, the TCP pellets produced as described in Section 2.2.1 were inserted into glass cups containing DI-water and kept in a closed water bath at a constant temperature of $37\text{ }^\circ\text{C}$ for prolonged times (3 days)

to ensure complete for conversion into CDHAp. The liquid:solid ratio in hardening reaction was 2.1. The hydrated pellets were then taken out and dried with acetone, and blow-dried with air.

The complete conversion to CDHAp was evidenced by XRD analyses of broken test samples (data not shown here). The mechanical properties of unreacted TCP pellets and CDHAp pellets of cement-type conversion are summarized graphically in Figure 3.11. The average fracture strength of TCP compacts before hydration was found as 0.17 ± 0.01 MPa. The measured average strength increased to 4.5 ± 0.1 MPa after hydration and conversion into CDHAp.

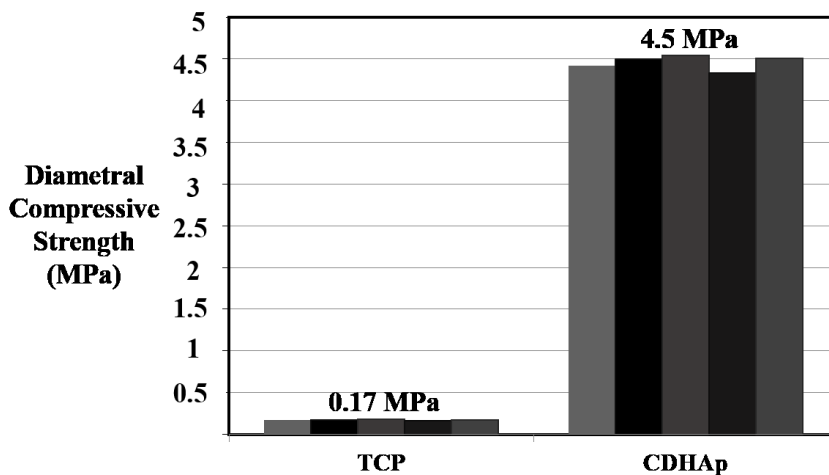


Figure 3.11 Diametral compressive strength of TCP and its hydration product (CDHAp).

The strength enhancement accompanied by a density change. Upon cement reaction, the porosity changes from an initial value of 59 ± 1 % (in vol.) to 45 ± 1 %. However, the increase in strength is mostly due to microstructural change, i.e. due to conversion of poorly-packed isolated TCP granules into reticulated and entangled flake-like new crystals (CDHAp) as discussed with the SEM analyses. This is common for almost all hydration-based cement type setting reactions involving dissolution and re-precipitation. [Dorozhkin, 2013]. Despite a remarkable increase in strength, diametral compression strength of 4.5 MPa is still not sufficient for a bone substitute material when compared tensile strength of cancellous (porous) bone, which is around 10 MPa [Meyers et al., 2008].

CHAPTER 4

CHARACTERIZATION AND PROPERTIES OF TCP:CSH HYBRID CEMENT BLENDS

In this chapter, results on cement behavior of TCP-based pre-cement mixtures 10 or 25 wt. % calcium sulfate hemihydrate (CSH, $\text{CaSO}_4 \cdot \frac{1}{2}\text{H}_2\text{O}$) addition has been presented. The change in cement-type reactivity of TCP in the presence of CSH was investigated. The microstructural and morphological change as a result of cement reaction (hydration with water) have been explored. In addition, mechanical properties of CSH-containing mixtures were examined to reveal the effect of CSH on hardening/setting behavior of TCP:CSH hybrid pre-cement blends. As discussed in the previous section, milled TCP exhibiting relatively higher hydraulic reactivity was used in these studies. The TCP:CSH pre-cement mixtures were prepared according to the experimental protocol explained in Section 2.2.3.

4.1 Effect of CSH incorporation on cement-type reaction kinetics of TCP

The heat flow curves obtained by isothermal calorimetry presented in Figure 4.1 shows the hydration behavior/kinetics of the powder forms of hybrid blends; 10 or 25 wt. % CSH (will be referred as CS-10 and CS-25). The heat flow curve for pure TCP is also shown for direct comparison purposes. The presence of additional heat peaks during the initial period of hydration (time shorter than 10 h) suggest that calcium sulfate addition changes the mechanistic path and the rate of heat evolution during conversion of TCP to CDHAp. Beside nucleation and growth peaks assigned for TCP to CDHAp conversion, additional initial and quick heat release events (within the time frame shorter than 2 h) can be observed in heat flow curves of hybrid cement mixtures. The additional heat release events and respective additional peak is associated with hydration of CSH to gypsum (CSD), which is also a cement-type conversion.

This calorimetric data also show that the calcium sulfate addition elongates the time for complete conversion of TCP to CDHAp in the hybrid cement mixtures. Upon 10 or 25% wt. CSH addition, the heat release saturates at 58 h and 98 h, respectively. These times points designate no further heat release and practically the end of the cement-type reaction(s). The termination of heat release was at around 36 h (at the same reaction temperature of 37 °C) in the case hydration of plain TCP powders, without any CSH addition.

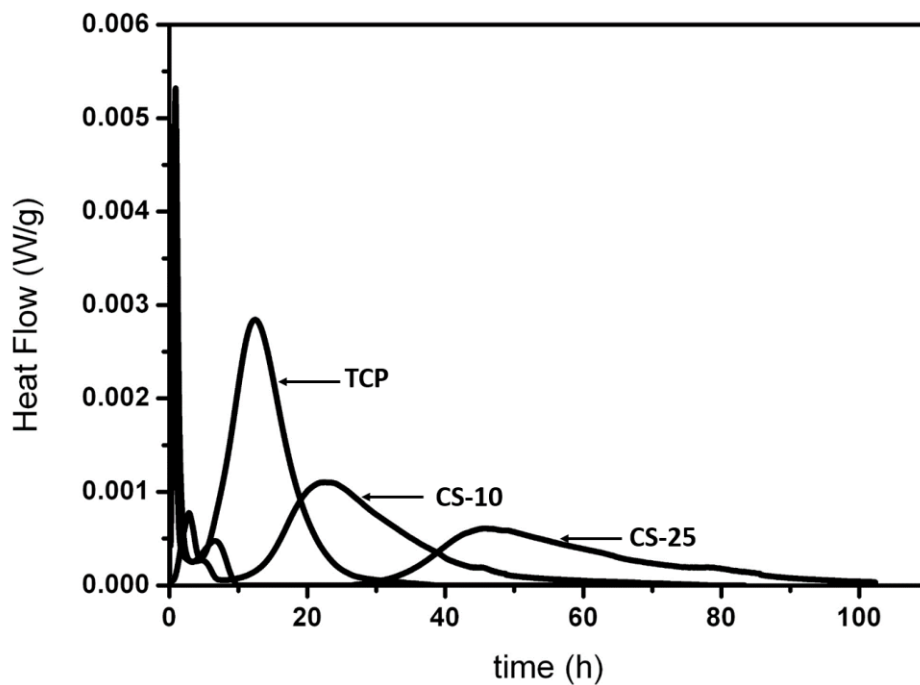


Figure 4.1 The heat flow curves for hydration of plain TCP (α -TCP(M)), and 10 wt. (CS-10) or 25 wt.% (CS-25) calcium sulfate hemihydrate (CSH, $\text{CaSO}_4 \cdot \frac{1}{2}\text{H}_2\text{O}$) containing hybrid blends. The reaction temperature was 37 °C.

4.2 Characterization of cement-end products

In order to obtain representative samples for phase and microstructural analyses again hydration of hybrid cement systems reactions were terminated at transitional state (48 h of reaction). This was again done washing the wet setting mass with acetone and then air blowing. Figure 4.2 and 4.3 shows the XRD diffractograms of cement-end

products of CS-10 and CS-25 hybrid blends after 48 h hydration at 37 °C. Compared to the hydration product data of plain TCP (Figure 3.7) these cement products contain much higher amount of unreacted TCP phase; again indicating limited conversion to CDHAp parallel to the calorimetric findings. There are also additional phases as expected and as revealed by additional diffraction peaks. One set of additional peaks are for gypsum (JCPDS card no 33-0311). Furthermore, when the XRD diffractograms of the end products for two hybrid blends of different amount of CSH incorporation are compared, it is clear that TCP→CDHAp conversion was more distinctly hampered in the case of CS-25. This blend contains higher amount of CSH.

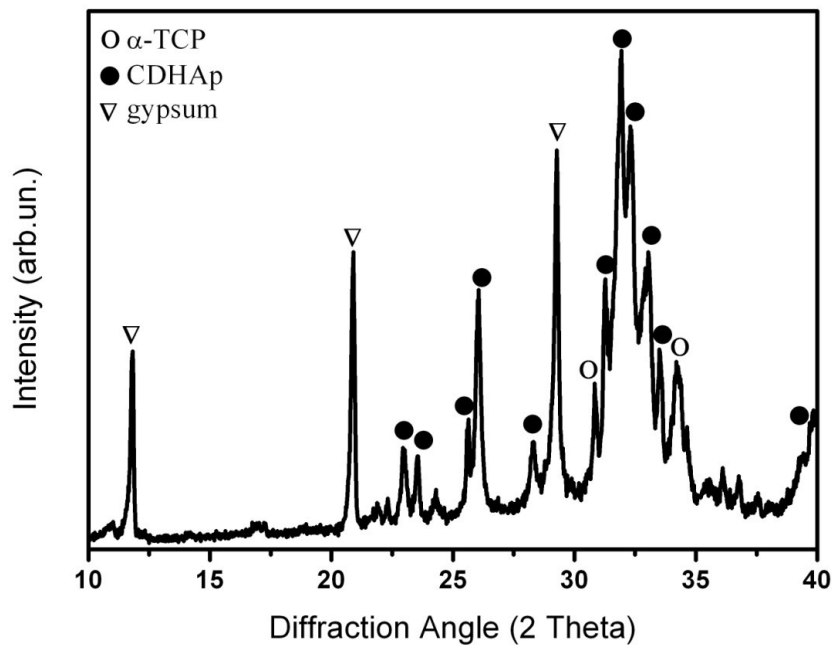


Figure 4.2 XRD diffractogram of 10 wt. % CSH-containing hybrid TCP:CSH blend after hydration at 37 °C for 48 h.

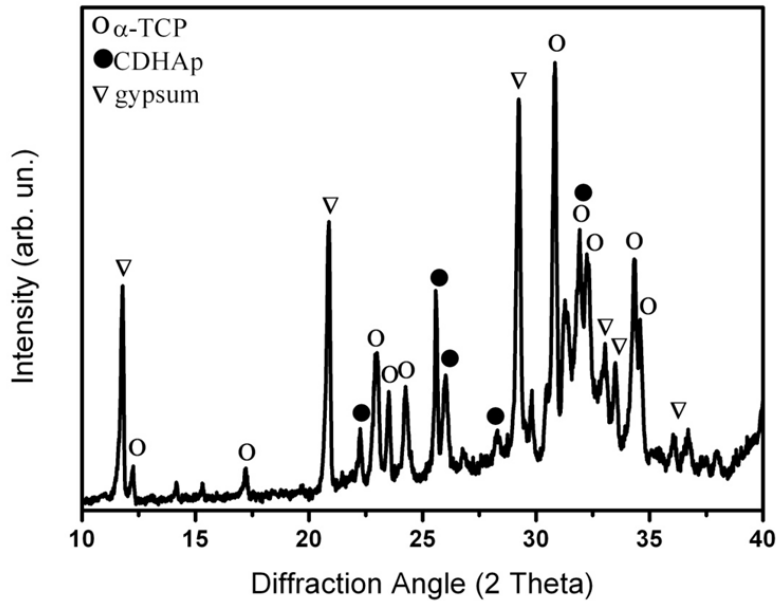


Figure 4.3 XRD diffractogram of 25 wt. % CSH-containing hybrid TCP:CSH blend after hydration at 37 °C for 48 h.

XRD data along with isothermal calorimetry data emphasize that CSH addition suppress the TCP→CDHAp conversion. In order to support this with additional analytical data, the microstructure/morphology of same samples before hydration and after 48 h hydration were examined with SEM and compared.

Microstructure of CS-10 and CS-25 before and after hydration are shown by the SEM micrographs in Figures 4.4 and 4.5; respectively. As shown in Figure 4.4a, the microstructure of non-hydrated hybrid blends consists of TCP particles granules and rod-like CSH crystals. Similarly, the non-hydrated state SEM micrograph of relatively higher amount of CSH containing CS-25 hybrid blend as shown in Figure 4.5a exhibits same features as captured at higher magnification providing more distinctive morphological difference between TCP (granules) and CSH (columnar/rod-like) constituent.

In hydrated state the composite microstructure is still evident as can be seen both in Figure 4.4b and 4.5b, and both flake-like CDHAp crystals formed upon partial

hydration of TCP and rod-like gypsum crystals developed upon hydration of CSH can be seen in these SEM images. The circular region marked as Figure 4.5b presents un-reacted TCP granules along with the CDHAp crystals developed with flake-like morphology for CS-25 system. In Figure 4.5b, regions labeled as 1 and 2 respectively show relatively higher amount of un-reacted TCP granules compared to those in Figure 4.4b and flake-like CDHAp crystals in CS-10. Based on SEM findings, when hydrated and non-hydrated state microstructure were compared it can be said that a structural integration occurs upon cement type reaction.

In parallel to isothermal calorimetry and XRD findings, these representative SEM images also reveal the difference between hydraulic properties of two cement mixtures. Extent of TCP to CDHAp conversion and hydraulic reactivity of TCP decreases for hybrids. This somewhat negative behavior in cement character becomes more obvious, as the amount of CSH increases in the pre-cement blend.

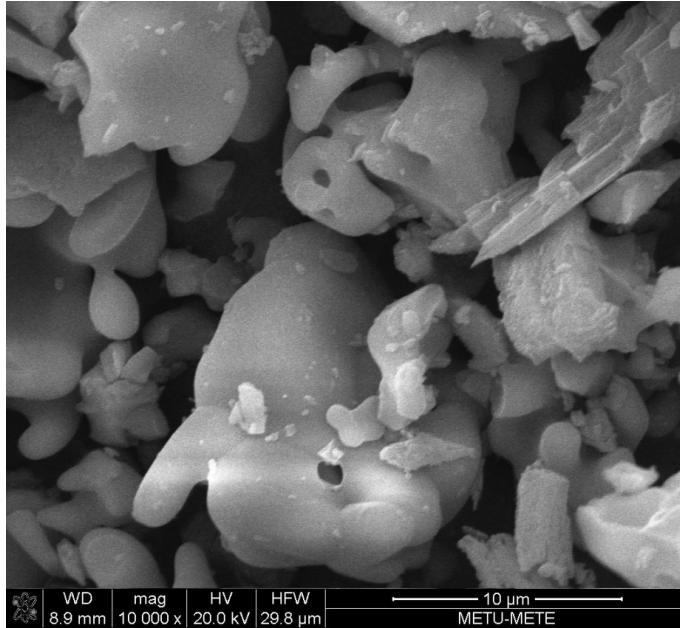


Figure 4.4a SEM micrograph of 10 wt. % CSH-containing hybrid TCP:CSH blend before hydration.

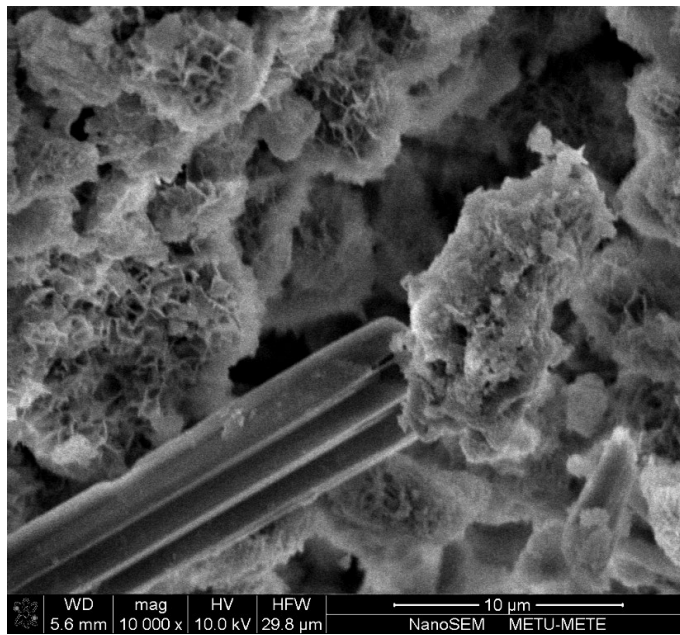


Figure 4.4b SEM micrograph of 10 wt. % CSH-containing hybrid TCP:CSH blend after hydration at 37 °C for 48 h.

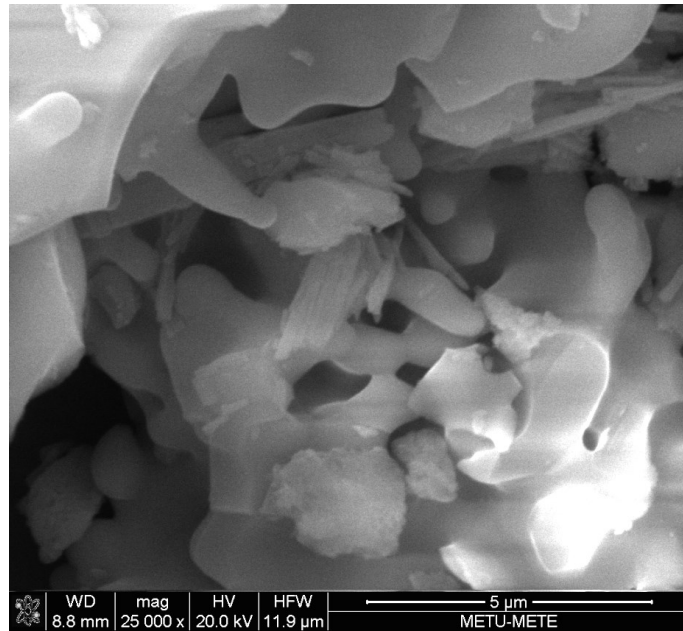


Figure 4.5a SEM micrograph of 25 wt. % CSH-containing hybrid TCP:CSH blend before hydration.

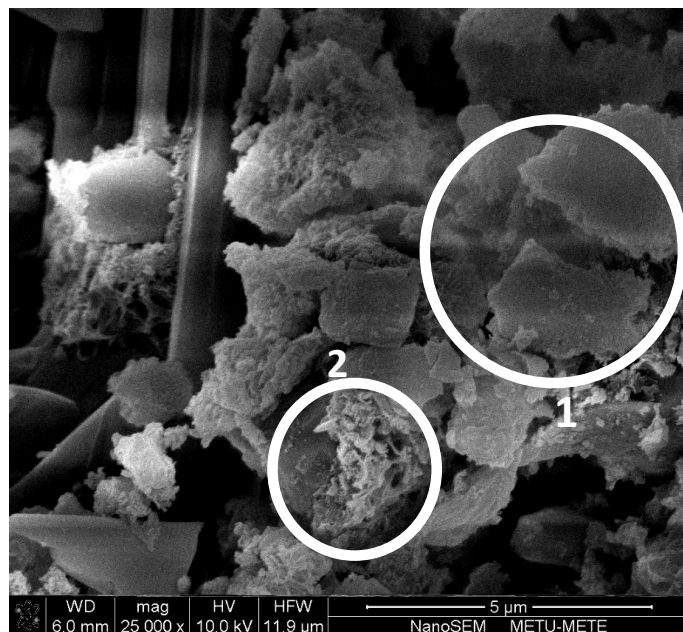


Figure 4.5b SEM micrograph of 25 wt. % CSH-containing hybrid TCP:CSH blend after hydration at 37 °C for 48 h.

4.3 Mechanical properties CSH incorporated hybrid cements

The effect of CSH addition on mechanical properties of cement end products was reported in the light of some qualitative observations and diametrical compression test results. For mechanical testing, TCP:CSH pellets were prepared by pressing as described in Section 2.2.3.

Physical appearance of cement putties obtained from hydration of powder starting materials give clues on hardening/setting behaviour and mechanical properties in a qualitative manner. Figure 4.6 provides images of cement end products of plain TCP, CS-10 and CS-25 hybrid blends after hydration of 48 h at 37 °C. The chunky and more consolidated appearance of cement products of CS-10 and CS-25 blends as shown in Figure 4.6 b and 4.6 c suggest an improved setting for the hybrid cement blends. The CDHAp cement product obtained by hydration of plain TCP, on the other hand, exhibits only limited consolidation upon hydration and reaches only semi-hardened bulky granulated form shown in Figure 4.6a. This preliminary qualitative analysis on cement end products indicates an improvement in mechanical properties with CSH addition. This of course is indirect evidence, yet a clear and obvious conclusion based practically visual observation.

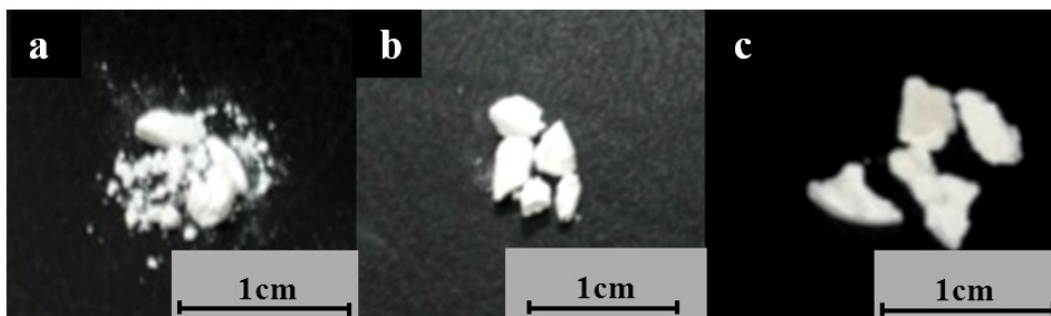


Figure 4.6 The images of CDHAp-based cement putty products after hydration of (a) plain TCP (b) 10 wt. (CS-10) or (c) 25 wt. % (CS-25) CSH containing hybrid TCP:CSH blends. (The scale is 1 cm)

In order to reach more valid and definite conclusion, the fracture strengths of samples were evaluated by Figure 4.7a and 4.7b diametral compression test shows fracture strength values of plain TCP, CS-10 and CS-25 before and after hydration. Consistent

with qualitative analysis, with increasing CSH content, higher fracture strength values were achieved. Additionally, it is worth to emphasize that the average porosity amounts of non-hydrated TCP, CS-10, and CS-25 compacts consolidated by pressing were determined to be 59 ± 1 vol. %, 58 ± 1 vol. %, 57 ± 2 vol. %; respectively as listed in Table 5.1. Porosity levels and fracture strengths of non-hydrated samples are nearly same for plain TCP and hybrid systems. There was not an observable effect of CSH on integrity of cements.

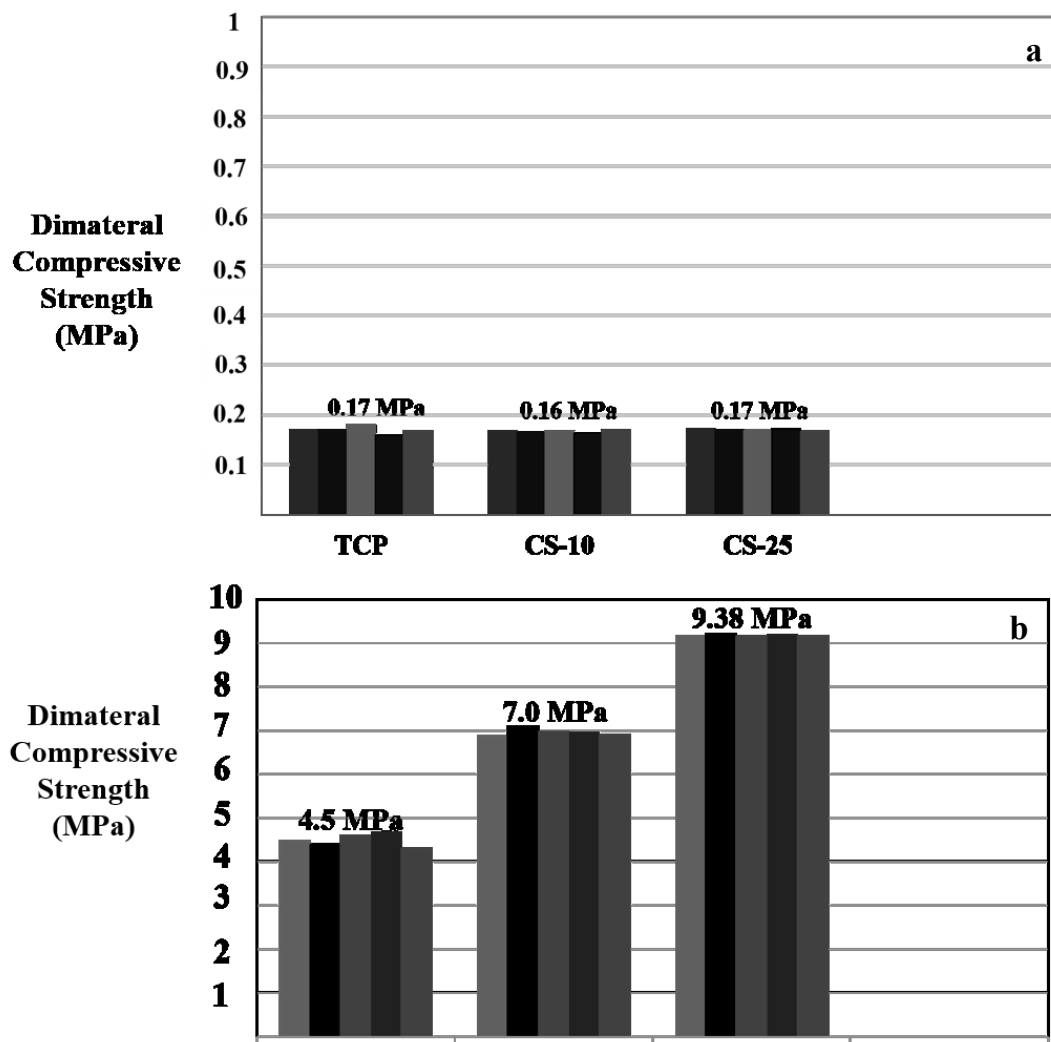


Figure 4.7 Diametral compressive strength of TCP and hybrid TCP:CSH pellets; CS-10, CS-25 (10, and 25 wt. % CSH) (a) before and (b) after hydration.

Table 4.1 Porosity values of mechanical test samples before and after hydration

Porosity (% vol)	TCP	CS-10	CS-25
Non-hydrated	59±1	58±1	58±2
Hydrated	45±1	44±1	46±1

A considerable increase in fracture strength of samples was observed after hydration. From microstructural point of view, increase in mechanical properties and density based on conversion of sphere-like TCP granules into entangled CDHAp plates/flakes. Porosity amount varying between 58-59 vol. % in non-hydrated samples decreased to 44-46 vol. % via cement-type conversion. The fracture strength for hydration product of plain TCP 4.50 MPa increased to 7.00 MPa and 9.38 MPa by addition of 10 wt. % and 25 wt. % CSH, respectively. Porosity levels of cement-end products were comparable. The additional strengthening is due to CSH hydration into gypsum evidenced in XRD diffractograms given in Figure 4.3. As proposed earlier interlocked gypsum crystals and adhesion forces between them during setting provide additional strength to the structure [Finot et al., 2000]. CSH incorporation is promising in terms of improving strength. By 25 wt. % CSH addition, the tensile strength value of cancellous bone (10 MPa) is almost achieved.

CHAPTER 5

CHARACTERIZATION AND PROPERTIES OF TCP:PCL HYBRID CEMENT BLENDS

In this chapter, the results in regard to cement behavior of PCL-added TCP-based hybrid blends are presented. First, the effect of PCL addition on cement-type TCP→CDHAp conversion kinetics and efficiency was investigated as a function of PCL amount by isothermal calorimetry. In addition to this, PCL amount-based preliminary parametric investigation, a detailed analysis on microstructural and phase/chemical property changes as a function of reaction time for a selected hybrid blend (with 3 wt. % PCL addition) has been conducted. Moreover, interaction between organic (PCL) and inorganic (TCP or CDHAp) constituents of composite cement were examined by spectroscopic/chemical analyses. Mechanical properties of cement-end products and effect of PCL on hardening behavior of TCP were evaluated by diametrical compression tests.

5.1 Effect of PCL incorporation on cement-type reactivity of TCP

The rate of heat evolution (dQ/dt vs. time) during cement-type reactions for TCP:PCL hybrid pellets of different PCL amount (3, 6 or 9 wt. % or T3CP, T6CP and T9CP) are illustrated in Figure 5.1. The heat evaluation curve for plain TCP pellet is also inserted for comparison. The isothermal calorimetry analyses were performed at around physiological temperature (37 °C) for all samples. These curves indicate that hydration reactions for the PCL-containing hybrids are exothermic, similar to that for plain TCP, as presented in previous chapters.

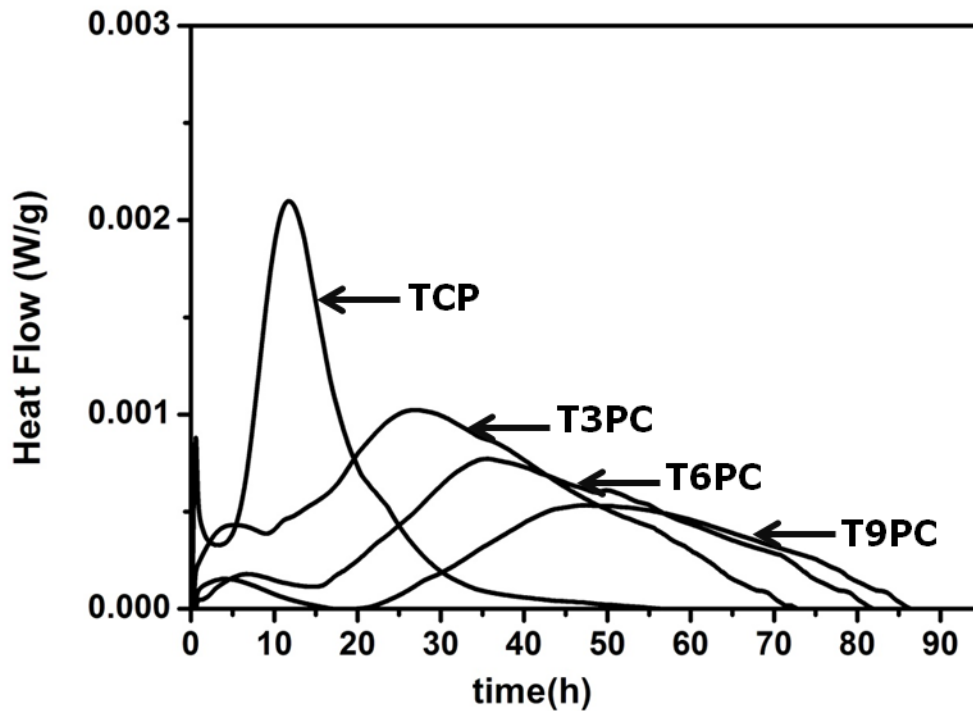


Figure 5.1 The heat flow curves for hydration (at 37 °C) of TCP and hybrid TCP:PCL pellets; T3CP, T6CP and T9CP (3, 6 or 9 wt.% PCL).

The time for complete conversion are different for TCP and TCP:PCL cement systems, however the general appearance of heat evolution rate curves is same for all; exhibiting a short low heat intensity peak at the early times of reaction and one broad highly intense peak expanding to longer times saturating at the end of conversion. The first low heat peak expands longer time periods and somewhat delayed in the case of hybrids.

The heat evolution rate during hydration of TCP indicates that pure TCP compacts converted into CDHAp completely after 42-45 h. The time for complete conversion extended to longer times; 72, 82 and 85 h by addition of 3, 6 and 9 wt. % PCL additions, respectively. PCL affects the hydraulic reactivity of TCP with significantly hampering initial formation as well as growth of CDHAp crystals, as can be seen from positional shifts for heat peaks, and PCL retards the completion. Isothermal calorimetry findings indicate that increase in PCL content suppresses TCP to CDHAp

cement-type conversion and among the hybrid cement composition used in this, T3PC with 3 wt. % PCL addition shows relatively higher hydraulic property, i.e. higher potential for complete conversion to hardened cement.

5.2 Microstructural and chemical properties of TCP:PCL hybrid cement blends

The effect of PCL on hydraulic reactivity of TCP was explored more in detail with phase evaluations and microstructural investigation. This was done by reaction time-based XRD and SEM analyses for plain TCP and T3PC. Figure 5.2 a and b illustrate sets of XRD diffractograms representing phase evaluations during cement-type reaction of TCP and T3PC as a function of reaction time of 2 h up to 48 h or longer.

Regardless of PCL addition, initial XRD diffractograms of both systems exhibited the characteristic peaks of TCP (JCPDS card no 9-348). First appearance of CDHAp evidenced by low intensity peaks at around $2\theta \approx 26.5$ and $2\theta \approx 31-33$ matching with characteristic peak positions of CDHAp (JCPDS card no 9-342) upon 2 h and 8 h hydration for TCP and T3PC, respectively. XRD findings show that with 3 wt. % PCL addition, first appearance of CDHAp during hydration of TCP retarded by 6 h. In XRD diffractograms of both systems, a gradual conversion from TCP to CDHAp can be observed. Ultimately, there was no left-over TCP and XRD diffractograms suggested a complete conversion to HAp at the end of 42+ h for TCP and 72 h for T3PC. Comparison of phase evaluations as a function of reaction time for two selected systems shows that PCL delays both first appearance of CDHAp and complete conversion into CDHAp. In parallel to isothermal calorimetry findings, XRD results also suggest retarding effect of PCL on cement-type conversion of TCP to CDHAp.

Figure 5.3 illustrates microstructural changes during cement-type reaction of plain TCP pellet as a function of reaction time up to 42 h. The TCP particles preserve their equiaxed-like granulated morphology in the early stages of hydration; for reaction times up to 2 h. A gradual morphological change from granules to flake form can be seen from SEM images representing different times (8, 18, 24 or 48 h) of reaction. In order to clearly show the details of microstructural changes during TCP to CDHAp conversion; such as first appearance of CDHAp crystal and time for complete

conversion to CDHAp, some related SEM micrographs in enlarged scale are provided in Figure 5.4 and 5.5.

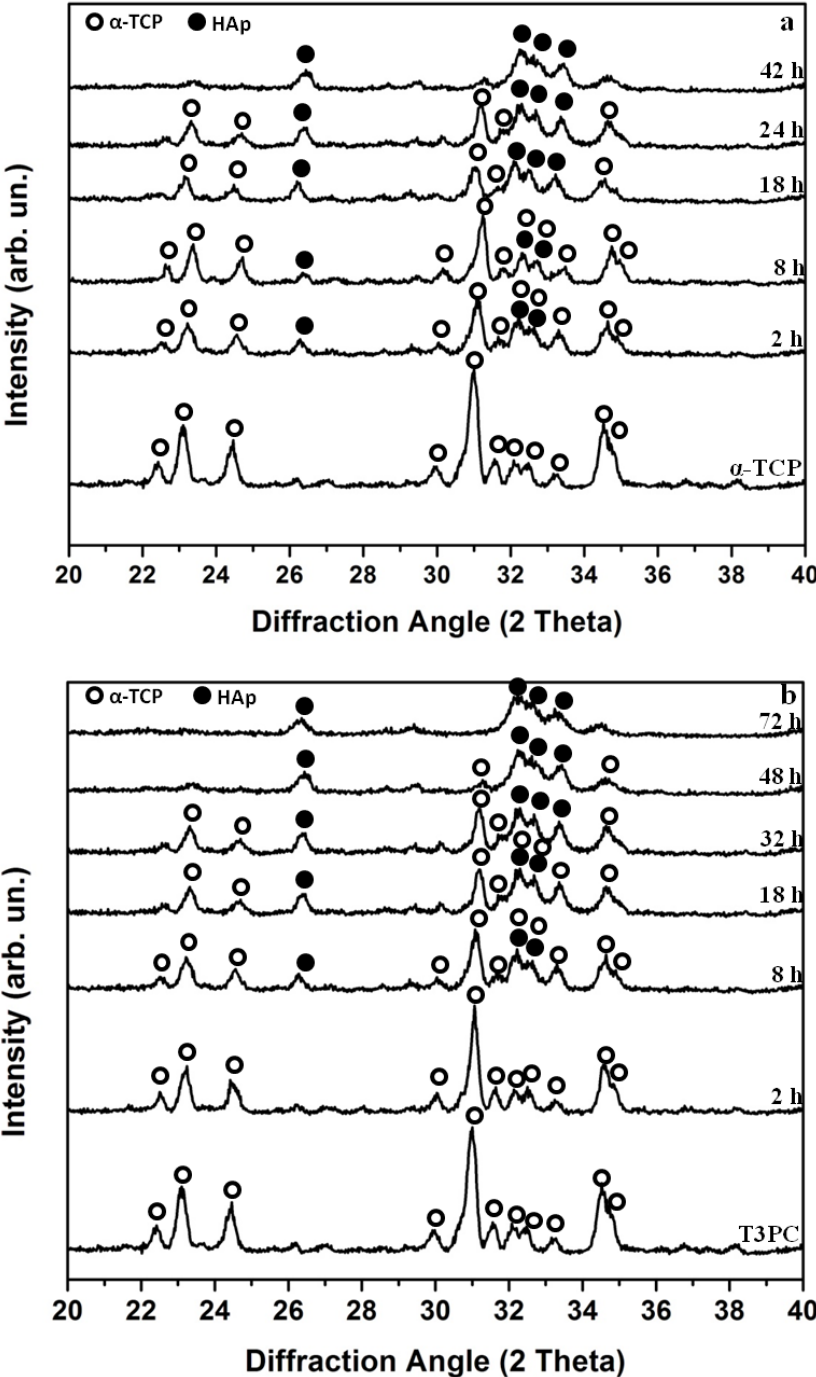


Figure 5.2 The XRD diffractograms as a function of reaction time for (a) plain TCP pellet, (b) T3PC (3 wt.% PCL) hybrid pellets.

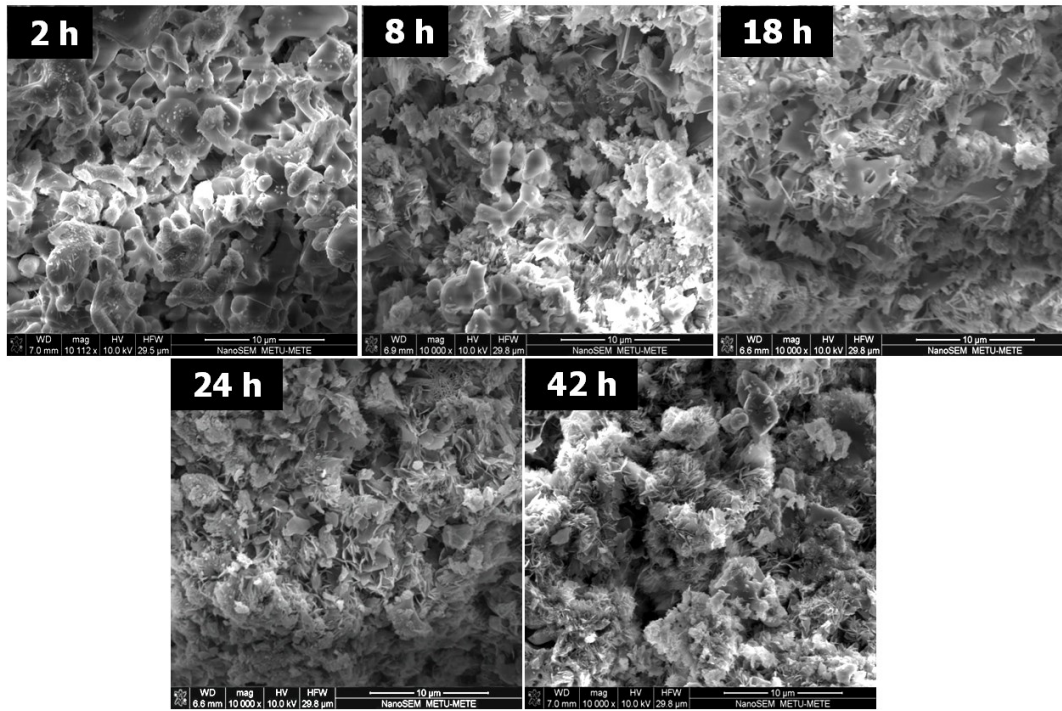


Figure 5.3 Microstructural changes during hydration TCP pellet as a function of reaction (at 37 °C) time.

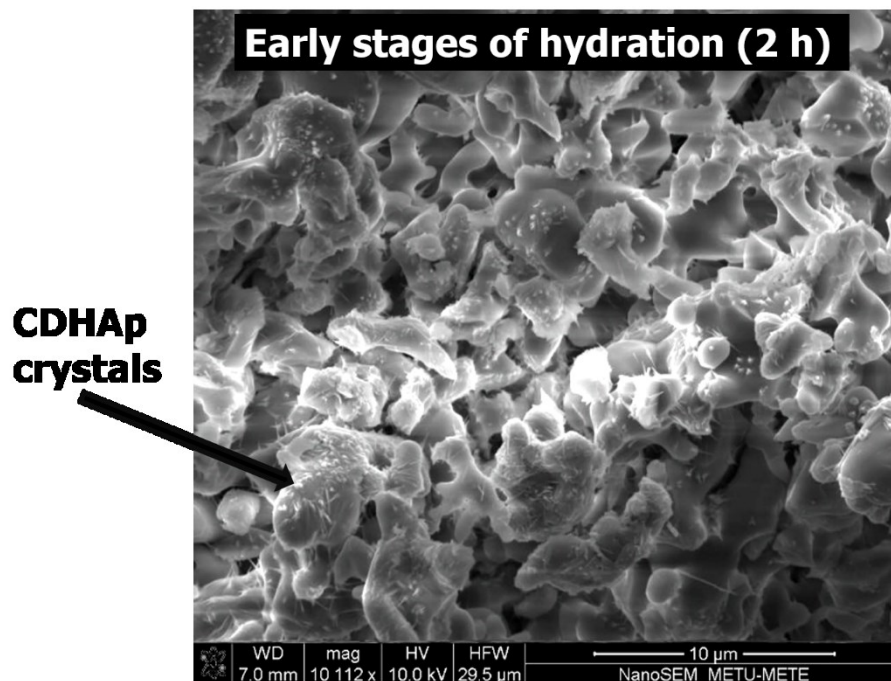


Figure 5.4 SEM micrograph of 2 h hydrated TCP pellet.

The micrograph in Figure 5.4 representing the microstructural changes after 2 h points out formation of some new crystals at this time. Based on XRD analyses, these new crystals are CDHAp, and as it can be seen from arrow mark and they preferentially precipitate on TCP particle surfaces. This image also provides some information about the mechanism of TCP to CDHAp conversion, which in fact is a hydration reaction. The TCP phase which is a relatively more soluble calcium phosphate compared to CDHAp dissolves in the early stages of reaction. When adequate supersaturation levels are reached upon dissolution, thermodynamically more stable new crystals (here CDHAp) heterogeneously precipitates on available TCP surfaces. Previous work also suggests a dissolution and precipitation based mechanism for cement type conversion of TCP [Durucan and Brown, 2000].

SEM micrograph given in Figure 5.5 shows microstructural features for plain TCP pellet after 42 h of hydration. Complete conversion of TCP to CDHAp evidenced by entangled CDHAp flakes without any unreacted TCP with granulated morphology. SEM analyses with in parallel with the XRD findings indicate a complete conversion into CDHAp flakes after 42 h of hydration with DI water



Figure 5.5 SEM micrograph of 42 h hydrated TCP pellet.

Similar reaction time-dependent microstructural analyses were also performed on hybrid blend with PCL, i.e. T3CP, as provided in Figure 5.6 for direct comparison purposes. SEM micrographs in Figure 5.6 reveal that initial granulated morphology of TCP particles were connected via PCL network and this mass gradually converts into reticulated CDHAp crystals. To be able to highlight the details and difference with respect changes with those of plain TCP, explanatory and bigger SEM micrographs are provided in Figure 5.7, 5.8 and 5.9. These are representative for 2 h, 8 h and 72 h of hydration. At 2 h of hydration, there was not any change in microstructure consisting irregular TCP granules linked via PCL network (Figure 5.7). As shown by Figure 5.8 at the end of 8 h hydration, sub-micron sized CDHAp crystals partially cover the surfaces of TCP granules. This takes place only after 2 h for plain TCP pellet. Consistent with XRD analyses, SEM micrographs also propose a retarding effect of PCL on initial formation (nucleation) of CDHAp crystals.

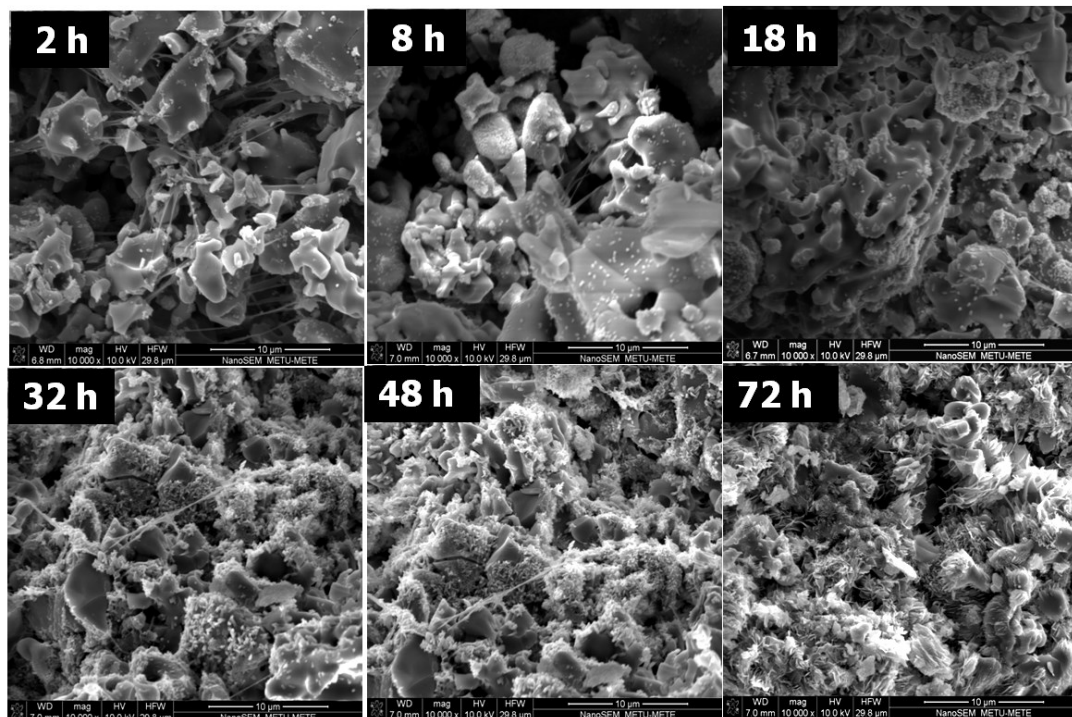


Figure 5.6 Microstructural changes during hydrolysis of T3CP (3 wt. % PCL) as a function of reaction time.

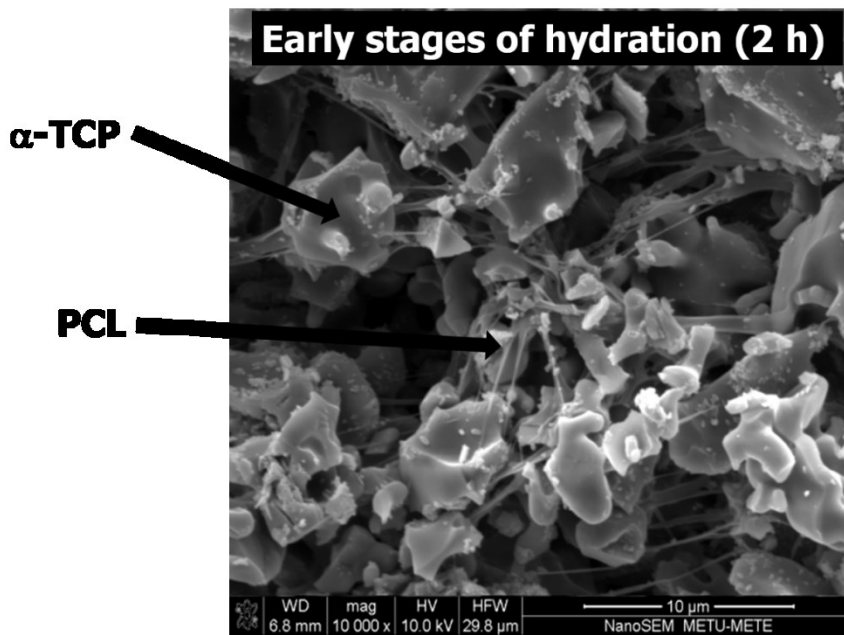


Figure 5.7 SEM micrograph of T3PC (3 wt. % PCL) after 2 h hydration.

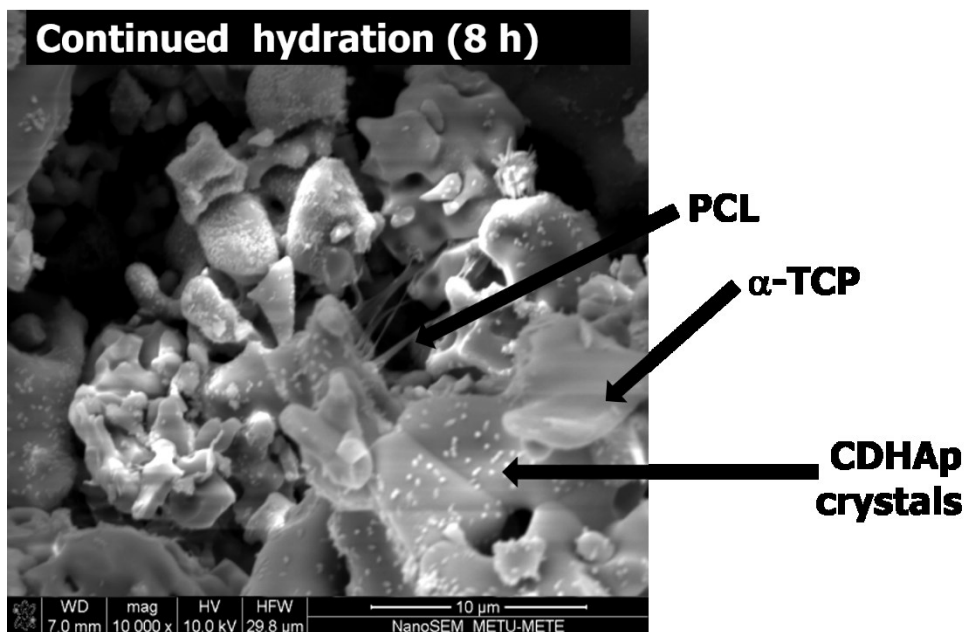


Figure 5.8 SEM micrograph of T3PC (3 wt. % PCL) after 8 h hydration.

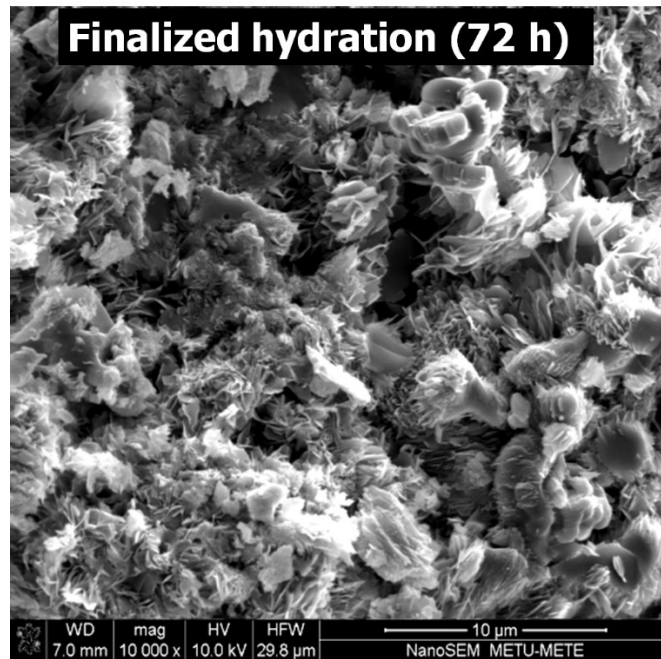


Figure 5.9 SEM micrograph of T3CP after 72 h hydration

As reaction progresses, similar to plain TCP cement, granulated morphology of TCP was replaced by entangled flake-like crystals of CDHAp (Figure 5.9). Complete conversion to entangled flake-like crystals of CDHAp without any unreacted TCP particles was accomplished after 72 h hydration as also indicated by XRD analysis. Comparison of morphological changes of TCP and T3PC as a function of reaction time reveals that the time for first appearance of CDHAp and end time of reaction were delayed by addition of 3 wt. % PCL.

The SEM findings in a general manner are consistent with XRD and isothermal calorimetry analyses and propose that addition of PCL results in poor hydraulic reactivity for TCP-based hybrid cements. This retarding effect may be due to the fact that, PCL is a biodegradable polymer with low glass transition ($-60\text{ }^{\circ}\text{C}$) and melting temperature ($60\text{ }^{\circ}\text{C}$) [Woodruff et al., 2010]. The hydration temperature ($37\text{ }^{\circ}\text{C}$) of samples is significantly higher than glass transition temperature but slightly lower than melting point of PCL. Therefore, PCL may obstruct and retard access of water to inorganic constituent of hybrid cements by wetting and covering the surfaces of TCP.

5.3 Compositional effects on cement behavior of TCP:PCL hybrid blends

After determining the effect of PCL on cement-type reaction of TCP for one specific hybrid composition. The extent of CDHAp conversion was also checked for higher amount of PCL containing hybrid blends. In other words, the isothermal calorimetry based findings were confirmed by XRD analyses of hydrated hybrids. The times for complete conversion was determined as 42 h, 72 h, 82 h and 85 h for TCP, T3PC, T6PC, T9PC, respectively, by isothermal calorimetry. Figure 5.10 illustrates XRD diffractograms of cement end products of pure TCP and three hybrid cements at same reaction times. In all cement systems, regardless of PCL amount, diffraction patterns match with characteristic peaks of HAp without any unreacted TCP or additional phase. Detailed kinetic analyses performed by SEM and XRD showed that PCL addition resulted in relatively poor hydraulic reactivities of cement systems. However, for all hybrids (T3PC, T6PC and T9PC) TCP completely converted to HAp at the end, only requiring longer conversion times compared to that needed for plain TCP, and requiring longer times with increasing PCL amount.

SEM micrographs of three hybrid system before and after hydration illustrated in Figure 5.11. For all systems, initial equiaxed-like inorganic constituent granules (TCP) connected via polymer bridges completely converted into entangled needles of CDHAp crystals. SEM micrographs correlate with XRD findings emphasizing that all three hybrid systems with different reaction kinetics are reactive and completely converted into CDHAp at the end.

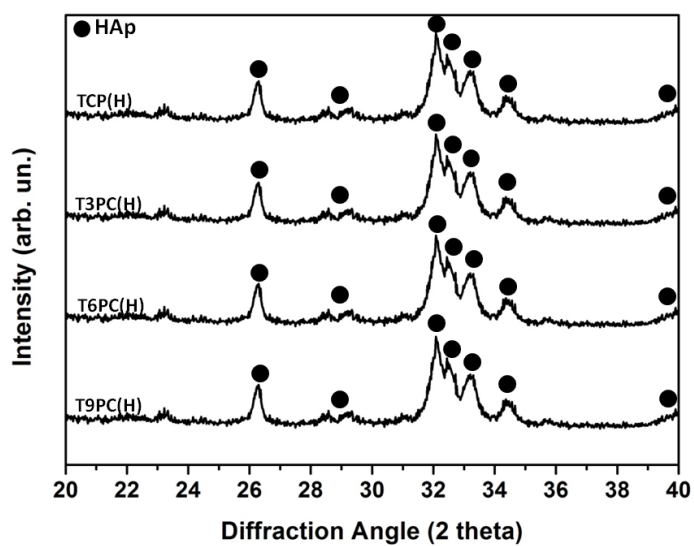


Figure 5.10 XRD diffractograms of hydration products of T3CP, T6CP and T9CP (3, 6 or 9 wt. % PCL) pellets.

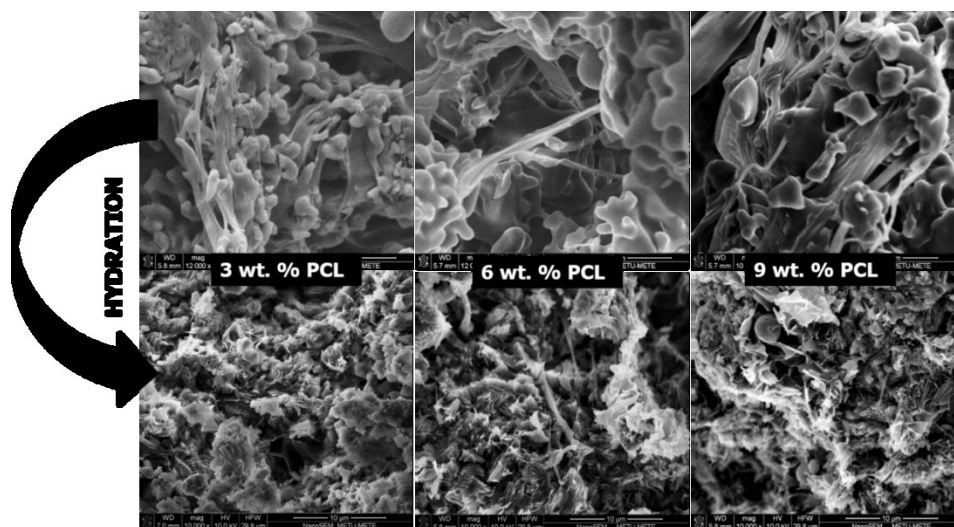


Figure 5.11 SEM micrographs of hybrid pellets of T3CP, T6CP and T9CP (3, 6 or 9 wt. % PCL) (top line), and their hydration products (bottom line).

5.4 Spectroscopic analysis of TCP:PCL hybrid blends

In this section, the chemical states of respective constituents and possible chemical interaction between organic and inorganic components of TCP:PCL hybrids composite before and after hydration were examined. Another reason for performing such chemical investigation was to reveal a possible change in the chemical structure of PCL or its degradation during hydration of TCP, presence investigated. Figure 5.12 and Figure 5.13 show FTIR spectra of TCP and all TCP:PCL hybrid cement systems before and after hydration, respectively. FTIR spectrum of pure PCL is also given as reference in Figure 5.12 for comparison purposes.

When spectra of non-hydrated and hydrated samples are compared, there are changes in the characteristic bands of inorganic constituent. As previously discussed, changes in the main PO_4 group related absorbance events are due to TCP to CDHAp cement-type reaction. The other changes marked with square (■) and star (★) at 630 cm^{-1} and 872 cm^{-1} or are again due same phase change, assigned $(\text{OH})^-$ and $(\text{HPO}_4)^{2-}$ groups of CDHAp. In parallel with XRD and SEM findings, FTIR analyses also indicates complete conversion of TCP to calcium deficient HAp.

Further, presence of any change in the structure of the organic component PCL upon hydration and any chemical reaction between inorganic and organic components were elucidated based on these data. Presence of PCL is evidenced both non-hydrated and hydrated hybrid cements with the most intense characteristic absorption band of PCL at 1727 cm^{-1} shown by triangle mark (▲) on spectra corresponding to carbonyl stretching [Elzein et al., 2004]. Additionally, it is worth to emphasize that the position of characteristic band of PCL is same for all compositions, before and after hydration, which indicates that during hydration of TCP, there isn't any change in the structure of PCL. Further, as no additional band in spectra of hydrated products was observed, a chemical interaction between PCL and inorganic constituent does not occur during hydration. FTIR investigation highlights that TCP:PCL pre-cement blends completely converted to CDHAp:PCL composites with any degradation or chemical change for PCL.

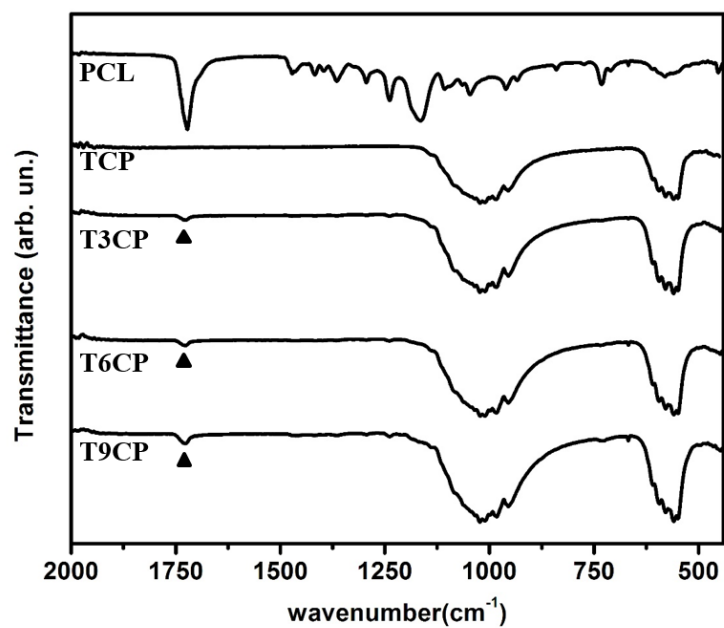


Figure 5.12 FTIR spectra of PCL, TCP and hybrid TCP:PCL pellets; T3CP, T6CP and T9CP

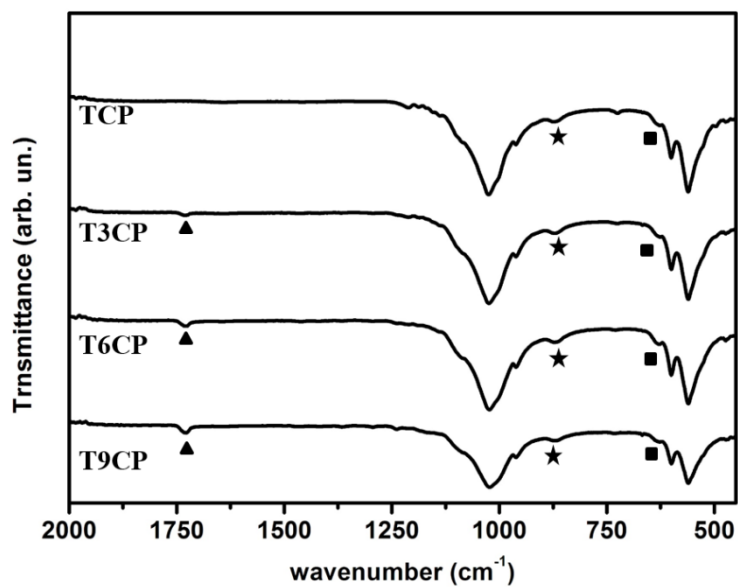


Figure 5.13 FTIR spectra of TCP and hybrid TCP:PCL pellets; T3CP, T6CP and T9CP (3, 6 or 9 wt.% PCL) after hydration (at 37 °C).

5.5 Mechanical properties of PCL incorporated hybrid cements

Mechanical properties of T3CP, T6CP and T9CP were evaluated before and after hydration. Effect of cement-type conversion and PCL addition on fracture strength values of samples were evaluated and related with the physical properties (% porosity) of the hardened compact.

Fracture strengths of TCP and TCP:PCL hybrid systems prior to hydration containing 3 wt.%, 6 wt.% and 9 wt.% PCL are illustrated in Figure 5.14. The strength values were obtained by averaging five tests. The initial diametral compression strength of pure TCP compacts prior was determined as 0.17 ± 0.05 MPa. This value increased to 0.18 ± 0.05 MPa, 0.33 ± 0.05 MPa and 0.34 ± 0.05 MPa by addition of 3 wt. %, 6 wt. % and 9 wt. % PCL, respectively.

Additionally, it is worth to emphasize that the average porosity amounts of non-hydrated TCP, T3PC, T6PC and T9PC compacts which were consolidated by pressing were determined to be comparable at 60 vol.%, 58 vol.%, 56 vol.% and 55 vol.%; respectively (listed in Table 5.1). Porosity measurement of non-hydrated compacts consistent with the fracture strength values indicates that PCL behaves as a binder by acting connecting links between the TCP particles and filling the spaces between during pressing as also evidenced in SEM micrographs in Figure 5.7. This improves the mechanical integrity of the pre-cement compact.

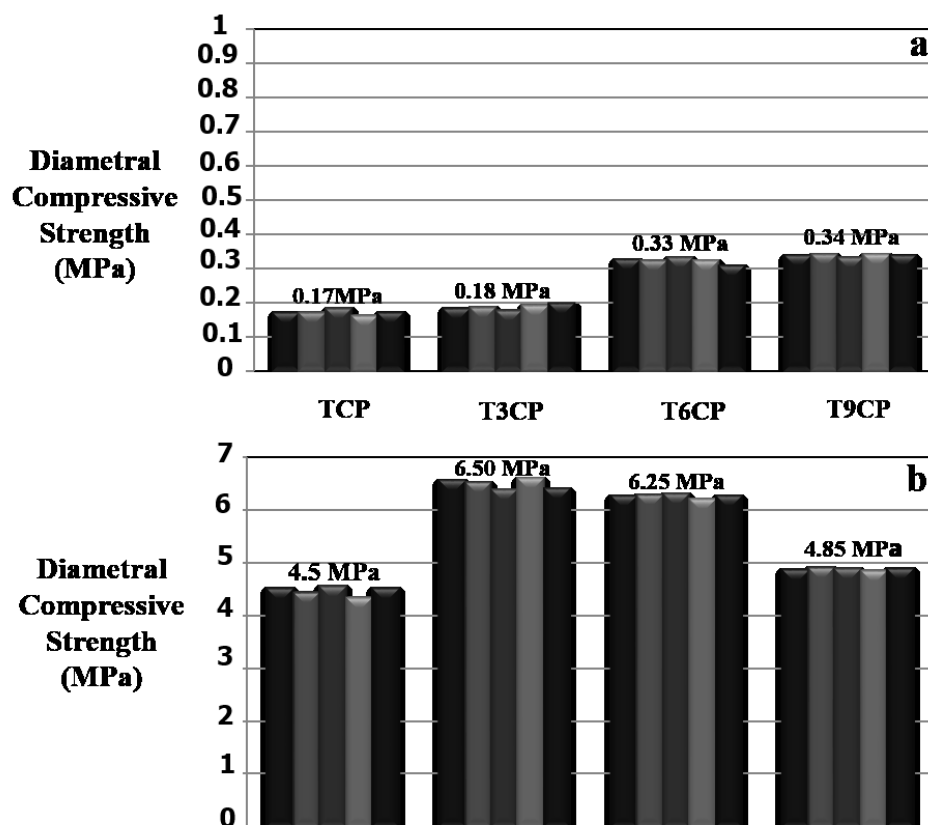


Figure 5.14 Diametral compressive strength of TCP and hybrid TCP:PCL pellets; T3CP, T6CP and T9CP (3, 6 or 9 wt.% PCL) (a) before and (b) after hydration.

Table 5.1 Porosity values of mechanical test samples before and after hydration.

Porosity (% vol)	TCP	T3CP	T6CP	T9CP
Non-hydrated	59±1	58±2	56±1	54±3
Hydrated	45±1	40±2	40±3	41±2

Figure 5.14b shows the effect of hydration on mechanical properties of hybrid cements containing 3 wt. %, 6 wt. % and 9 wt. % PCL. A significant increase in mechanical properties at the end of cement-type reaction was observed.

Meanwhile, the porosity values also decreased upon TCP to CDHAp conversion, as a result of morphological change. From microstructural point of view, increase in

mechanical properties and density based on conversion of sphere-like TCP granules into entangled CDHAp flakes. Porosity amount changing between 54-59 vol. % for non-hydrated samples decreased to 40-45 vol. % after hydration. Further, hydrated TCP, T3PC, T6PC and T9PC exhibited average diametral compression strength of 4.50 ± 0.1 MPa, 6.50 ± 0.1 MPa, 6.25 ± 0.1 MPa and 4.85 ± 0.1 MPa, respectively. Since all composites exhibited higher diametral compression strength with respect to plain CDHAp, it can be stated that PCL increased mechanical properties of CDHAp based composite cements by behaving as reinforcing agent. However, a decrease in strength was observed beyond 3 wt. % PCL incorporation. This may be due to the fact that in the presence of PCL, extent of CDHAp entanglement giving strength to the structure has decreased as observed in SEM microstructures provided in Figure 5.11. T3PC exhibits the highest diametral compression strength of $6.50 \text{ MPa} \pm 0.1 \text{ MPa}$, which is relatively lower than that of cortical bone which is about 70-150 MPa [Dorozhkin, 2010]. However, it is comparable with that of cancellous bone which is around 10 MPa [Dorozhkin, 2010; Meyers, 2008].

The mode of fracture of compacts are also modified by addition of PCL. While hydration product of TCP failed in tension mode (breaking into two solid piece along to loading axis), the hybrid products failed in shear mode (shattered into three or more pieces), which indirectly indicates a possible improvement in fracture toughness. Mechanical test results with density measurements suggest that cement-type reaction results in hardening and PCL improves mechanical integrity/strength and fracture toughness of the CDHAp-based product by providing a mechanical interlocking effect between the hard/stiff inorganic cement particles without any chemical interaction as determined and evidenced by FTIR spectroscopy.

CHAPTER 6

CONCLUSIONS

α -TCP was custom synthesized by solid state reaction of proper inorganic precursors. The composite cements were formed by incorporation of various amounts of calcium sulfate hemihydrate (CSH) and polycaprolactone (PCL) into α -TCP. Mainly, effect of these additives on cement-type reactivity of α -TCP and mechanical properties of its hydration product were elucidated. In addition, physical and chemical properties of all cement systems before and after hydration have been examined. The general findings of the thesis are summarized as followings;

Synthesis and cement characteristics of TCP

Phase pure and highly reactive TCP was obtained by solid state reaction between monetite (CaHPO_4) and calcium carbonate (CaCO_3) at 1200 °C for 2 h in air. As-synthesized TCP with average particle size of 17.8 μm converted into CDHAp at the end of 55 h hydration with DI water at 37 °C. When particle size decreased to 8.4 μm , reaction was completed in 36 h; improved reaction kinetics were observed with decreasing particle size. The cement conversion was also evidenced by XRD and SEM analyses. In addition, exact chemical stoichiometry and calcium deficiency for hydroxyapatite of cement reaction was proved by FTIR analysis. Furthermore, mechanical properties and densities of TCP cement before and after hydration were evaluated. An increase in density and fracture strength were observed after cement-type conversion owing to entangled crystals of CDHAp. Porosity level around 59 ± 1 % for TCP cement was decreased to 45 ± 1 % after cement-type conversion. Consistent with change in porosity, fracture strength was increased from 0.17 MPa to 4.5 MPa via TCP \rightarrow CDHAp conversion.

Calcium-deficient hydroxyapatite:calcium sulfate hemihydrate (CDHAp:CSH) hybrid cements

TCP:CSH hybrid blends were prepared by incorporating 10 wt. % and 25 wt. % CSH into TCP. By hydration of hybrid blends, CDHAp:CSD composites were obtained. The phase and microstructural/morphological changes for both components during hydration were examined in detail (by XRD and SEM) and related to cement conversion efficiency and mechanism. By this way, TCP to CDHAp and CSH to CSD conversion efficiencies were assessed qualitatively. However, even after a reasonably long reaction, some TCP remained unreacted for both compositions indicating limited conversion to CDHAp. Meanwhile, hydration behaviour of composite cements were investigated by isothermal calorimetry and directly compared with plain TCP. As amount of CSH incorporation increases, the completion reaction delayed and CSH hampered TCP to CDHAp cement-type conversion. There was not any remarkable change in densities of samples in the presence of CSH. All cements before hydration exhibit approximately 58 vol. % porosity level which decreased to 45 vol. % after cement-type conversion. Moreover, fracture strengths of non-hydrated samples were approximately same with plain TCP around 0.17 MPa. However, a remarkable increase was observed in fracture strengths of hydrated samples. Despite their similar porosity level, by addition of 10 and 25 wt. % CSH, 4.5 ± 0.1 MPa fracture strength of CDHAp was increased to 7.0 and 9.28 MPa; respectively. This change is due to presence of CSD (gypsum) providing reticulated needle-like crystals and adhesive forces between them. Although CSH significantly improves mechanical properties, poor hydraulic reactivities of TCP:CSH hybrids remain as a concern for ultimate use, i.e. irregular bone defect filling operations.

Calcium-deficient hydroxyapatite:polycaprolactone (CDHAp:PCL) hybrid cements

TCP:PCL hybrid blends were prepared by adding 3, 6 and 9 wt. % PCL into TCP. Hybrid blends were hydrated at 37 °C and converted to CDHAp:PCL composites. Cement-type reaction kinetics of α -TCP in the presence of PCL were evaluated by SEM, XRD and isothermal calorimetry analyses and compared with plain TCP. It was

revealed that PCL slow down α -TCP to CDHAp conversion. As PCL content increases, conversion times to CDHAp were increased. Phase identification and morphological investigation as a function of reaction time were performed on pure TCP and TCP with 3 wt. % PCL addition, in a systematic manner. However, all of hybrid cements completely converts into CDHAp at extended (longer than 85 h) as evidenced by phase and microstructural analysis. Moreover, FTIR analysis indicated that there is not any chemical interaction between PCL and inorganic constituents. It was also revealed that PCL was not affected from cement reaction. At the end of hydration, all composite cements exhibited higher strength when compared with plain TCP. 4.50 MPa fracture strength value of hydration product of TCP was increased to 6.50 MPa, 6.25 MPa and 4.50 MPa by addition of 3, 6 and 9 wt. % PCL; respectively. An increase in density for non-hydrated samples were observed as PCL acts as an interconnecting bridge between TCP particles. 59 vol. % porosity level of cement-end product of TCP was lowered to approximately 58, 56 and 54 vol. % by addition of 3, 6 and 9 wt. % PCL. Similar effect of PCL on porosity level was also observed in hydrated products. However, maximum fracture strength value was achieved by the cement with 3 wt. % PCL. Further PCL addition decreased fracture strength due to relatively lower extent of CDHAp entanglement in the presence of PCL. An optimum amount of PCL addition (3 wt. %) was determined for effective fracture strength improvement with minimum adverse effect on hydration kinetics.

REFERENCES

- Albee, F., Morrison, H. (1920). Studies in bone growth. *Annals of Surg*, 71, 32-38.
- Andrianjatovo, H., Jose, F., Lemaître, J. (1996). Effect of β -TCP granulometry on setting time and strength of calcium orthophosphate hydraulic cements. *J. Mater. Sci. Mater. Med.*, 7, 34-39.
- Aoki, H. (1994). *Medical Applications of Hydroxyapatite*. Ishiyaku EuroAmerica, Inc.: Tokyo.
- Barrelet, J. A., Hofmann, M., Grover, L.M., Gbureck, U. (2003). High-strength apatitic cement by modification with -hydroxy acid salts. *Adv. Mater.*, 15, 2091-2094.
- Beaudoin, J.J. (1990). *Handbook of Fibre-Reinforced Concrete*. Noyes Publications, New Jersey.
- Bigi, A., Bracci, B., Panzavolta, S. (2004). Effect of added gelatin on the properties of calcium phosphate cement. *J. Biomater.*, 25, 2893-2899.
- Bohner, M., Malsy, A.K., Camiré, C.L., Gbureck, U. (2006). Combining particle size distribution and isothermal calorimetry data to determine the reaction kinetics of α -tricalcium phosphate-water mixtures. *Acta Biomater.*, 2, 343–348.
- Bohner, M. (2000). Calcium orthophosphates in medicine: From ceramics to calcium phosphate cements. *Injury, Int. J. Care Injured*, 31, 37-47.
- Bohner, M. (2007). Reactivity of calcium phosphate cements. *J. Mater. Chem.*, 17, 3980-3986.
- Bohner, M., van Landuyt, P., Merkle, H.P., Lemaître, J. (1997). Composition effects on the pH of a hydraulic calcium orthophosphate cement. *J. Mater. Sci. Mater. Med.*, 8, 675-681.
- Bourgeois, B., Laboux, O., Obadia, L., Gauthier, O., Betti, E., Aguado, E., Daculsi, G., Bouler, J.M. (2003). Calcium-deficient apatite: a first in vivo study concerning bone ingrowth. *J. Biomed. Mat. Res.*, 65A, 402-408.
- Brown, W.E., Chow, L.C (1986). A new calcium phosphate water setting cement. In *Cements Research Progress*; Brown, P.W., Ed.; American Ceramic Society: Westerville, OH, USA, 352-379.
- Brunner T. J., Grass R.N., Bohner M., Stark W.J. (2007). Effect of particle size, crystal phase and crystallinity on the reactivity of tricalcium phosphate cements for bone reconstruction. *J. Mater. Chem.*, 17, 4072-4078.
- Burguera, E.F., Xu, H.H., Takagi, S., et al. (2005). High early strength calcium phosphate bone cement: effects of dicalcium phosphate dihydrate and absorbable fibers. *J. Biomed. Mater. Res. A*, 75, 966–975.

- Camiré, C.L., Jegou Saint-Jean, S., Hansen, S., McCarthy, I., Lidgren, L. (2005). Hydration characteristics of α -tricalcium phosphates: comparison of preparation routes. *J. Appl. Biomater. Biomech.*, 3, 106–111.
- Camiré, C. L., Gbureck, U., Hirsiger, W., and Bohner, M. (2005). Correlating crystallinity and reactivity in an α -tricalcium phosphate. *J. Biomater.*, 26, 2787–2794.
- Canal, C., Ginebra, M.P. (2011). Fibre-reinforced calcium phosphate cements: A review. *J. Mech. Behav. Biomed. Mater.*, 4, 1658-1671.
- Carey, L.E., Xu, H.H., Simon, C.G. Jr., et al. (2005). Premixed rapid-setting calcium phosphate composites for bone repair. *Biomaterials*, 26, 5002–5014.
- Carrodegua, R., De Aza, S. (2011). α -Tricalcium phosphate: Synthesis, properties and biomedical applications. *Acta Biomater.*, 7, 3536-3546.
- Chen, W.C., Lin, J.H.C., Ju, C.P. (2003). Transmission electron microscopic study on setting mechanism of tetracalcium phosphate/dicalcium phosphate anhydrous-based calcium phosphate cement. *J. Biomed. Mater. Res.*, 64, 664-671.
- Cherng, A., Takagi, S., Chow, L.C. (1997). Effects of hydroxypropyl methylcellulose and other gelling agents on the handling properties of calcium phosphate cement. *J Biomed Mater Res A*, 35, 273–277.
- Constantz, B., Barr, B., Ison, I., Fulmer, M., Baker, J., McKinney, L., Poser, R. (1998). Histological, chemical, and crystallographic analysis of four calcium phosphate cements in different rabbit osseous sites. *J. Biomed. Mater. Res.*, 43, 451-461.
- De Groot, K. (1983). Ceramics of calcium phosphates: preparation and properties. In: *Bioceramics of Calcium Phosphate*. deGroot K (Ed). CRC Press: Boca Raton, pp. 100–114.
- Dorozhkin, S. (2011). Biocomposites and hybrid biomaterials based on calcium orthophosphates. *Biomater*, 1, 3-56.
- Dorozhkin, S. (2013). Self-setting calcium orthophosphate formulations. *J. Funct. Biomater.*, 4, 209-311.
- Dorozhkin, Sergey. (2013). A detailed history of calcium orthophosphates from 1770s till 1950. *J. Mater. Sci. Eng. C*, 33, 3085-3110.
- Dos Santos, L.A., de Oliveira, L.C., da Silva Rigo, E.C., Garcia Carrodéguas, R., Ortega Boschi, A., Fonseca de Arruda, A.C. (2000). Fibre reinforced calcium phosphate cement. *Artif. Organs*, 24, 212–216.
- Driessens, F.C.M. (1999). Chemistry and applied aspects of calcium orthophosphate bone cements. In *Concepts and clinical applications of ionic cements*. In *Proceeding of 15th European Conference on Biomaterials*, Arcachon, Bordeaux, France.
- Durucan, C., Brown, P. (2000). α -Tricalcium phosphate hydrolysis to hydroxyapatite at and near physiological temperature. *J. Mater. Sci. - Mater. Med.*, 11, 365-371.

- Durucan, C., Brown, P. (2002). Reactivity of α -tricalcium phosphate. *J. Mater. Sci.*, 37, 963-969.
- Elliott, J.C. (1994). Structure and chemistry of the apatites and other calcium orthophosphates; Elsevier: Amsterdam, Holland.
- Hattori, T., Iwadata, Y. (1990). Hydrothermal preparation of calcium hydroxyapatite powders. *J. Am. Ceram. Soc.*, 73, 1803–1805.
- Hench, L. L. (1988). Bioactive ceramics, in Ducheyne P and Lemons J E, *Bioceramics: Materials Characteristics vs. in vivo Behavior*, New York, Ann. of the New York Academy of Science, 523, 54–71.
- Ikenaga, M., Hardouin, P., Lemaître, J., Andrianjatovo, H., Flautre, B. (1998). Biomechanical characterization of a biodegradable calcium phosphate hydraulic cement: a comparison porous biphasic calcium phosphate ceramics. *J. Biomed. Mater. Res.*, 40, 139-144.
- Ishikawa, K., Asaoka, K. (1995). Estimation of ideal mechanical strength and critical porosity of calcium phosphate cement. *J. Biomed. Mater. Res.*, 29, 1537-1543.
- Ishikawa, K., Takagi, S., Chow, L.C., Ishikawa Y., Eanes, E.D., Asaoka, K. (1994). Behavior of a calcium orthophosphate cement in simulated blood plasma in vitro. *Dent. Mater.*, 10, 26-32.
- Ishikawa, K., Takagi, S., Chow, L.C., Ishikawa, Y. (1995). Properties and mechanisms of fast-setting calcium phosphate cements. *J. Mater. Sci. Mater. Med.*, 6, 528-533.
- Jarcho, M. (1976). Hydroxylapatite synthesis and characterization in dense polycrystalline forms. *J. Mater. Sci.*, 11, 2027–2035.
- Kim, J.Y., Cho, B.C. (2007). Effect of calcium sulfate pellets on early bone mineralization in distraction osteogenesis for craniofacial microsomia in adults. *J. Craniofac. Surg.*, 18, 1309-1321.
- Lee D. D., Rey C., Aiolova M. , US Pat. No 5676976, 1995.
- Loher, S., Stark, W. J., Maciejewski, M., Baiker, A., Pratsinis, S.E., Reichardt, D., Maspero F., Krumeich F. (2005). Fluoro apatite and calcium phosphate nanoparticles by flame synthesis, *Chem. Mater.*, 17, 36–42.
- Lieberman, J. and Friedlaender, G. (2005). *Bone regeneration and repair*. New Jersey: Humana Press.
- Mariño, F.T., Mastio, J., Rueda, C., Blanco, L., Cabarcos, E.L. (2007). Increase of the final setting time of brushite cements by using chondroitin 4-sulfate and silica gel. *J. Mater. Sci. Mater. Med.*, 18, 1195-1201.
- Mariño, F.T., Torres, J., Hamdan, M., Rodríguez, C.R., Cabarcos, E.L. (2007). Advantages of using glycolic acid as a retardant in a brushite forming cement, *J. Biomed. Mater. Res. B Appl.*, 571-579.

- Monma, H., Goto, M. (1983). Behavior of the α - β phase transformation in tricalcium phosphate. *Yohyo-Kyokai-Shi*, 91,473-475.
- Monma, H., Kanazawa, T. (1976). The hydration of α -tricalcium phosphate. *Yogyo-Kyokai-Shi*, 84, 209-213.
- Moreau, J.L., Weir, M.D., Xu, H.H. (2009). Self-setting collagencalcium phosphate bone cement: mechanical and cellular properties. *J. Biomed. Mater. Res. A*, 91, 605-613.
- Nilsson, M., Fernandez, E., Sarda, S., Lidgren, L., Planell, A. (2002). Characterization of a novel calcium phosphate/sulphate bone cement. *J. Biomed. Mater. Res.*, 61, 600-607.
- Park, J. (2008). Hard tissues: structure, properties, healing, remodeling, and biocompatibility. In *Bioceramics: Properties Characterization and Applications*. NewYork: Springer Science Business Media.
- Peltier, L.F. (1961). The use of plaster of Paris to fill defects in bone. *Clin. Orthop. Res.*, 21,1-29.
- Perez, R.A., Altankov, G., Jorge-Herrero, E., et al. (2012). Micro- and nanostructured hydroxyapatite-collagen microcarriers for bone tissue-engineering applications. *J. Tissue Eng Regen. Med*.
- Perez, R.A., Kim, H.W., Ginebra, M.P., (2012). Polymeric additives to enhance the functional properties of calcium phosphate cements. *J. Tissue Eng.*, 3(1).
- Ramay, H.R., Zhang, M. (2003). Preparation of porous hydroxyapatite scaffolds by combination of gel-casting and polymer sponge methods. *Biomaterials*, 24, 3293-3302.
- Ray, R., Degge, J., Gloyd, I., Mooney, G. (1952). Bone regeneration. *J. Bone Joint Surg.*, 34A, 638-647.
- Sarda, S., Fernández, E., Nilsson, M., Balcells, M., Planell, J.A. (2002). Kinetic study of citric acid influence on calcium phosphate bone cements as water-reducing agent. *J. Biomed. Mater. Res.*, 61, 653-659.
- Singh, N., Middendorf, B. (2007). Calcium sulphate hemihydrate hydration leading to gypsum crystallization. *Prog. Cryst. Growth Charact. Mater.*, 53, 57-77.
- Suchanek, W.L., Yoshimura, M. (1998). Processing and properties of hydroxyapatite based biomaterials for use as hard tissue replacement implants. *J. Mater. Res.*, 13, 94-117.
- Sun, L., Xu, H.H., Tagaki, S., et al. (2007). Fast setting calcium phosphate cement-chitosan composite: mechanical properties and dissolution rates. *J. Biomater.*, 21, 299-315.
- Tagaki, S., Chow, L.C., Hirayama, S., et al. (2003). Properties of elastomeric calcium phosphate cement-chitosan composites. *Dent. Mater.*, 19, 797-804.

- Tamimi, F., Kumarasami, B., Doillon, C., et al. (2008). Brushite-collagen composites for bone regeneration. *Acta Biomater*, 4, 1315–1321.
- Tancred, D.C., McCormack, B.A., Carr, A.J. (1998). A synthetic bone implant macroscopically identical to cancellous bone. *J. Biomater.*, 19, 2303–2311.
- Tang, R., Nancollas, G. H., Orme C.A. (2001). Mechanism of dissolution of sparingly soluble electrolytes., *J. Am. Chem. Soc.* 123, 5437–5443.
- Thomas, M.V., Puleo, D.A. (2008). Calcium sulfate: Properties and clinical applications. *J. Biomed. Mater. Res. B Appl. Biomater.*
- Weiner, S., Wagner, H. D., (1998). The material bone: Structure-mechanical function relations. *Annu. Rev. Mater. Sci.*, 28, 271-298.
- Wilson, C.E., de Bruijn, J.D., van Blitterswijk, C.A., Verbout, A.J., Dhert, W.J. (2004). Design and fabrication of standardized hydroxyapatite scaffolds with a defined macro-architecture by rapid prototyping for bone-tissue-engineering research, *J. Biomed. Mater. Res.*, 68,123–132.
- Xu, H.H.K., Eichmiller, F.C., Giuseppetti, A.A., (2000). Reinforcement of a self-setting calcium phosphate cement with different fibres. *J. Biomed. Mater. Res.* 52, 107–114.
- Xu, H.H.K., Quinn, J.B. (2002). Calcium phosphate cement containing resorbable fibres for short-term reinforcement and macroporosity. *J. Biomater.*, 23, 193–202.
- Xu, H.H.K., Weir, M.D., Burguera, E.F., Fraser, A.M. (2006). Injectable and macroporous calcium phosphate cement scaffold. *J. Biomater.*, 27, 4279–4287.
- Yu, T., Ye, J., Gao, C., et al. (2010). Effect of biomedical organic compounds on the setting reaction of calcium phosphates. *Colloids Surf B Biointerfaces*, 75, 363–369.
- Zhou, W., Xue, Y., Ji, X., Yin, G., Zhang, N., Ren, Y. (2011). A novel injectable and degradable calcium phosphate/calcium sulfate bone cement. *African Journal of Biotechnology*, 10, 19449-19457.
- Zuo, Y., Yang, F., Wolke, J.G.C., Li, Y., Jansen, J.A. (2010). Incorporation of biodegradable electrospun fibres into calcium phosphate cement for bone regeneration. *Acta Biomater*, 6, 1238–1247.